UNIVERSITY OF KWAZULU-NATAL ™

INYUVESI YAKWAZULU-NATALI

RESEARCH AND DEVELOPMENT OF A HYBRID KINEMATIC PLATFORM, WITH ASSOCIATED CONTROL METHODOLOGY, FOR SEVERAL LOW DEGREE OF FREEDOM SERIAL KINEMATIC MANIPULATORS

Submitted by Mr Bryan Kelly (BSc Eng – UKZN – 212501838) – May 2023

Supervisor: Prof. G. Bright

Co-Supervisor: Dr J. Padayachee

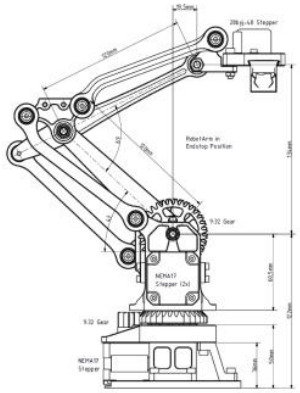

Submitted in the fulfilment of the academic requirements for the degree of Master of Science in Engineering (Mechanical Engineering) at the School of Mechanical Engineering, University of KwaZulu-Natal.

“The factory of the future will have only one human and one dog. The human will be there to feed the dog, and the dog will be there to keep the human from touching the machines.”

THE THREE LAWS THAT GOVERN ROBOTS:

1. A robot may not injure a human being or, through inaction, allow a human being to come to harm.

2. A robot must obey the orders given to it by human beings, except where such orders would conflict with the First Law.

3. A robot must protect its own existence as long as such protection does not conflict with the First or Second Law.

- Isaac Asimov 1942.

Declaration 1: Submission

As the candidates' supervisor, I agree to the submission of this dissertation.

Supervisor: _____ Date: _____

Dr Jared Padayachee.

As the candidates' co-supervisor, I agree to the submission of this dissertation.

Supervisor: _____ Date: _____

Prof. Glen Bright.

Declaration 2: Plagiarism

I, Bryan Sherwood Kelly, declare that:

i. The research reported in this dissertation, except where otherwise indicated, is my original research.

ii. This dissertation has not been submitted for any degree or examination at any other university.

iii. This dissertation does not contain other persons' data, pictures, graphs or other information, unless specifically acknowledged as being sourced from other persons.

iv. This dissertation does not contain other persons' writing, unless specifically acknowledged as being sourced from other researchers. Where other written sources have been quoted, then:

   a. Their words have been re-written, but the general information attributed to them has been referenced.

   b. Where their exact words have been used, then their writing has been placed in italics and inside quotation marks and referenced.

v. This dissertation does not contain text, graphics or tables copied and pasted from the Internet, unless specifically acknowledged, and the source being detailed in the dissertation and in the References sections.

Signed:  Date: 30 April 2023

Bryan Kelly.

Declaration 3: Publications

Details of contribution to peer-reviewed publications that include research presented in this dissertation. The undersigned agree that the following submissions were published and submitted as described and that the content therein is contained in this research.

ICINCO 2019:

B. Kelly, J. Padayachee, and G. Bright, "Quasi-serial Manipulator for Advanced Manufacturing Systems," in *ICINCO (2)*, 2019, pp. 300-305.

Bryan Kelly was the lead author of this paper and conducted all research and experimentation under the supervision of Doctor Jared Padayachee and Professor Glen Bright.

RobMech 2020:

B. Kelly, J. Padayachee, and G. Bright, "Quasi-Serial Manipulator - Inverse Kinematics and Workspace Analysis for Industrial Automation," in *2020 International SAUPEC/RobMech/PRASA Conference*, 2020, pp. 1-6: IEEE.

Bryan Kelly was the lead author of this paper and conducted all research and experimentation under the supervision of Doctor Jared Padayachee and Professor Glen Bright.

Signed: [redacted] Date: 30 April 2023

Bryan Kelly.

ABSTRACT

Industry has placed focus on efficiency and flexibility, for this reason it is beneficial to propose a method in which serial manipulators can be reoriented into a parallel system when needed. This reorientation allows industry to implement less robotic manipulators, which reduces cost and space requirements; while still being able to receive the benefits that are associated with serial and parallel robotic manipulators.

This research focuses on the development of a hybrid kinematic platform that consists of the combination of several low degree of freedom Serial Kinematic Manipulators (SKM) into a Parallel Kinematic Manipulator (PKM). Special attention was placed on the initial selection of the serial manipulators to be combined into a hybrid SKM PKM platform. The aim of the hybridization is to create the ability to have several serial manipulators that can operate within a collaborative workspace for tasks that require dexterity, such as assembly operations. As well as, become an individual parallel mechanism to perform tasks that require increased rigidity, such as machining.

Several desktop models were produced via rapid prototyping methods. An electronic system that included stepper motors, limit switches, Arduino, RAMPS breakout board and motor drivers were installed onto each RobotArm. Several design optimizations were implemented to improve the potential of the final platform.

Full serial kinematic analysis was performed on the individual serial RobotArms, including full 3D forward and inverse derivations via a geometric approach. A parallel inverse kinematic derivation was performed for the combined system, which includes a rotation matrix. The rotation matrix was required due to the added degrees of freedom that became available in the combined hybrid kinematic platform. The kinematics were used for the control system that were implemented via Arduino and a Python GUI. The kinematics also allowed for investigation into the workspace, and the singularities present in that workspace. Both the workspace and the singularity plots were performed via Monte Carlo randomization scripts performed in Octave/MATLAB and Python.

Testing was then performed to identify how well the platform works as individual collaborative serial manipulators as well as a single combined hybrid platform. The tests focused on the accuracy and repeatability present within the different combination of the platform. It was found that the combined hybrid kinematic platform outperformed the individual serial kinematic manipulator in accuracy as well as displaying a lower level of deflection to load. The combined hybrid kinematic platform was able to achieve three further degrees of freedom compared to the individual serial kinematic manipulator.

The results obtained validate the research question of whether it is possible to combine several low degree of freedom serial kinematic chains into a single hybrid platform and how such a platform would be controlled.

CONTENTS

LIST OF FIGURES

LIST OF TABLES

NOMENCLATURE

$\vec{m}$	Vector m
θ_1	Theta One
2D	Two Dimensional
3D	Three Dimensional
CAD	Computer Aided Drawing
CNC	Computer Numerically Controlled
DC	Direct Current
DH	Denavit-Hartenberg
DOF	Degrees Of Freedom
FK	Forward Kinematics
GUI	Graphical User Interface
IK	Inverse Kinematics
PKM	Parallel Kinematic Mechanism
PLA	Polylactic Acid
PWM	Pulse Width Modulation
SCARA	Selective Compliance Articulated Robot Arm
SKM	Serial Kinematic Mechanism

1. INTRODUCTION

As an introduction to the remainder of the research outlined in this dissertation, several considerations need mentioning. These include the motivation for why the research is necessary, how it is going to be of value to the market, and a breakdown of how the research will be performed, with specific aims and objectives required to answer the research question posed.

1.1 Research Background

Global industrial manufacturing output is a function per captia as well as the level of automation that has been implemented. From Figure 1 and Figure 2, the level of factory output for countries with a lower capita count is dominated largely by those that have a higher level of robotic automation implemented.

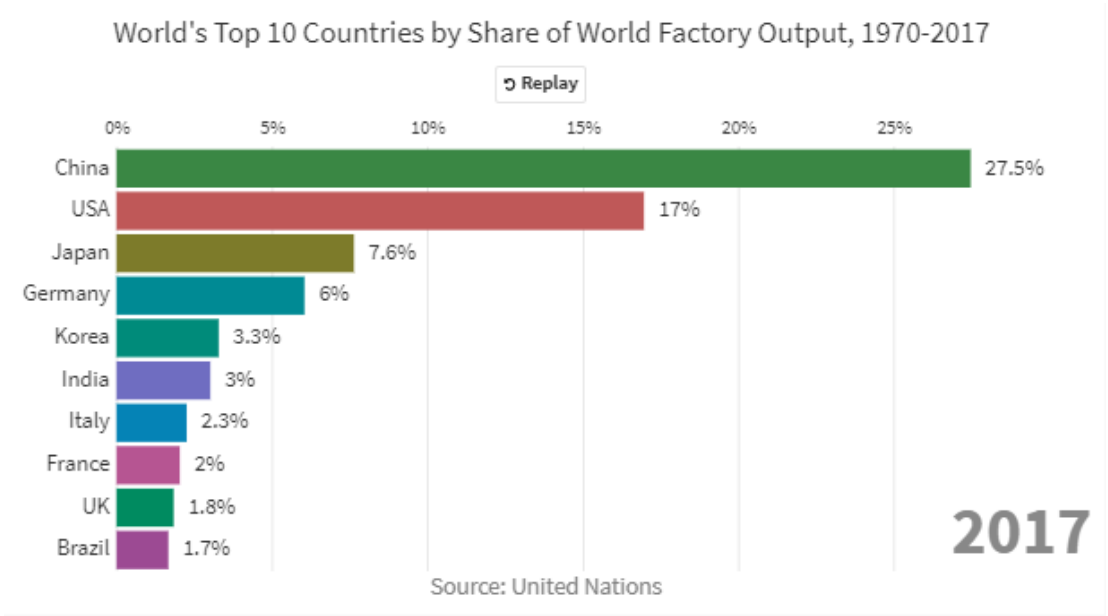

Figure 1: Top 10 manufacturing countries 2017 [1].

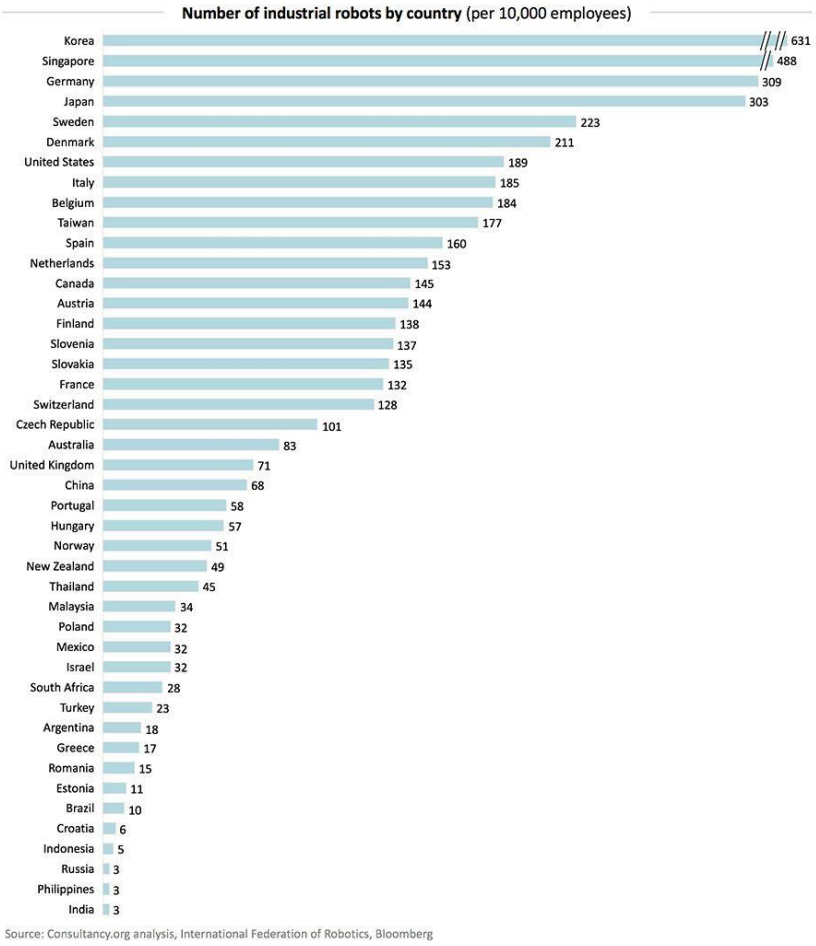

Figure 2: Number of industrial robots by country [2].

This trend of industrial automation increasing the overall output and hence increasing the country's Gross Domestic Product (GDP) should be viewed as a direct correlation. This is backed up by the scientific community in a number of research contributions, including the paper by *Cali et al.* [3] and *Sharif et al*. [4]. The paper outlines an increase in production, with up to 20% reduced product defect rate due to increased industrial automation.

It is further noted by *Carbonero et al.* [5] that there is a decrease in outsourcing aspects of manufacture to other countries when increased automation is present within the country of origin. This decrease in offshoring can be viewed as a method to increase in countries employment in aspects that surround the manufacture, as well as increased overall GDP of the country.

With this in mind, a method of achieving greater automation within countries that already have an industrial automation footprint, but perhaps do not have a large enough GDP to increase this level of automation should be of focus to researchers.

The ability to achieve a greater amount of output via a lower level of automation potential can be viewed as a flexibility efficiency problem. Hypothetically, the ability to achieve more flexibility from the current level of automation would allow for a higher level of production output without the need to increase the number of industrial robots.

This could be achieved if the current industrial manipulators could perform a wider range of tasks, enabling more automation to become available from the same number of implemented manipulators. For emerging countries such as Brazil, Russia, India, China, and South Africa - the BRICS collaboration, this would mean a greater footprint in the global manufacturing environment, whilst controlling the overall costs involved with the increase in automation experienced by established countries, such as the United States of America [6].

1.2 Research Motivation

Industry has become hugely reliant on automating production and manufacturing. This has allowed for people to perform more holistic tasks rather than menial repetitive tasks. Automation has allowed the production to become more streamlined with greater potential for output volume and quality.

In the past, the cost of automation was extremely high, with hugely complex mechanisms designed to perform a single task. This, although still occurs in some cases, has become less of the majority thanks to the implementation of flexible multi-task capable robotic manipulators. These robotic manipulators could perform several tasks; or at the very least are reprogrammed to perform a completely new task when required. This has allowed the cost of automation to reduce significantly.

Within industrial robotics there are two separate fields of study: namely the parallel and serial archetypes. Each archetype has its own advantages and disadvantages, however there is no clear link between the two [7] [8].

Although there now is a large amount of flexibility available within industry to reprogram robotic manipulators to perform different tasks; there still is a clear differentiation between the major types of tasks available to the different types of robotic manipulator archetypes. The integration of each type of archetype is separate in industry and this leads to the requirement of having many specific robotic platforms for individual tasks. Namely parallel mechanisms are focused on rigidity and accuracy, but are difficult to calibrate, while serial mechanisms are focused on articulation throughout a larger workspace [8]. This tends to be a bulky system requiring large amounts of space, as well as a costly system due to the personalized tasks performed by each specific type of robotic manipulator [9] [10].

The focus of industry in the recent past has been to become as efficient and streamlined as possible. This efficiency has been applied to many aspects, namely space, costs, material and energy requirements with a large focus on becoming more eco-friendly [11].

The next step was to create a system in which the robotic manipulators can perform any task; by reconfiguring or combining to other manipulators to become a new system that can achieve the desired result. This would allow for a reduction in the number of robotic platforms required within a production or manufacturing facility, which in turn reduces the space and overhead costs involved.

The goal of this research was to propose a methodology into which hybridisation, and therefore more flexibility, can be introduced between the two major industrial robot archetypes.

The scientific contributions outlined for this research were the novel implementation and integration of simple serial kinematic chains in parallel in order to achieve the effective working envelope and flexibility of a serial robotic configuration, whilst being rigid enough to perform the machining operations of a conventional CNC machine. Additionally, the scientific contribution included a novel unified method of automation and control of the hybrid system [12] [13] [14].

Several outcomes were to be achieved throughout the research: with a focus on the combining of several low degree of freedom serial kinematic chains into one hybrid kinematic platform. This outcome relied on the integration of several low degree of freedom serial kinematic manipulators achieving harmonious combined articulation that could be implemented additionally, or the ability to achieve greater articulation when compared to the individual serial manipulators. It was discovered throughout the performed research that although possible to achieve acceptable working accuracy and repeatability obtained through the methodology followed, future research should focus on a unified control system, utilizing a single, more powerful, control hardware configuration.

1.3 Research Aims & Objectives

The aim of the project was to develop a scaled prototype of a multipurpose, hybrid kinematic robotic platform. The platform consisted of multiple low degree of freedom serial kinematic robotic manipulators that have the potential to operate as individuals, collaboratively, within the same workspace; as well as a single combined hybrid platform that can operate as a unified manipulator with greater potential when compared to the individual.

Focus of the research was to illustrate that it is possible to achieve increased flexibility and collaboration between multiple, otherwise considered independent, low Degree Of Freedom (DOF) serial kinematic manipulators; and on the control methodology of the individual manipulators, while presenting a unified control approach to allow for combined operation.

The hypothesis is that it is possible to achieve greater flexibility within industrial automation by creating systems that can work independently, collaboratively as well as transform into a new system when combining. It Is hypothesised that the combined system will demonstrate greater potential over the individual components.

Research Question:

“Can simple serial kinematic chains be incorporated in parallel to create a hybrid robotic system? Subsequently, how would such a system be automated and controlled?”

Research Objectives:

- Research and establish the state-of-the-art in parallel kinematic and serial kinematic robotic systems, with focus on low DOF serial kinematic robots that can be incorporated into larger parallel systems.

- Integrate low DOF serial robots in parallel, model the inverse kinematics and implement a suitable electronic system to create a combined hybrid system.
- Perform comparative experiments on the low DOF serial and the combined hybrid kinematic systems.

The scope of this research is limited to the objectives outlined above, and does not consider the dynamic properties, the trajectory or path planning algorithms, or the methods of calibration involved with the setup of industrial robotic manipulators. The research has focus on reconfigurability, however this is limited to a non-autonomous reconfiguration of the robotic manipulators from SKM to PKM.

1.4 Research Methodology Overview

A mechatronics approach was utilized to guide the research and development process. The mechatronics approach is considered a multi-disciplinary research and design approach that emphasises concurrent engineering practices. Listed below are the stages in which this project was executed:

- Perform research on the state-of-the-art in robotic systems.
- Research and develop a set of specifications that outline the functionality and performance required for a proof-of-concept prototype.
- Research and formulate schemes of reconfiguration that can be applied to mechanical architecture, electronic design and software control system.
- Research and innovate on methods of kinematic modelling to describe the changing motion capabilities of a reconfigurable system.
- Research, design and construct a mechanical prototype of a reconfigurable hybrid kinematic robotic system.
- Research, design and implement a suitable electronic and software control system.
- Research, design, plan and execute a series of experiments and tests that verify the system performance.
- Report on the findings of this research in an MSc dissertation as well as in conference and journal publications.

1.5 Outline of Dissertation

Chapter One:

This chapter introduces and outlines the research aims objectives and proposed goal. Along with the methodology proposed and the scientific contributions achieved. Chapter one is a summary of the proposed research.

Chapter Two:

This chapter develops a literature review of the current state of the art within industrial robotics. The goal of this chapter was to develop and outline a full understanding into the current methods and key factors within robotics. Focus has been placed on the major archetypes currently found within industry and research.

Chapter Three:

This chapter outlines the research concept which includes the potential advantages of such a hybrid system.

Chapter Four:

Begins to move onto the specifics of the research – including the selection of the suitable robotic platform that would be the focus of the hybridisation and control research. This chapter outlines the manufacture of desktop models, including design upgrades.

Chapter Five:

This chapter provides a full understanding of the 3D SKM kinematics, as well as the workspace and singularities of the chosen robotic platform.

Chapter Six:

Chapter six outlines the collaboration and hybrid platform. This chapter dove into the hybrid kinematics which includes PKM as well as the possible working envelope the mounting pattern of the individual robotic platforms could achieve when coupled together into a single hybrid kinematic manipulator.

Chapter Seven:

Investigation into the software employed to make such a hybrid kinematic manipulator operate. This involves the integration of several control and programming methods into one cohesive system.

Chapter Eight:

Testing and experimentation was the focus of how well the research has been performed. This chapter outlines what has been achieved and what is possible as individual low DOF serial manipulators as well as the combined hybrid mechanism.

Chapter Nine:

This chapter discusses the findings from the research.

Chapter Ten:

The conclusion to the research.

Appendixes:

All raw data, code and testing sequences outlined as reference to the preceding chapters are made available within the Appendix A to F.

1.6 Introduction Chapter Summary

The first chapter outlines the research, including the research question to be answered; as well as the motivation for the research. The chapter outlines the aims and objectives involved with answering the research question.

The chapter outlines the methodology involved in achieving the aims and objectives and is accompanied by the outlines of the remainder of the chapters to follow in the dissertation.

2. LITERATURE REVIEW

2.1 Literature Review Introduction

Industry 4.0 is defined by the following definition, “a collective term for technologies and concepts of value chain organisation which draws together Cyber-Physical Systems, the Internet of Things (IoT), and the Internet of Services” [15]. Essentially Industry 4.0 has developed to become the factory of the future, or “smart factory”, in which the major operations are automated, with the use of Cyber-Physical Systems, and controlled through the Internet of Things [16] [17].

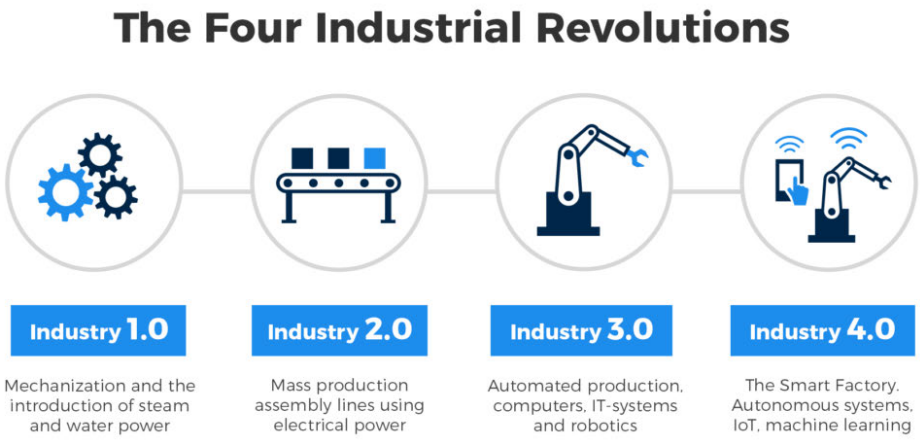

Figure 3: The four industrial revolutions [18].

The factory of the future, or smart factory, has developed with several driving factors, including the ability to have more flexible manufacturing, to be more adaptable and efficient in space requirements, time and production rate [19]. These driving factors have allowed manufacturing to advance beyond what was previously achievable before the introduction of automation.

Autonomous industrial robots are the major driving factor towards the Industry 4.0. An industrial robot, as defined by Robotics Industries Association (RIA), is *"a reprogrammable, multifunctional manipulator designed to move material, parts, tools, or special devices through variable programmed motions for the performance of a variety of tasks"* [20] [21].

There are multitudes of commercially available industrial robots, each with unique geometries and applications. However, they can generally be classified as either a serial, or a parallel mechanism. A combination of a serial and parallel mechanism may be considered a hybrid mechanism. Hybrid configurations, although not a new concept, do not have nearly as much research and development behind it, when compared to its serial and parallel counterparts.

It is known from the extensive research and development previously conducted on the different mechanisms that each geometric configuration has its accompanying advantages, as well as its

disadvantages. A graph illustrated in Figure 4: Overview of industrial robots [21]. illustrates the relationship between the common types of industrial manipulators, comparing the flexibility to the dynamic response properties.

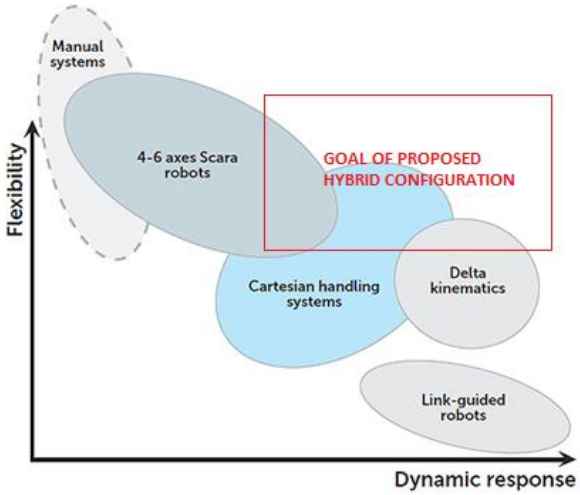

Figure 4: Overview of industrial robots [21].

The flexibility of a robotic manipulator is its ability to achieve a large workspace; and the ability to change the orientation of the end-effector within that workspace. This means that the end-effector can achieve complex working trajectories, either to perform an operation on a complex shaped part, or to manoeuvre around obstacles as necessary.

The dynamic response of an industrial manipulator is linked to the ability of the mechanism to move around the achievable workspace in a rapid manner, whilst being able to overcome the inertial forces involved with moving a mass at speed. The dynamic response capabilities of a manipulator either allow it or exclude it from being able to perform certain tasks accurately and repeatedly.

Serial robot configurations, such as the 4-6 axes Selective Compliance Articulated Robot Arm (SCARA), have great flexibility at the expense of dynamic response. These in comparison to the parallel configuration, such as the Delta, have great dynamic response; however, have limited flexibility.

The research outlined in this report was aimed at bridging the gap between the serial and parallel configurations, with the goal of achieving a mechanism that exhibits a high degree of flexibility, as well as high dynamic response. The goal of the proposed hybrid mechanism is illustrated Figure 4: Overview of industrial robots [21].

In order to achieve the desired output from the hybrid mechanism to be designed; intensive investigation into the current state of the art of serial and parallel industrial robots must be conducted.

Factors to consider when selecting an industrial robot: [22] [23]

- Load – weight and shape
- Orientation
- Degrees of Freedom - DOF
- Speed & Travel
- Actuation & Control
- Working environment

- Stiffness
- Inertia
- Backlash
- Singularities
- Vibrations
- Accuracy & Repeatability

2.2 A Review of Industrial Robot Application

In the modern manufacturing currently being experienced, several duties and operations have been tasked to robotic counterparts. A robot is made use of if the task is dirty, dull, dangerous or difficult to perform. Occasionally some manufacturing procedures are implemented via industrial robots; however these tasks are limited to procedures that do not require a large amount of rigidity [24] [25].

Some of the current applications of industrial robots are materials handling, processing operations, assembly procedures, as well as perform quality control inspection.

Figure 5: Industrial automation [26].

From Figure 5: Industrial automation [26]. there are several operations and tasks being performed, by both specialised CNC machines as well as industrial robots. The machines labelled A (i-iii) are examples of specialised CNC machines, whereas the mechanisms labelled B (i-iv) are examples of industrial robots. All of the industrial robots depicted are that of serial configurations, as most industrial robots are serial for the advantage of their large and flexible workspace, but at the cost of stiffness and accuracy [25].

Ultimately, the factory of the future would consist of highly flexible mechanisms such as the articulated industrial robots, whilst exhibiting the rigidity and accuracy of the specialised CNC machines. This would allow for all operations and tasks to be performed by the same robot. At the moment, this is not intensively implemented within industry due to the fact that achieving a large amount of articulation, coupled with suitable rigidity is expensive to implement within a single architecture [27] [28].

2.3 A Brief Review of Serial Mechanisms

A serial robotic arm is such that each node or joint is connected to the previous in a sequential manner. This means the system is a linear chain of joints, anatomically representative of a human arm. Serial mechanisms can take on many different configurations depending on the required outputs of each task. For example, a 2R or RR mechanism is one in which there are two revolute joints connected sequentially [29].

Serial robotic manipulators have been the focus of research for many years and hence there is a large amount of information available. Therefore, there will not be a large focus on defining all the characteristics of already well documented serial manipulators, rather a brief outline of some of the most common architectures will be mentioned for reference.

The cartesian or gantry configuration makes use of three perpendicular axis, that allow linear translational movement in 3 DOF. This configuration can be referred to as a 3P or PPP system, as it contains 3 prismatic joints. The cartesian configuration is very rigid due to the linear axis being supported at both ends. This allows for the movement of heavy loads with a good degree of accuracy and repeatability. The cartesian configuration requires the largest surface area for a given workspace as it requires linear guiding surfaces. These guides need to be maintained to ensure fluid movement [23]. A gantry configuration is the same as a cartesian configuration, with the X and Y-axes elevated. In a factory, a gantry configuration allows for access to multiple workstations due to the overhead clearance.

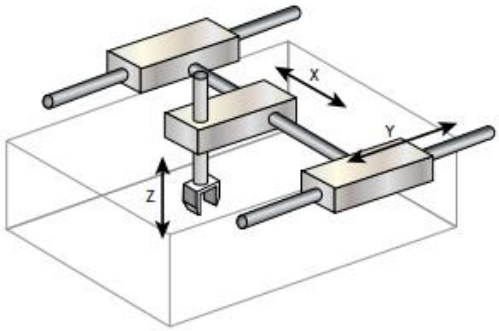

Figure 6: Cartesian configuration [30].

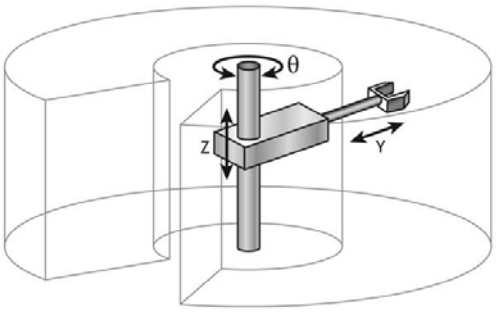

Figure 7: Cylindrical configuration [30].

By replacing the first prismatic joint in the cartesian configuration to a rotational joint one is able to achieve a cylindrical coordinate robot, or a RPP mechanism [31]. A cylindrical mechanism has the advantage of being able to perform a full circular operation about its base; however, it cannot reach above its own height.

A spherical mechanism has two revolute joints and is therefore considered to be a RRP mechanism. The spherical manipulator has the advantage over a cylindrical mechanism in that it can reach higher than its own height.

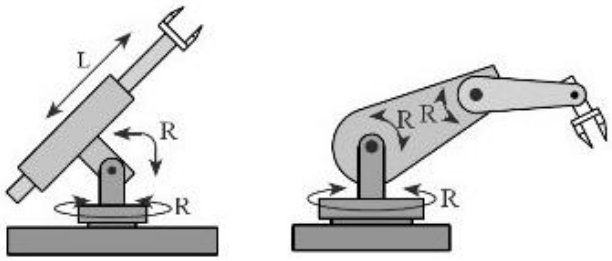

Figure 8: Spherical configuration [32].

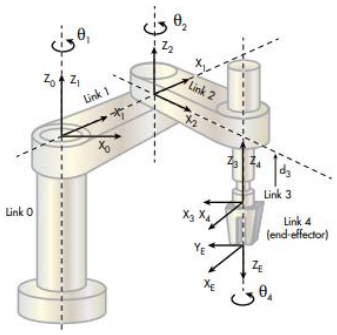

Figure 9: SCARA configuration [30].

SCARA or Selective Compliance Articulated Robot Arm refers to a class of configurations of robots that was devised for assembly work, specifically high speed pick and place procedures [33]. Unlike the cartesian configuration, in which there are guide rails that create the working envelope within their boundaries, the SCARA robot configuration makes use of a single central pedestal that allows rotational movement, thus creating the working envelope.

The SCARA configuration achieves movement in the X-Y plane, however, has either very little, or no freedom in the Z-axis. The design of the SCARA configuration means that there is a bending moment on the joints; therefore, require robust bearings and high torque motors. A SCARA configuration can also be referred to as a 2R in horizontal and 1P in vertical, or an RRP mechanism [31]. The kinematics of such a configuration are more complex than that of the Cartesian configuration, however the speed is greatly increased for the same accuracy and repeatability [33].

A robot is fully articulated if each of the joints are revolute. If there are six joints that are revolute, an articulated configuration can then be referred to as a 6R system. Articulated robots make use of a central pedestal like that of the SCARA configuration. A 6 DOF articulated configuration is the robotic analogue of a human arm. This configuration has the most flexibility; however has the most complicated kinematic model [33].

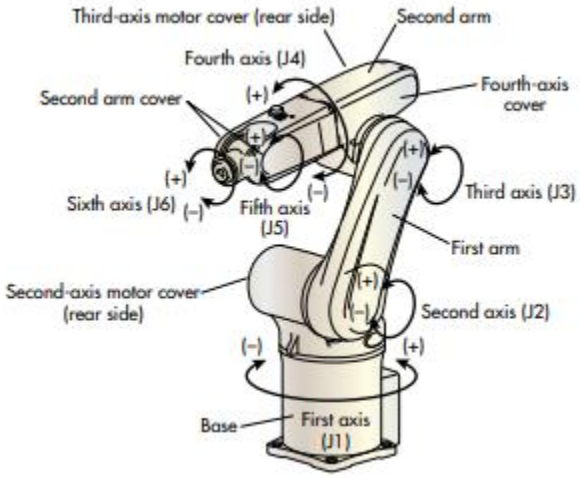

Figure 10: Articulated configuration [30].

Articulated robots are primarily used for complex processing and assembly operations due to their great flexibility. However, in order to achieve a high level of accuracy and repeatability, great insight into the inertia, joint stiffness and bending moments are required. These factors can cause non-linear movements

of the linkages, as well as the compounding of errors though the serial linkages, and therefore close attention must be placed on these parameters in order to optimise productivity [25] [34].

2.4 A Brief Review of Parallel Mechanisms

Unlike serial configurations, parallel configurations have their linkages connected in a parallel orientation with the base and end-effector joined via multiple links. Although there are a great number of geometric variants of parallel mechanisms, they are all similar in the fact that two or more parallel linkages, or arms, which span from a common base to a common platform, control their end effector [29].

Parallel kinematic manipulators have commanded a firm position in research due to their high theoretical dynamic potential [35]. A parallel configuration operates within a limited workspace, significantly smaller than that if a serial configuration, however, the parallel configurations exhibit high rigidity and accuracy when compared to that of serial configurations. For this reason, parallel configurations are more suited to high load and high-speed applications. Parallel kinematic systems can achieve high accuracy due to the closed kinematic loops and no accumulation of errors through the joints. However, careful consideration of singularities for parallel configurations must be conducted [25, 36].

There are in excess of 200 different PKM architectures currently. According to *Carricato* and *Parenti-Castelli,* Parallel Kinematic Mechanisms or PKM's may be classed as Mixed (MPM), Spherical (SPM) and Translational (TPM) [37] [38].

Gough and *Whitehall* in 1962 and then *Steward* in 1965 were the first to design and investigate the opportunities surrounding parallel mechanisms [37]. This Gough-Steward Platform/Hexapod architecture consists of a fixed base that have six legs connected via universal joints on the base and spherical joints on the end-effector platform. This mechanism can be considered to be a 6-UPS system [39]. However it is also possible to achieve a 6-SPS system [40]. These are illustrated in Figure 11: 6-UPS and Figure 12: 6-SPS.

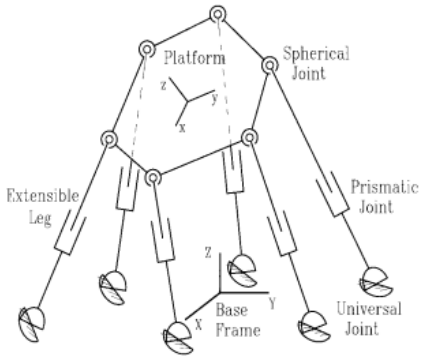

Figure 11: 6-UPS [40].

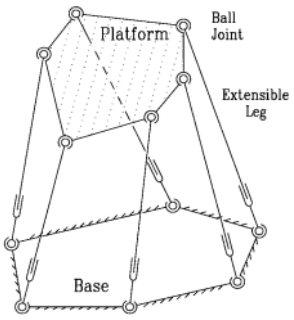

Figure 12: 6-SPS [40].

Both the 6-UPS as well as the 6-SPS have 6 DOF and are both actuated by six prismatic joints. However, the 6-SPS configuration exhibits six passive DOF relating to the rotation of each leg [40].

A Stewart platform, as it is commonly referred to, has very high rigidity and payload capabilities, however has a limited workspace and complicated forward kinematics [39]. *Hopkins* and *Williams* designed a variant

of the Stewart Platform such that it has a 6-PSU model. This configuration allows for the active prismatic joints to be actuated from the base allowing for better inertial characteristics [41].

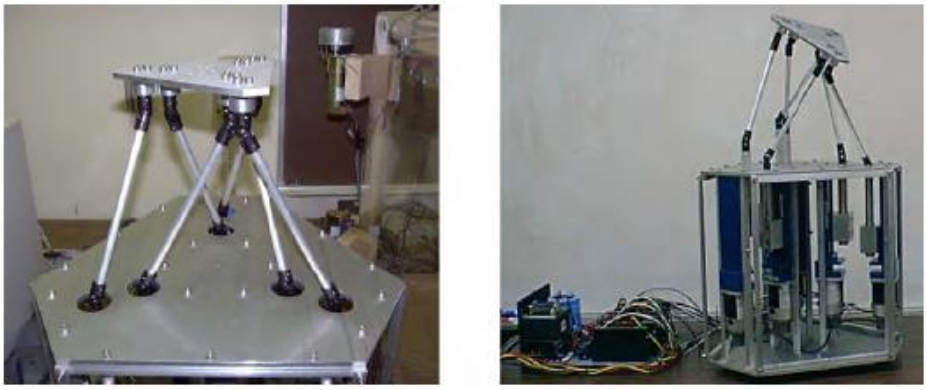

Figure 13: 6-PSU Platform [41].

Unlike that of the six legged 6 DOF Steward Platform, a delta robot has three legs and can achieve 3 DOF, or four legs to achieve 4-DOF. The three legs allow for the end-effector to be restricted to 3 translational movements in the X, Y and Z Cartesian axis. This movement is actuated by rotational joints on the base platform, and therefore can be considered a 3-RPR system. Delta configurations are considered to be one of the most famous translational parallel manipulators, TPM [42].

The delta configuration can be achieved via several different combinations of joints and actuation methods. Several of these combinations are illustrated Figure 14: 3 DOF delta parallel planar robots [38].

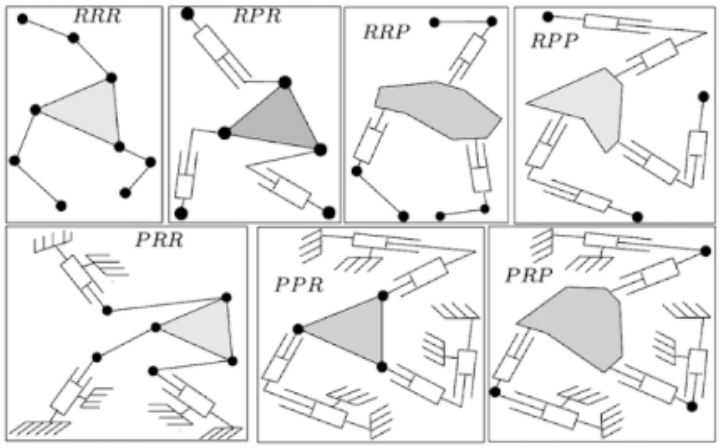

Figure 14: 3 DOF delta parallel planar robots [38].

One of the most well-known delta robots is the Flex Picker developed and produced by ABB Robotics. This robot has been extensively used in Pick-and-Place movements due to its high-speed capabilities and rigid design [39]. The design of the Flexpicker is a 3-RRR system.

The TORX achieves the same end-effector movements as the Flex Picker however achieves it via different linear actuation. It can be observed from

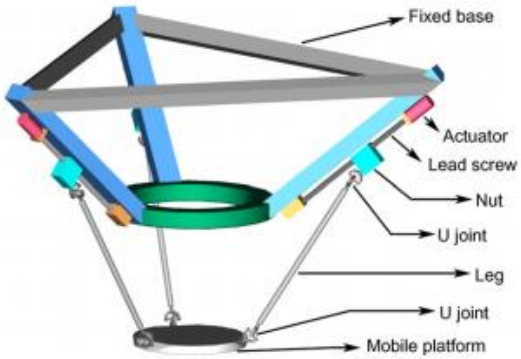

Figure 16: TORX 3-PUU PKM [44]. that the TORX uses prismatic actuation compared to revolute actuation in the Flex Picker.

Figure 15: ABB Flex Picker [43].

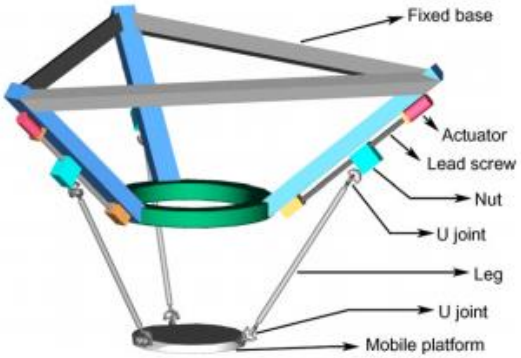

Figure 16: TORX 3-PUU PKM [44].

A modified version of the TORX was introduced by *Righettini* such that constant orientation of the end-effector was maintained. The modified TORX achieves the constant orientation due to the 3-PSS parallelograms unlike the 3-PUU parallelograms of the TORX [39].

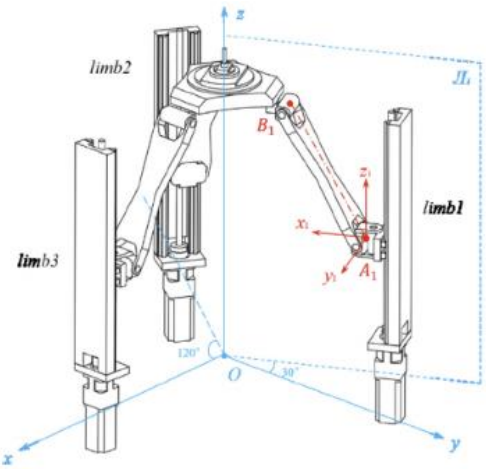

Figure 17: 3-PSS [45].

2.5 A Brief Review of Hybrid Mechanisms

There are several hybrid kinematic mechanisms in industry due to their combined serial and parallel qualities [46].

The 3-DOF Tricept consist of three UPS limbs used for actuation, a passive UP limb for guiding the end-effector, and a 2-DOF rotating head [47] [48]. The tricept is a 5 DOF machine that exhibits a robust design which combines high stiffness and force handling, together with high flexibility [49].

A variation to the Tricept, the TriVariant, was introduced in which the passive UP limb was adapted to be an active limb, hence achieving the same DOF as the Tricept however has fewer components [50]. The Tricept and TriVariant both exhibit high rigidity and can be used for several manufacturing applications.

Figure 18: 3-UPS&UP Tricept [48].

Figure 19: 2-UPS&UP TriVariant [48].

The majority of PKM mechanisms exhibit a symmetrical design such that the Jacobian matrix is homogenous. This allows for pure translational or pure rotational DOF, and therefore, ease of analysis and optimisation [51].

The Exechon PKM has an asymmetrical design and has a mixed translational/rotational DOF. This design exhibits non-homogeneity within the Jacobian matrix [51].

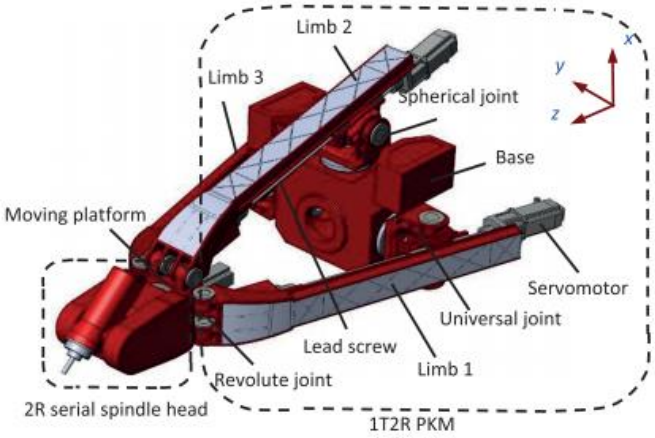

Figure 20: Exechon [52].

It can be observed that much of the hybrid kinematic platforms take the orientation of a regular PKM with serial aspects. However, it is also possible to incorporate parallel theory into a serial configuration via the use of four-link mechanisms, such as those present in quasi-serial architectures. This essentially creates a closed loop kinematic parallelogram within the serial arm. This closed loop kinematic parallelogram allow for increased dynamic properties of the mechanism by relocating some of the mass, and hence decreasing inertial and stiffness effects [53] [54] [55].

Within industry, this concept has been utilised for multiple palletising robot designs. Several variations from the major industrial robot manufacturers are currently available. Examples of these are described as follows.

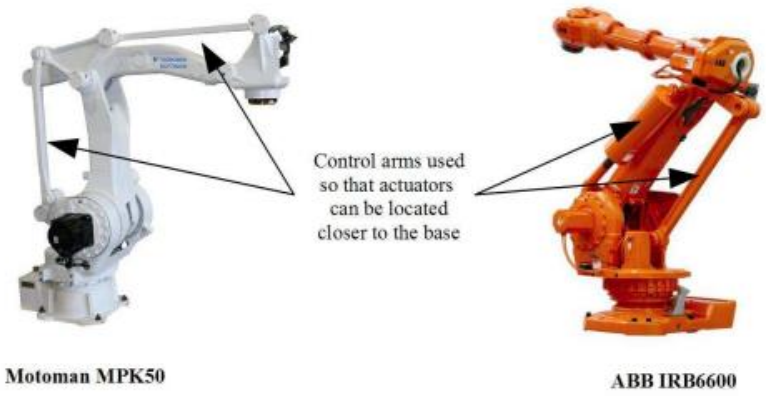

Figure 21: Quasi-Serial examples [53].

A quasi-serial manipulator can have one or two closed loop kinematic parallelograms within their geometry; however, each closed loop kinematic parallelogram reduces the overall degree of freedom by one. The FANUC M-410iB/140H and the Motoman MPK50 have two closed loop kinematic parallelograms and hence have 4 degrees of freedom [56].

The ABB IRB6600 has one closed loop kinematic parallelogram and has an articulated wrist; hence it has 5 or 6 degrees of freedom. Theoretically, one could put an articulated wrist onto the FANUC M-410iB/140H and Motoman MPK50 in order to get 5 degrees of freedom.

2.6 A Review of Collaborative and Combined Platforms:

There have been few attempts by researchers in the past two decades to produce a platform that is a true hybrid – being a collaboration and combination of several other robotic manipulators into a single unit that is able to have added characteristics otherwise unavailable to the individual manipulators.

The most notable attempts are outlined as follows:

2.6.1 Hybrid (parallel-serial) Robot Manipulator

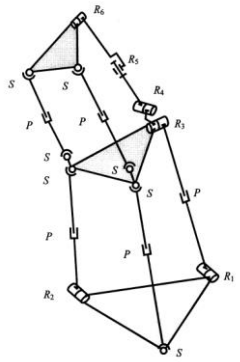

Figure 22: Hybrid manipulator by Tanio K. Tanev [57].

Here we have illustrated *Tanevs'* [57] approach to producing a hybrid platform that takes a serial form but consists of multiple parallel mechanism connected serially. This is an interesting approach as the combination of the two 3 DOF parallel mechanisms into a serial chain, according to his research allowed for 6 DOF to become available to the combined mechanism.

2.6.2 Collaborative Welding Platform

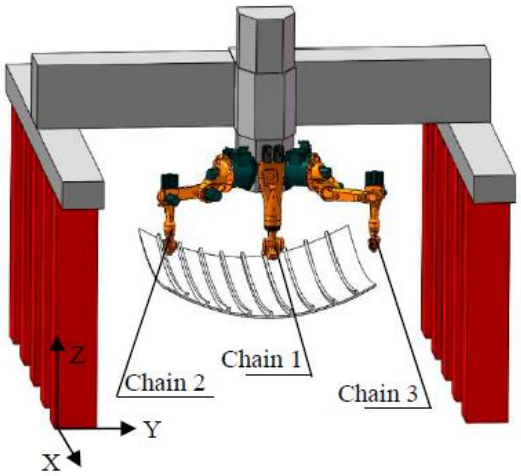

Figure 23: Liu et.al collaborative welding platform [58].

Liu et.al [58] proposed a robotic manipulator that has cartesian and serial combinations to its architecture. There are multiple serial industrial robotic manipulators connected to a single base that can move along an XYZ Cartesian gantry system.

Liu et.al [58, 59] papers focused on the kinematic analysis and trajectory planning of such a system for welding purposes, however the major notes were that a collaborative system such as this is a more energy and space efficient approach to conventional industrial robotic welding practices.

2.6.3 Transformable Serial to Parallel Manipulator for Machining

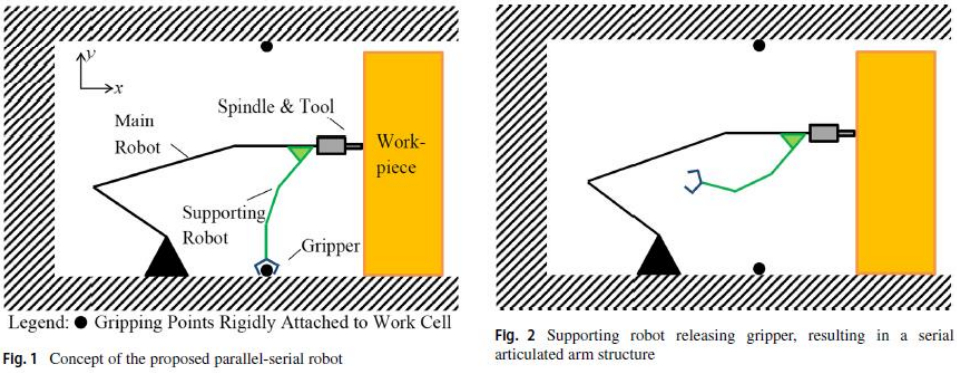

Figure 24: Lai et.al transforming serial/parallel mechanism for machining [60].

A concept that is more closely related to the research proposed in this dissertation, is that of *Lai et.al* [60] in which they are attempting to produce a reconfigurable robotic manipulator that is capable of performing machining operations due to the increased dexterity available when compared to traditional CNC machining centres.

As mentioned in the beginning of this chapter, serial kinematic manipulators have great flexibility but lack rigidity to perform machining. Conversely a parallel arrangement has sufficient rigidity to perform

machining but lacks the flexibility to articulate around complex tool paths. *Lai et.al* [60] have proposed a serial kinematic manipulator that is able to grip physical points within the workspace and hence convert itself into a form of parallel mechanism, in order to perform machining operations. The paper outlines that the stiffness characteristics increased, and the overall workspace available was far greater than if a regular parallel mechanism was used.

2.6.4 Multi-Robot Collaboration on Single Task

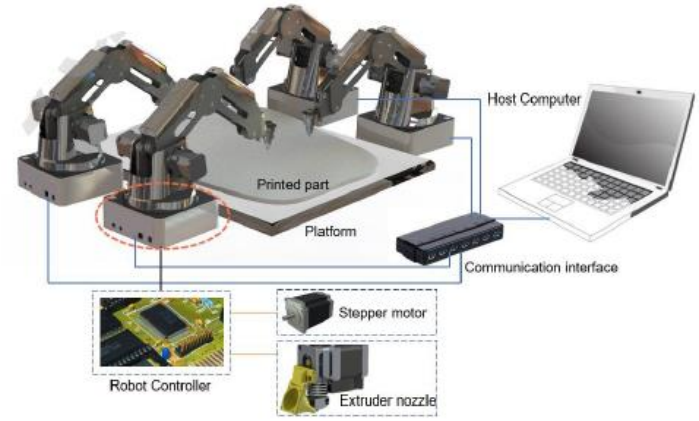

Figure 25: Collaborative serial kinematic robots 3D printing a single item [61].

Shen et.al [61] introduce a collaborate set of serial manipulators working on the same task simultaneously – in their case, an additive manufacturing or 3D printing task. This collaborative approach allowed the working envelope available to be drastically increased, and therefore the component to be produced could be of much greater size when compared to standard 3D printers' construction.

Although this is not a hybridized serial parallel mechanism, the collaborative aspect associated with this research outlines the potential for the ability to have multiple serial kinematic manipulators work collaboratively within the same workspace.

2.6.5 CoBots

Alternative to the previously mentioned hybridization attempts, there has been a large focus on recent research into cobots, or collaborative robots. These cobots usually take the form of a humanoid structure, in which the two individual arms operate as serial mechanisms, but within a combined workspace; with the ability to move workpieces between one another. Little research has been performed with the combination of the two serial arms into a single hybrid parallel manipulator.

Figure 26: YuMi Cobot [62].

Afsari et.al [62] in the paper "*Applications of collaborative industrial robots in building construction*" discuss the introduction of cobots to industry. These collaborative serial kinematic chains are generally coupled to a common base (torso) and are designed to be able to perform tasks like a human on a production line. Suited for high articulation and dexterity, however lack the strength to perform tasks greater than small component inspection or assembly [62].

These cobots generally run from a single controller unit, which allows the kinematic control to perform collision free movement of both arms simultaneously.

A large focus of cobots is the integration within the human environment in industry. In the past robots were confined to an enclosed workspace in which a human was not permitted to enter during operation. The cobots have been designed to have smaller inertial forces as well as methods to reduce force on a human if collision occurs. Baxter cobot have springs within his limbs to reduce forces [63].

2.6.6 Humanoid Robots

Alternatively, research has been performed in a non-industrial application of humanoid robotic systems. They do take into consideration the hybridization of serial and parallel mechanisms working collaboratively, however there is no focus on these systems working as a single combined mechanism.

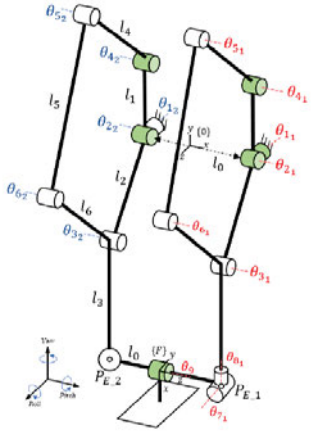

Figure 27: Schematic of a humanoid leg that consists of nested parallelograms within a serial configuration [64].

A key note from *Kumar et.al* [65] and *Gim et.al* [64] is the identification of the added benefits of having nested parallelograms within a serial structure, illustrated in Figure 27, in the same way a palatizing robot has, which was outlined previously. This consideration concurs with the direction this research is taking in the attempt of pure hybridization.

2.6.7 Combined Systems

The closest to a true hybrid system, as this research proposed, is the following combined system that was introduced and examined by *Montemayor et.al* [66], however the focus of the paper is in the combined carrying capabilities of two independent serial manipulators working in tandem.

This has been researched quite extensively in the 1990s, notably by *Sugar* and *Kumar* in which they present multiple papers focused on the control of this collaboration between two robots. They focus on a leader follower approach between the two individual arms, either via trajectory plan with known geometry, or via constant force control [67] [68]. This combination is illustrated in Figure 28.

Although this is the closest, we have discovered to multiple robots conducting themselves in a hybrid manner, they are still individual robots. There is no parallel kinematics taking place within the control structure.

This research has been aimed to produce a platform that is able to work via serial kinematics for the individual robots, but then could switch to a unified parallel kinematic set up in which the individuals are part of the whole. This would remove the need to have a leader follower arrangement for hybrid manipulation.

Figure 28: Multiple serial manipulators working together to lift [66].

2.7 Literature Review Chapter Summary

This chapter outlines the current conventions and state of the art within industrial robots currently in place within industry.

Beginning with the introduction to what industrial robots are, and how they are implemented throughout the manufacturing process. How they are implemented depends on the characteristics of that industrial robot. The characteristics of an industrial robot depend on several factors including the number of degrees of freedom and the associated movement available due to those DOF. The associated movement is dependent on the combinations of the different types of joints that link together the limbs or axes.

From this understanding, different styles of manipulators were explored. This includes the most popular industrial archetypes being a serial kinematic manipulator and a parallel kinematic manipulator. Several different well researched and implemented serial and parallel manipulators were explored in detail to establish the advantages and disadvantages of each type.

With this foundation, an investigation into the current methods of hybridization of serial parallel mechanisms was performed. This includes individual mechanisms that take aspects of serial and parallel into their design. The quasi-serial architecture displayed several desirable characteristics that made it a suitable candidate for further research and hybridization. It was found that the quasi-serial combination of closed loop nested parallelograms within a serial structure gave a combination of the advantages of both serial and parallel mechanism. The quasi-serial architecture displays a high level of rigidity and stiffness. It also possesses good dynamic properties due to the relocation of motors lower down away from the joints. This was a great low DOF serial kinematic manipulator to develop a hybridized platform.

The chapter then moved onto the investigation of the current methods in which researchers have attempted to combine several robots into a unified system, either via collaboration or via combination. The closest to the research performed within this dissertation is that of the transforming serial to parallel manipulator for machining; however, that is still an individual robot and not the combination of several into a single hybrid system when required.

3. RESEARCH CONCEPT

3.1 Research Concept Introduction

The proposed concept of the research was to create a combined hybrid platform, and control methodology, that would be the accumulation of several low DOF serial kinematic robotic arms that were already implemented in a smart factory, operating within the same workspace on individual tasks. The concept of combining robotic manipulators that were already implemented in a factory was derived from the original motivation of the research in which emerging countries such as the BRICS collaboration, whom already have a small automation footprint, but do not have a great enough GDP for small to medium sized businesses to outlay capital on the import of more dedicated manipulators to perform additional tasks.

The concept was such that the research could provide developing countries a method to enable them to increase the amount of automation available within their production, without the need to purchase additional industrial manipulators. Not only does this concept allow the emerging countries to become more competitive within the global manufacturing environment; but also allows the leading industrially automated Industry 4.0 smart factories to achieve more in a smaller floorspace. This is a factor that has become a large overhead cost for the European markets.

With this concept in mind the research was tending towards using a set of low degree of freedom robotic manipulators that are currently widely utilized and bring an increased level of flexibility and range of possible tasks.

3.2 Theoretical Advantages Due to Hybridization

There are several theoretical advantages that could be achieved through the addition of several serial manipulators into a combined hybrid platform. The main advantages are that of increased DOF, increased workspace, increased lifting potential, and reduced deflection/increased stiffness.

3.2.1 Increased Degrees of Freedom – DOF

The combination of the three translational freedoms, together with the three rotational freedoms gives a total of six degrees of freedom, or 6 DOF, as in Figure 29: Six degrees of freedom [69].

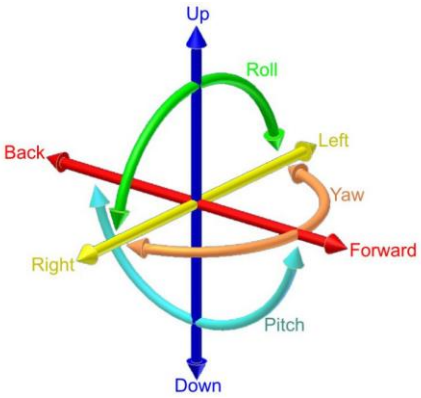

Figure 29: Six degrees of freedom [69].

It was proposed that the DOF available within the combined hybrid platform would increase with the addition of several low DOF serial manipulators. Therefore, the selection of the low DOF base serial platform in which the research would be conducted, was of importance to achieve a full 6 DOF system for the final combined hybrid platform.

The class of palletizing robots that are currently underutilised as 3 DOF pick and place mechanisms have large potential to be hybridized, due to their simple and cost-effective architecture. The 3 DOF present in most palletizing robots have a low complexity kinematic model.

3.2.2 Increased Rigidity / Decreased Deflection

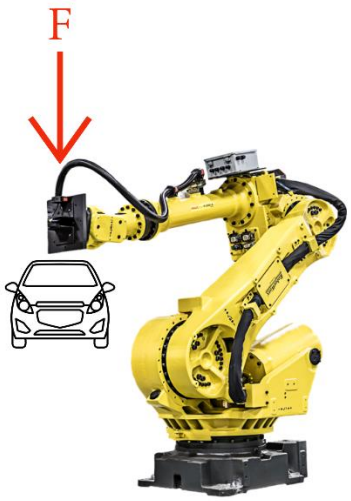

Figure 30: Deflection of single robot.

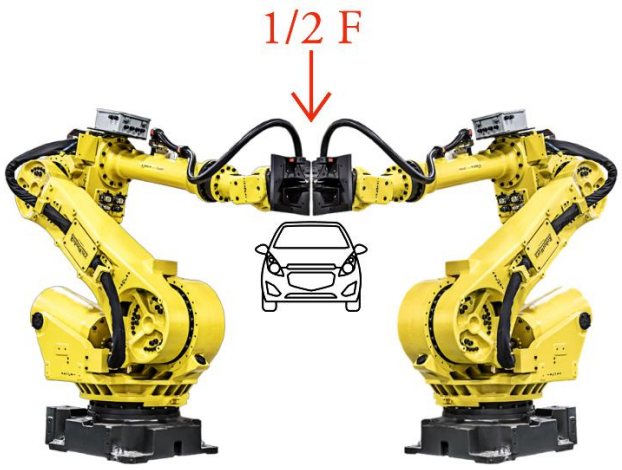

Figure 31: Deflection of hybrid robot.

A major advantage that could be achieved through the addition of several serial manipulators into a combined system is the increased rigidity, as illustrated in Figure 30 and Figure 31, that would become available through the reorientation of the manipulators from a serial configuration into a parallel configuration, as well as the increase in number of motors.

For the design, an important consideration was to choose revolute joints in a serial combination due to their high level of articulation and rigidity. Revolute joints allow for a large amount of torque to be translated through them, as well as could reduce backlash if the driving mechanism is well designed and

constructed. It can be noted that palletizing robots consist of 3 revolute joints, some of which are mounted in a co-linear arrangement, which in turn aids in the dynamic properties, and hence increase the torque that can be translated. A revolute joint, Figure 32, is a rotary joint that allows for one rotational DOF. Revolute joints come in many different geometric combinations [70]. The use of two revolute joints, connected orthogonally in series creates the same degrees of freedom as a universal joint [29].

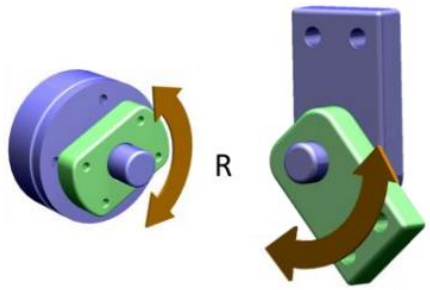

Figure 32: Revolute joints [29].

3.2.3 Increased Working Envelope

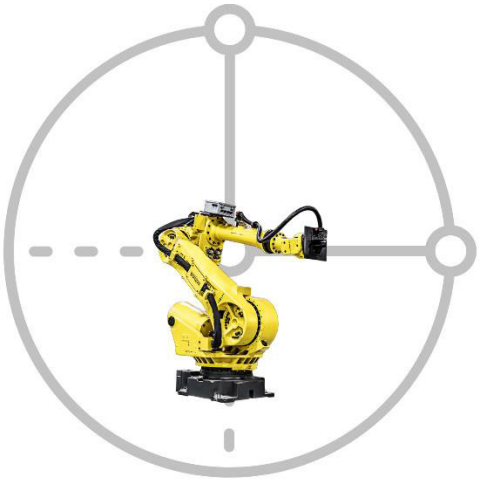

Figure 33: Workspace of single robot.

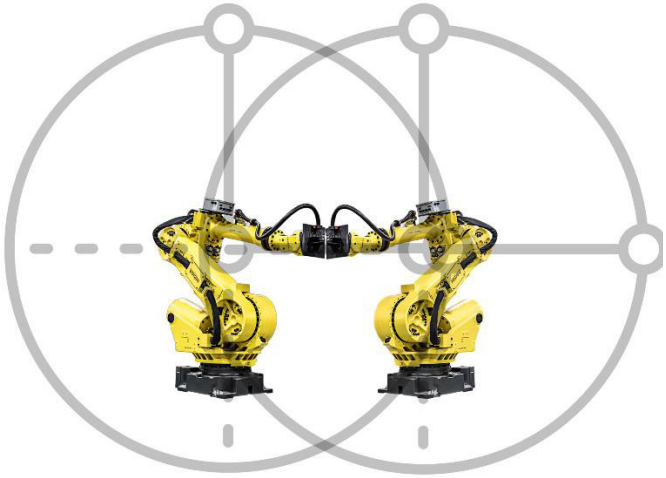

Figure 34: Workspace of hybrid robot.

The working envelope, Figure 33, is the area in which the robotic manipulator can achieve a pose that allows it to perform operations. The working envelope of each type of robotic configuration is determined by the combination of the joint types and their related degrees of freedom. The Articulated configuration (RRR) has three revolute joints and has a similar working envelope to that of the spherical configuration; however, the internal concentric sphere is smaller, hence a bigger working volume.

It should be noted that in general, serial kinematic manipulators have more articulation, and therefore a more flexible working envelope, when compared to a parallel kinematic manipulator. This means that ideally, the final hybrid mechanism of this research be more like that of a serial kinematic manipulator.

With the addition of several serial manipulators into one common working envelope allows the combined platform to extend the possible workspace by overlapping the individual workspaces, Figure 34. The palletizing industrial robots are considered to have a working envelope like that of the fully articulated RRR robot, as shown in Figure 35. By combining several of these into a collaborative common working environment, that working envelope can be extended for a wider variety of tasks. However, possible disadvantage of the combined system is that of a reduced working envelope, this is unfortunately the nature of a PKM.

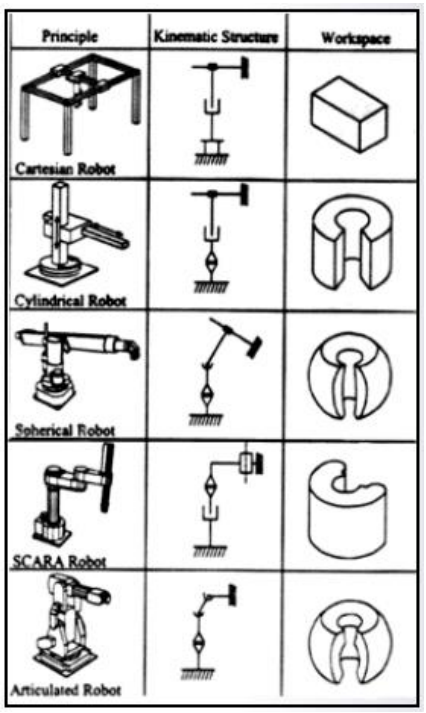

Figure 35: Working envelopes of serial configurations [71].

3.2.4 Increased Lifting Load

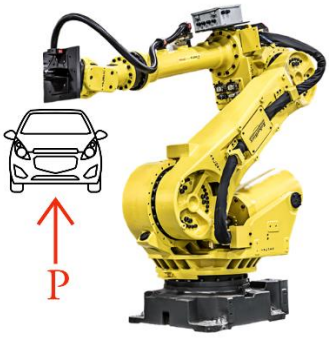

Figure 36: Lifting potential of single robot.

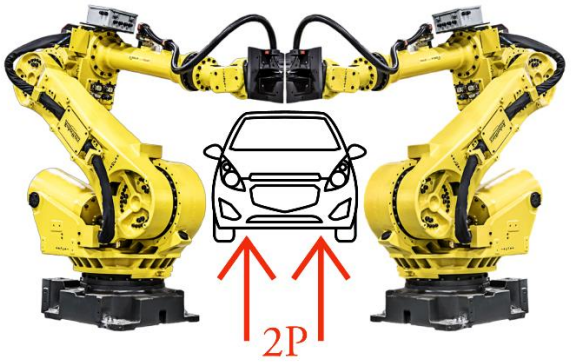

Figure 37: Lifting potential of hybrid robot.

Another major contribution that can be achieved through the addition of several serial robotic arms into a combined hybrid platform is the increase in force or lifting potential of the platform. Theoretically the

lifting force will be a multiple of the number of individual serial arms that are being combined, as illustrated in Figure 36 and Figure 37. If a single serial manipulator can lift x, then the addition of three serial arms into a combined hybrid platform should yield a lifting potential of 3x.

3.3 Research Concept Chapter Summary

The concept of the combined hybrid design was outlined, and options explored on the theoretical advantages of the concept. The literature review outlined that there is an abundance of robotic manipulators available within industry already. The design concept was to be able to achieve more potential from already implemented, but underutilized manipulators. The major increases in potential being the increase in DOF, lifting potential and workspace, while reducing the effects of deflection. Possible disadvantages of the research concept are that of the complex combination of individual SKM into the combined hybrid PKM. This would require further focus on the specific end-effectors that would need to be developed in order to maintain the accuracy and rigidity that the rest of the platform exhibits.

4. SELECTION AND CONSTRUCTION OF A SINGLE QUASI-SERIAL ARM

4.1 Selection and Construction Introduction

The literature has been trending toward the design and development of a 3 or 4-DOF hybrid platform, versus a 5 or 6-DOF machine. This is due to the inherent singularities coupled with unnecessarily complicated kinematics [46]. The research concept outlined the increased degrees of freedom available to a combination of several 3 or 4 DOF robotic manipulators.

In order to gain the most advantageous dynamic properties, it had been decided to combine several low DOF quasi-serial arms together. To prove the concept that multiple quasi-serial arms can work in tandem, several steps needed to be implemented and followed.

4.2 Quality Function Deployment

In order to create the most suitable product for market, designers and researchers utilize a Quality Function Deployment or QFD, in which engineering metrics are compared and weighted against the needs of the customer. These metrics can also be used to benchmark the design to the current market options of competitors [72]. A QFD was performed for this research and is available in Appendix A.

4.2.1 Relationship between Customer Requirements and Engineering Metrics

The driving factors the customer in emerging countries are focused on are that of the production adaptability, the costs involved with achieving the adaptability, the amount of actuator travel that can be

achieved and the overall precision that is available. These factors are all subject to the level of ease in which they can be implemented. The emerging countries have fewer skilled labourers available to them, and hence require a large amount of ease to achieve adaptability in order to compete with the more established automated production countries.

The engineering metrics that contain a relationship to the customer needs are as follows. The adaptability the customer requires is linked with the level of tooling and lifting requirements needed in order to perform the reconfiguration. The costs and precision directly relate to the level in which the manufacturing of parts and components has been undertaken. The material selection and machining tolerances effect the overall costs involved with production. The selection of the electronic system and high accuracy motors also directly relate to the costs involved.

The relationship of customer requirements and the engineering metrics have the strongest relationships in the aspect of adaptability of the hybrid platform. The second strongest relationships appear in the categories of the ease of use and the precision. Ease of use has 3 strong and 3 moderate relationships, whereas the high precision requirement has 3 strong and 2 moderate relationships.

The least strong relationships were the cost. This is mainly due to the consideration that the cost involved in the hybridized platform is not affected by the purchase of the individual robotic manipulators, but rather the purchase and implementation of the control system that would allow for the combination of existing manipulators. The major costs involved with the customers' requirements of high precision and joint travel are dependent on the existing robotic manipulator already present within the factory.

4.2.2 Correlations between Engineering Metrics

The correlations between the engineering metrics can help aid the design in a manner that outlines which metrics are most important and how they interact with the other outlined metrics. Some will have a strong impact on metrics, while others could have negative impacts. From the QFD performed, the engineering metrics of most value are that of the control user inputs, and the set-up time.

As mentioned, the major contribution of the research performed was focused on the ability to combine several already existing robotic manipulators into a new hybrid platform that is capable of more adaptability within the manufacturing environment. Therefore, the strong correlation between the customers desire for a user-friendly interface and the set-up time needed to achieve the hybrid platform is positive for the research.

To note, some negative correlations are that of the singularities and the range of motion available in the XYZ translation and the RPY rotations. Again, these factors are a direct function of the pre-existing robotic manipulator.

4.2.3 Importance Weighting and Difficulty of Implementation

The customers' requirements are weighted according to their importance. It was discovered for the emerging countries that a major weighting should be placed on the adaptability and cost of implementation. These were both out weighted by the ease of use, due to the lack of high skilled operators.

Similarly, the engineering metrics are weighted. It was noted that the most influential engineering metrics were that of the DOF and singularities, followed closely by the control interface and flexible setup.

The difficulty of implementation of the engineering metrics is that of the DOF, singularities and control interface. It should be noted that the control interface has influence over the DOF and singularities; and hence the control interface should be considered an aspect in which a large focus should be placed.

4.2.4 Target Specifications

The target specifications outlined in the QFD relate both to the industrial version of the research as well as the desktop model proposed to perform the research. Assuming the research will be implemented in an industrial environment; the most important specifications according to difficulty would be multiple configurations, DOF, singularities and the control interface.

For industrial purposes the multiple configurations and DOF can be a function of the control interface and its ability to accommodate more complex orientations and the associated kinematic models. The control system must accommodate a large motion range in 6 DOF, with accurate motor control, and reduce the singularities to a minimum.

4.2.5 Competitive Considerations

This research has been positioned such that there are no direct market competitors. However, inspiration can be drawn from similar approaches, such as the industrial CoBots. Furthermore, inspiration was taken from the literature, in which the design concept is compared to previous research, such as the PUMA combination outlined by *Montemayor et.al* [66], and the collaboration outlined by *Liu et.al* [58]. More importantly, competitive consideration was made for the transformable serial manipulator outlined by *Lai et.al* [60].

Although direct comparison is difficult with these examples, it is important to note that the design concept allows for greater adaptability with a lower cost to implement.

4.3 Selection of Quasi-Serial Arm

A design by Florin Tobler, Figure 38, accessible through Thingyverse.com under the Creative Commons Licence, was proposed as the initial design for consideration [73]. The design was that of a quasi-serial robot arm that had 4 degrees of freedom. The gripper can be considered the fourth degree of freedom. The arm had been designed to be a desktop model; however, it retains good stability and stiffness characteristics due to the quasi-serial architecture.

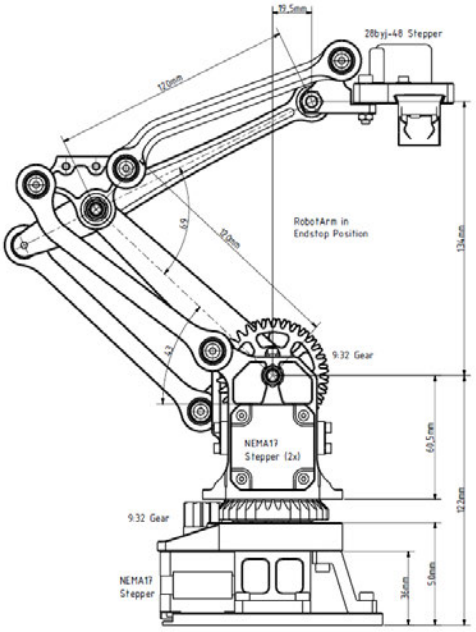

Figure 38: RobotArm by Florin Tobler [73].

4.4 Rapid Prototyping Components

Rapid prototyping is considered a method of creating physical models of 3D items via Computer Aided Drawing (CAD) packages and additive manufacturing procedures such as 3D printing. These methods have proven to be extremely timeous and cost effective, and therefore an ideal method of production for research purposes [74].

The robot arm designed by Florin Tobler had several mechanical components to be 3D printed. These components are illustrated in Figure 39: RobotArm 3D printed components. All of the components to be printed needed to have their print orientations considered with relation to the forces involved in each member.

An important consideration when 3D printing was that unlike standard manufacturing procedures, 3D printing relies on placing hundreds of similar layers upon each other. This leads to an inhomogeneous final product that is susceptible to delamination - process in which the fused layers separate from one another. This causes ultimate failure of the component.

Along with the orientation of the component when being printed; having a strong grasp of the print settings is advantageous. Table 1: 3D printing parameters [75]. outlines the print settings input into an open-source Graphical User Interface (GUI) called Cura 3.5.1 in order to slice the model for printing.

Table 1: 3D printing parameters [75].

PARAMETER	QUANTITY
Material	PLA+
Tensile breaking strength	57.8 MPa
Modulus of elasticity in flexure	2.3 GPa
Density	1.23-1.25 g/cm3
Layer Height	0.16 mm
Shells	4
Infill	Rectilinear
Infill %	60
Nozzle Temp	215 °C
Bed Temp	55 °C
Print Speed	50 mm/s

The printing was done on a Creality Ender 3 printer that is running on Crealitys' modified version of the open-source 3D printing software, RepRap Marlin.

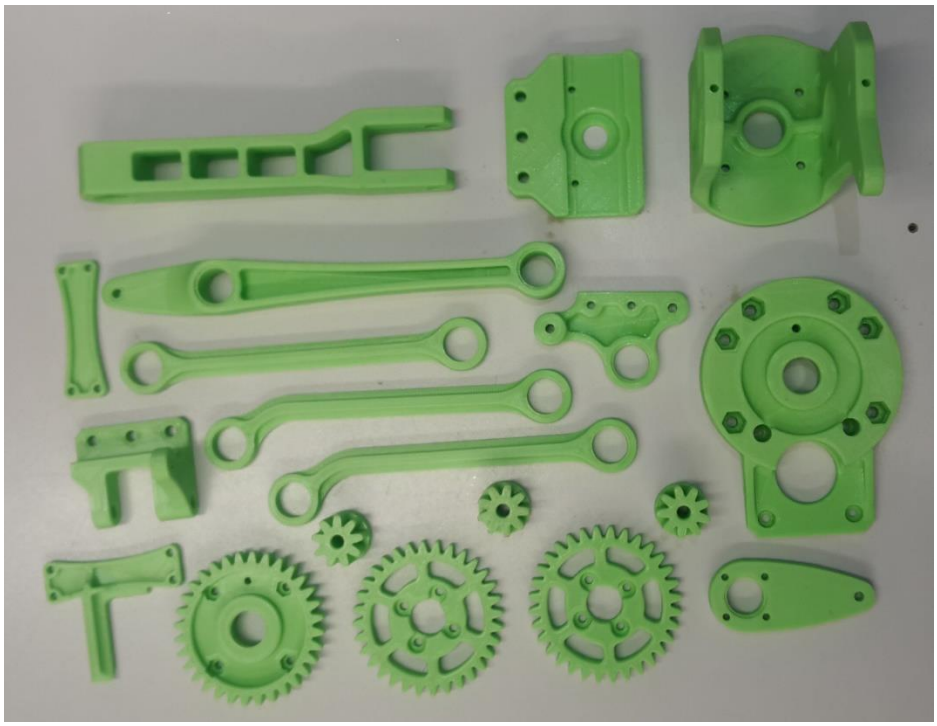

Figure 39: RobotArm 3D printed components.

4.5 Design Updates

The design proposed by Florin Tobler was a great starting point, however not enough optimisation had occurred in the initial design. In order to achieve greater success, further evaluation was performed.

Several items needed to be reconsidered from the original design. An initial issue was the control program that was non-operational. This meant that a new control program can be developed from first principals.

Further considerations found and implemented were as follows.

- The original RobotArm had no accommodation for limit switches to be mounted. Limit switches are a vital feedback loop required for the homing and initialization of the RobotArm in a production environment. Three limit switches needed to be incorporated into the body of the robot; and a way for each of them to be triggered at the maximum travel of the motor they represent.

- With the addition of limit switches, the cable management needed to be updated too.

- The electronics box needed to be updated to a more ergonomic design, which could also accommodate all the features and wiring.

- The end effector was redesigned for better articulation, due to reorientation and reduction in size and overall weight.

- The common mounting bracket was redesigned to accommodate the new end-effector as well as the control linkages. The main modification being that the new end effector accommodated a limit switch. This limit switch would be activated via the common end-effector in order to signal the control board that it has been coupled as a combined mechanism.

- A common end effector was then created with the intention of the robots being coupled.

A control program was developed sequentially as the functionality requirements increased. The program grew and progressed throughout the duration of the research; and therefore, will be investigated more thoroughly in Chapter 7.

Once these changes had been perfected on the initial robot, they were reproduced on two more RobotArms.

4.6 Electrical and Electronic Components

The following are the electrical and electronic components required for the movement and control of the quasi-serial robot arm.

- 3 NEMA 17 Stepper Motors

Stepper motors are some of the most versatile electric motors used within robotic systems. They are low cost compared to closed loop servo motors and can be controlled accurately via PWM. Thus, making them a great choice for the research.

- 1 Servo Motor

For the gripper to operate as a controlled lightweight system, the use of a single servo motor is the most suited for this application. The gripper however was not a major focus of this research.

- 1 Arduino Mega 2560 Microcontroller

Arduino, although not currently used in wide industrial applications, is a C++ based microcontroller that is affordable and robust enough to perform the control. The Arduino Mega 2560 has an AT660 control chip that runs on 16bit and communicated via serial USB. A powerful system used by many hobbyist controllers. Arduinos can be considered a non-industrial PLC.

The discoveries and coding applications can easily be transferred onto a less general, more robust control board for industrial integration.

- 1 RAMPS 1.4 Shield

A breakout board that has been designed to fit directly on top of the Arduino Mega 2560 microcontroller. The RAMPS board allows for the integration of several stepper motor as well as several servo motors. The RAMPS board can accommodate many inputs and outputs including limit switches, PWM, digital and analogue I/O pins. The RAMPS board also allows for several motor controller drivers to be coupled directly on top of it. This small form design allows for a compact and powerful control solution.

- 3 A4988 Stepper Motor Drivers

The A4988 stepper drivers couple directly to the RAMPS shield. They are responsible for converting and organising the electric pulses given from the control program into a form that can control the stepper motors. They can achieve speed and direction control.

- 3 Mechanical Limit Switches

As the main motors being implemented into this system was that of stepper motors, without the use of encoders, it is essential to have physical limit switches to perform vital homing and calibration procedures. Without a homing procedure, any industrial machine will have no starting reference from which to perform further kinematic calculations and relative movements.

This combination of components is essentially equivalent to that of a traditional RepRap 3D printer.

Table 2: Hardware Specifications [76].

ITEM	DISCRIPTION	SPECIFICATION
Stepper Motor	Frame Size	NEMA17
	Part No.	42BYGHW811
	Step Angle	1.8°

	Steps per Revolution	200
	Motor Length	48mm
	Voltage Rating	3.1V
	Current Rating	2.5A
	Phase Resistance	1.25 Ω
	Phase Inductance	1.8mH
	Holding Torque	4800g.cm
	Number of Lead Wires	4
	Rotor Inertia	68g.cm2
	Detent Torque	280g.cm
	Motor Weight	0.34kg
Stepper Motor Driver	Type	A4988
	Operating Voltage	8V to 35V
	Continuous Current Per Phase	– 1A (Max without Heat Sink) – 2A (Max with Heat Sink)
	Logic Voltage	3V to 5.5V
	Microstep Resolutions	Full; 1/2; 1/4; 1/8; 1/16
	Heat Sink	Included (With Adhesive Thermal Backing)
	Additional Features	– Overcurrent Protection – Under-Voltage Lockout – Automatic Chopping Control
	Dimensions	15 x 20mm
	Weight	1.3g
Servo Motor	Model	28BYJ-48
	Rated Voltage	5V DC
	Number of Phases	4
	Speed Variation Ratio	1/64
	Stride Angle	5.625°
	Frequency	100Hz
	DC Resistance	50ohms ±7%(25°C)
	Idle In-Traction Frequency	>600Hz
	Idle Out-Traction Frequency	>1000Hz
	In-Traction Torque	>34.3mN.m(120Hz)
	Self-Positioning Torque	>34.3mN.m
	Friction Torque	600-1200gf.cm
	Pull in Torque	300gf.cm
	Insulated Resistance	>10MΩ(500V)
	Insulated Electricity Power	600V AC / 1mA / 1s
	Insulation Grade	A
	Rise in Temperature	<40K (120Hz)
	Noise	<35dB (120Hz, No Load, 10cm)
Arduino Micro Controller	Microcontroller	ATmega2560
	Operating Voltage (Logic Level)	5V
	Input Voltage (Recommended)	7 to 12V
	Input Voltage (Limits)	6 to 20V
	Digital I/O Pins	54

	PWM Output Channels	15
	Analog Input Channels	12
	DC Current per I/O Pin	40mA
	DC Current for 3.3V Pin	50mA
	Flash Memory	256KB (8KB Reserved by Bootloader)
	SRAM	8KB
	EEPROM	4KB
	Clock Speed	16MHz
	LED_BUILTIN Pins	13
	Dimensions	101.52 x 53.3mm
	Weight	37g
Shield	RAMPS 1.4	
Limit Switch	Connections	Common / Normally Open / Normally Closed
	Switch Type	Mechanical Micro Limit Switch

4.7 Proposed Control

The proposed control hardware for this RobotArm was to use hobbyist Arduino microcontrollers along with some third-party shields. A shield is a purpose made PCB breakout board. In this case inspiration had been taken from the open-source 3D printing world, in which Arduino and RAMPS shield with additional motor controller shields.

Initial testing of code and its functionality was performed. However, the control code that was supplied with the RobotArm download files did not work correctly. In order to send commands to the Arduino control board – a second open-source program was used. Pronterface however, is designed as a G-code parser for Cartesian 3D printers. This meant that the kinematics of the robot was not being taken into consideration. Although the kinematics was not being considered in these preliminary movement tests, it did prove insightful to be able to toggle the RobotArm around manually.

In order to control the RobotArms, a modified version of Marlin, or similar, would need to be used. Alternatively, a custom control program would need to be written. This custom option seems more likely as the open-source Marlin control software does not accommodate the types of kinematics in question for this research.

4.8 Selection and Construction Chapter Summary

Through the QFD some important metrics and customer needs were compared. It was discovered that a large classification of underutilised robotic platforms is that of the palletizing robots. This class of manipulators have in the past only been used for generic pick and place operations in a XYZ translation. There is scope for this class of manipulator to be expanded upon to enable the emerging countries to perform an increased range of tasks within the manufacturing environment.

The major considerations discovered were that the customer requires a high level of precision at low cost, both monetary and time. The concept thus tends towards a control methodology that can expand the DOF, flexibility and rigidity of these palatizing robots.

An open-source quasi-serial robotic arm was proposed, and 3D printed as a desktop model for further investigation. The variables selected in order to print the model were outlined. The proposed control hardware solutions have been outlined and discussed.

The software solutions that could be applicable to this project were outlined and discussed. Several methods were selected but it was discovered that the most likely solution would be to develop a custom control algorithm from first principals.

From the investigations performed in this chapter, it was clear that the selection of the proposed RobotArm was a great foundation. The proof-of-concept aspect has been completed.

5. KINEMATICS AND MODELLING OF A SINGLE QUASI-SERIAL ARM

5.1 3D Inverse Kinematics of a RobotArm - Shifted from Origin

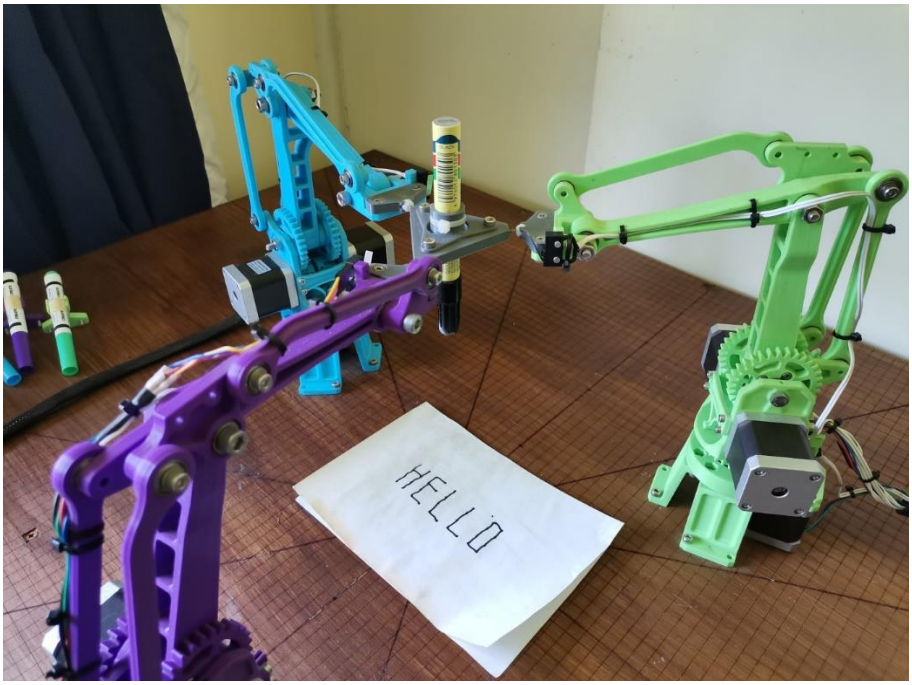

Figure 40: Combined RobotArms with marker pen.

The kinematic model has been derived using a graphical vector method, this method has been outlined in a paper published for the 2D inverse kinematics and workspace analysis [77].

There would ultimately be three robots that would have the same kinematic equations as follows. The inputs given vary between robots. I.e., theta11 (θ_{11}) is different to theta21 (θ_{21}) and theta31 (θ_{31}). As a

standard, the naming convention will be as follows: the variable, followed by a subscript. The first number of the subscript (θ_{n1} – n in this case) refers to the robot number.

$$m_n = radius\ from\ XYZ\ origin\ to\ the\ XYZ'origin.\ Given\ from\ mounting\ pattern.$$

m_n should be a standard value across the RobotArms.

$$\theta_{n1}\ (Theta1) = rotation\ of\ XYZ'origin\ from\ XYZ\ origin.\ Given\ from\ mounting\ pattern.$$

$$\theta_{nM}\ (ThetaM) = rotation\ of\ motor.\ \ Given\ from\ mounting\ pattern.$$

ThetaM refers to the rotation of the base of the RobotArm around the Z' axis. This is since the base does not complete a full 360-degree rotation. For this reason, the section that could not be achieved has been rotated out of the way, for optimal hybrid articulation.

$$\overrightarrow{m_n} = is\ the\ vector\ made\ up\ from\ m_n\ and\ \theta_{n1}$$

$$l_n = is\ the\ vector\ that\ makes\ up\ the\ EE\ offset.$$

$$\overrightarrow{t_n} = \begin{bmatrix} t_{nx} \\ t_{ny} \\ t_{nz} \end{bmatrix} is\ a\ vector\ of\ desired\ XYZ\ location\ from\ global\ origin \qquad \textit{Eq. 1}$$

For the robots to understand their position in space and motor orientation (ThetaM), during the robot start up, it initialises itself through a homing procedure. In this procedure the kinematics take into consideration the empirical home position and the rotations that have been placed on the robot arm during mounting. Refer to the figures below which illustrated the translation and rotations as individual operations. Each robot has gone through two rotations and a translation. A general case has been outlined.

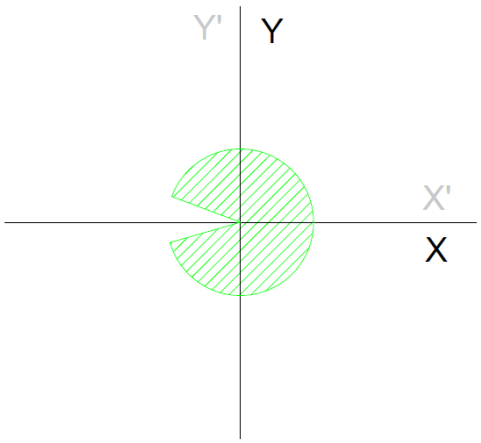

Figure 41: ThetaM origin.

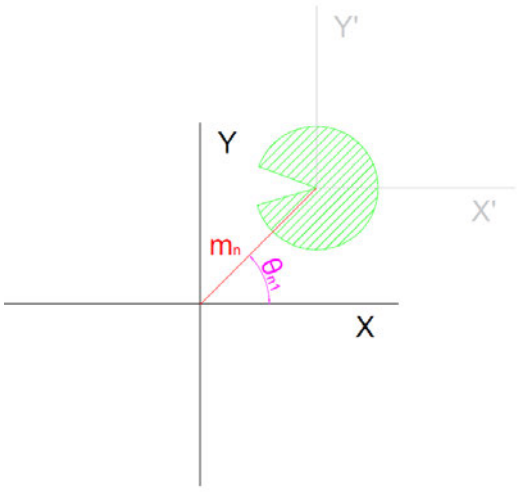

Figure 42: ThetaM translated by mn and theta1.

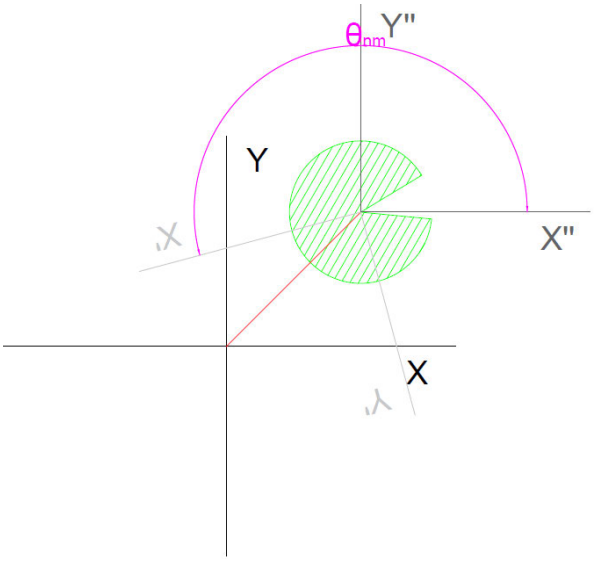

Figure 43: ThetaM rotated.

The position of home position of unrotated and un-displaced axis due to theta2max position i.e., homing

$$xinit = ((xHomeOrig + l) * cos(\theta_{n2MAX})) \quad \textit{Eq. 2}$$

$$yinit = \left((xHomeOrig + l) * \sin(\theta_{n2MAX})\right) \quad \textit{Eq. 3}$$

New home position due to displacement of vector m and rotation due to thetaM (motor rotation about Z)

$$x'' = (m * cos(\theta_{n1}) + xinit * cos(\theta_{nM}) - yinit * sin(\theta_{nM})) \quad \textit{Eq. 4}$$

$$y'' = (m * sin(\theta_{n1}) + (xinit * sin(\theta_{nM}) + yinit * cos(\theta_{nM})) \quad \textit{Eq. 5}$$

$$z'' = (zHomeOrig + q) \quad \textit{Eq. 6}$$

Where *q* is the z height from the mounting position to the first joint.

$xHomeOrig$ & $zHomeOrig$ were identified empirically from the physical robot arm.

The robot home position is now initialised, and it is ready to receive new coordinate positions.

In the X-Y Plane:

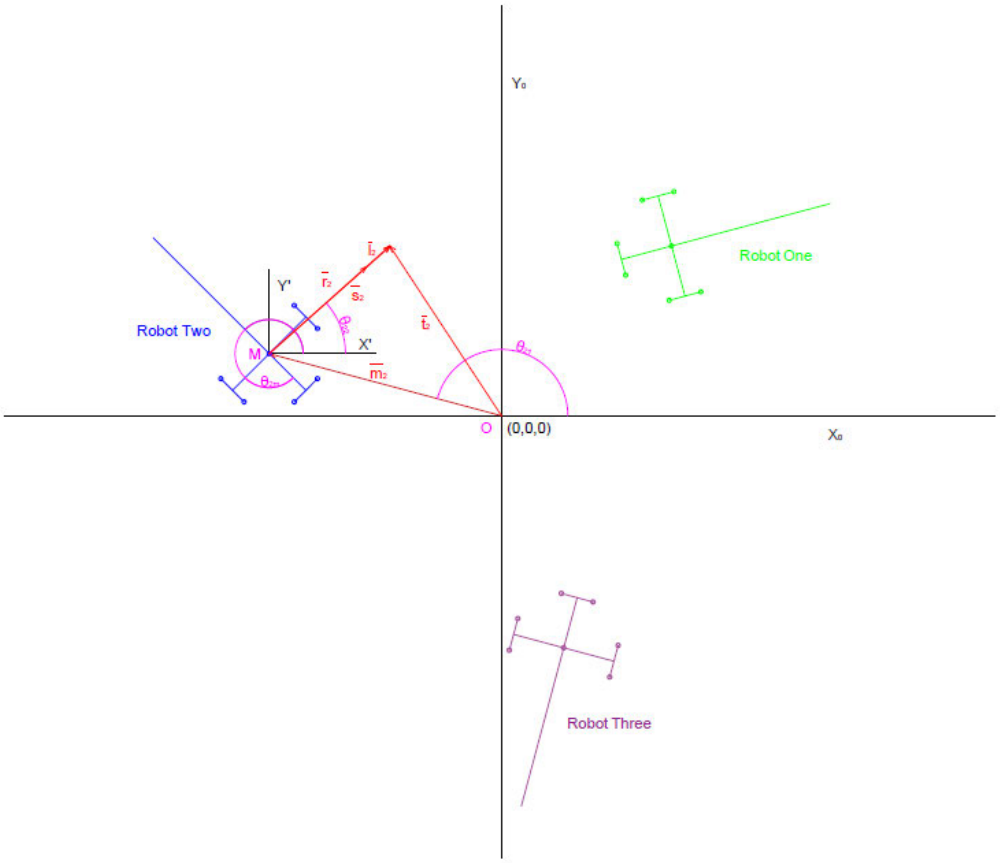

Figure 44: Collaborative Robots Kinematics: X-Y plane.

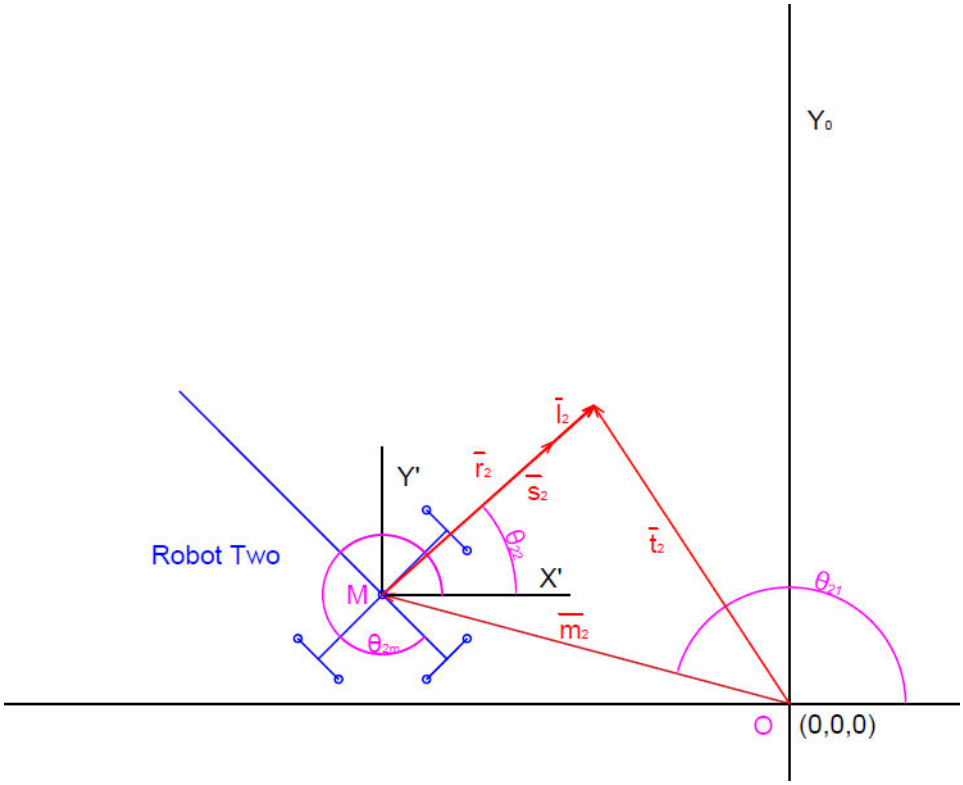

Figure 45: Collaborative Robots Kinematics: X-Y plane enlarged.

$$\bar{m}_n = \begin{bmatrix} m_{nx} \\ m_{ny} \\ m_{nz} \end{bmatrix} \quad \textit{Eq. 7}$$

$$\bar{m}_n = \begin{bmatrix} m_n * \cos(\theta_{n1}) \\ m_n * \sin(\theta_{n1}) \\ 0 \end{bmatrix} \quad \textit{Eq. 8}$$

$$\theta_{n2} = arctan\left(\frac{(t_{ny} - m_{ny)}}{(t_{nx} - m_{nx})}\right) \quad \textit{Eq. 9}$$

$$r_{nxy} - m_{ny} \quad \textit{Eq. 10}$$

$$\theta_{n1} = is\ given\ depending\ on\ mounting \quad \textit{Eq. 11}$$

$$\theta_{n1} = is\ given\ depending\ on\ mounting \quad \textit{Eq. 12}$$

$$r_{nxy} = \sqrt{(t_{nx} - m_{nx})^2 + (t_{ny} - m_{ny})^2} - l \quad \textit{Eq. 13}$$

In the XZ Plane:

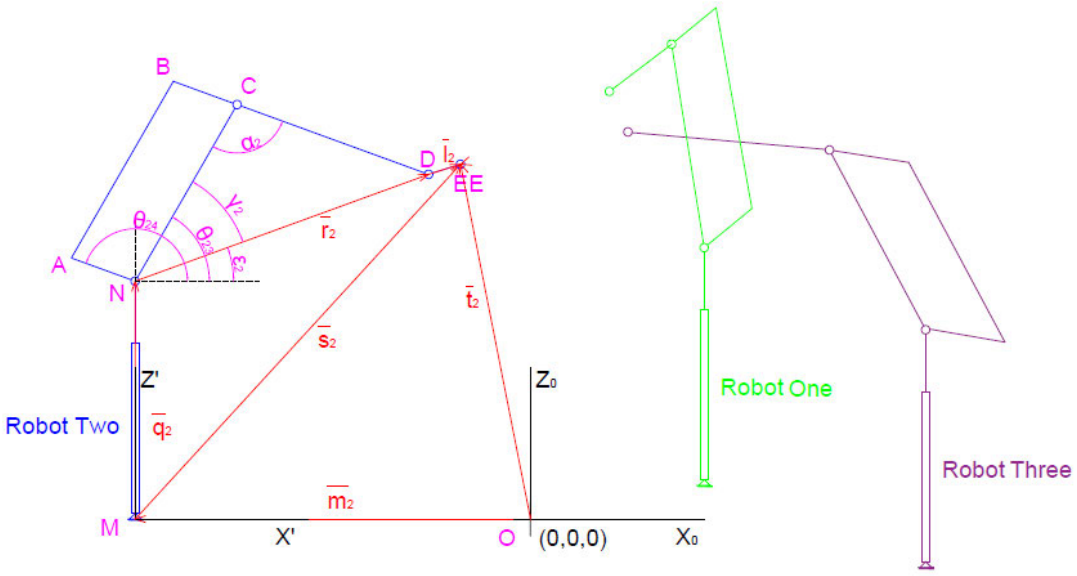

Figure 46: Collaborative Robot Kinematics: X-Z plane.

$$\varepsilon = arctan\left(\frac{(z_{n1} - q)}{r_{nxy}}\right) \quad \textit{Eq. 14}$$

$$r_{xz} = \sqrt{(r_{nxy})^2 + (z_{n1} - q)^2} \quad \textit{Eq. 15}$$

$$\gamma = arcos\left(\frac{{L_2}^2 - {L_1}^2 - {r_{xz}}^2}{-2 * L_1 * r_{xy}}\right) \quad \textit{Eq. 16}$$

$$\alpha = arcos\left(\frac{{r_{xz}}^2 - {L_1}^2 - {L_2}^2}{-2.L_1.L_2}\right) \qquad \textit{Eq. 17}$$

Finally:

$$\therefore \begin{Bmatrix} \theta_{n2} = \arctan\left(\frac{(t_{ny} - m_{ny)}}{(t_{nx} - m_{nx})}\right) \\ \theta_{n3} = \varepsilon + \gamma \\ \theta_{n4} = \theta_{n3} + \alpha \end{Bmatrix} \qquad \textit{Eq. 18}$$

Here they can operate freely as individuals with the ability of passing items between shared workspaces. For a combined hybrid kinematic system, each RobotArm must complete these IK and then in conjunction execute the move [78] [79].

5.2 Workspace Simulation – 3D Single RobotArm

The following plots were performed using Octave and a Monte Carlo randomization plot. The generated random sample points were run through the IK and if the result was determined to be possible that XYZ point that was generated was plotted [80].

The Octave script used to perform these simulations is available in Appendix B.

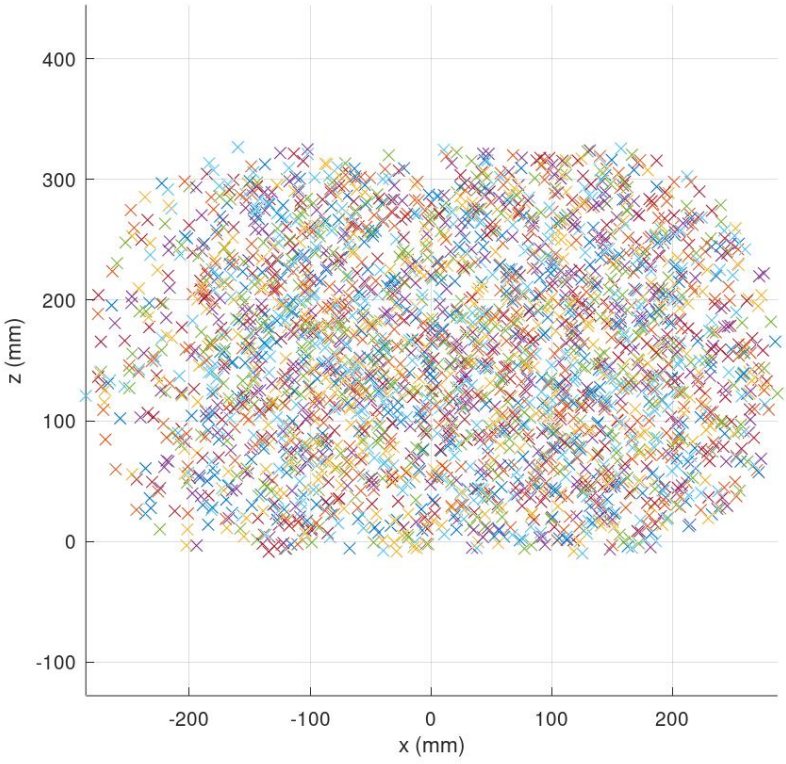

Figure 47: 3D Workspace simulation of single RobotArm - XZ plane.

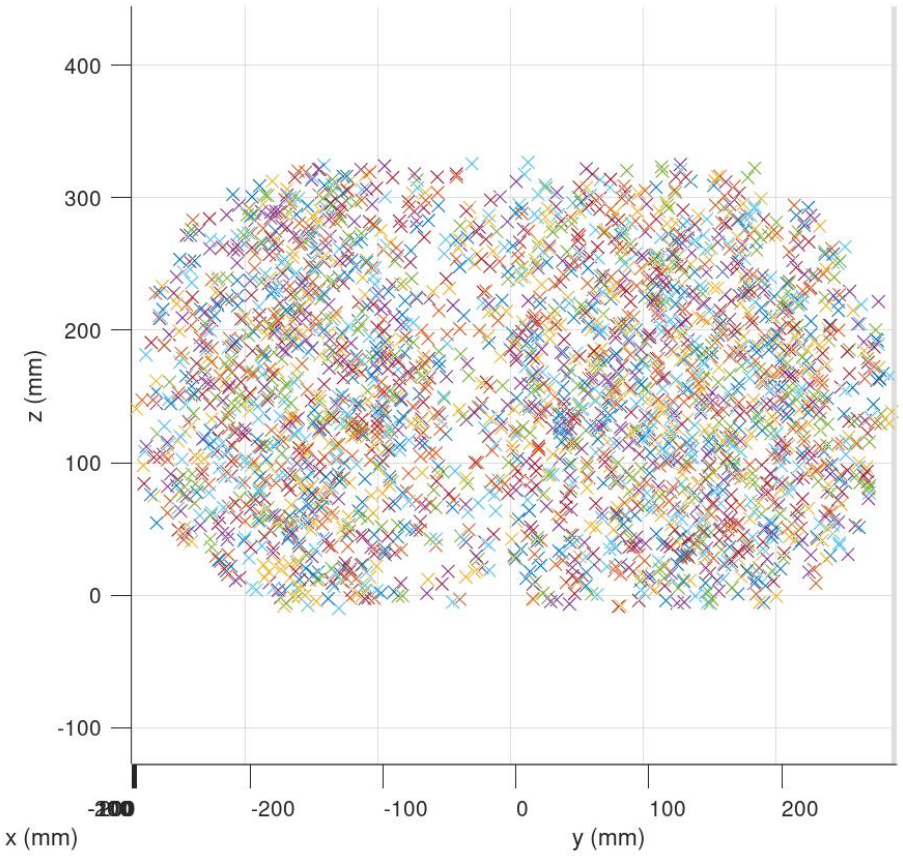

Figure 48: 3D Workspace simulation of single RobotArm - YZ plane.

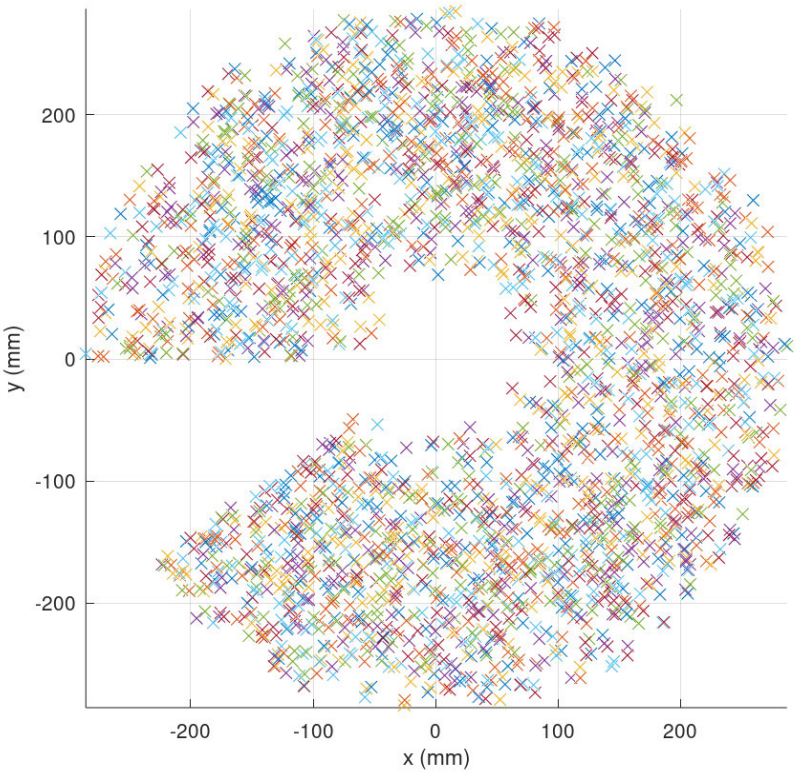

Figure 49: 3D Workspace simulation of single RobotArm - XY plane.

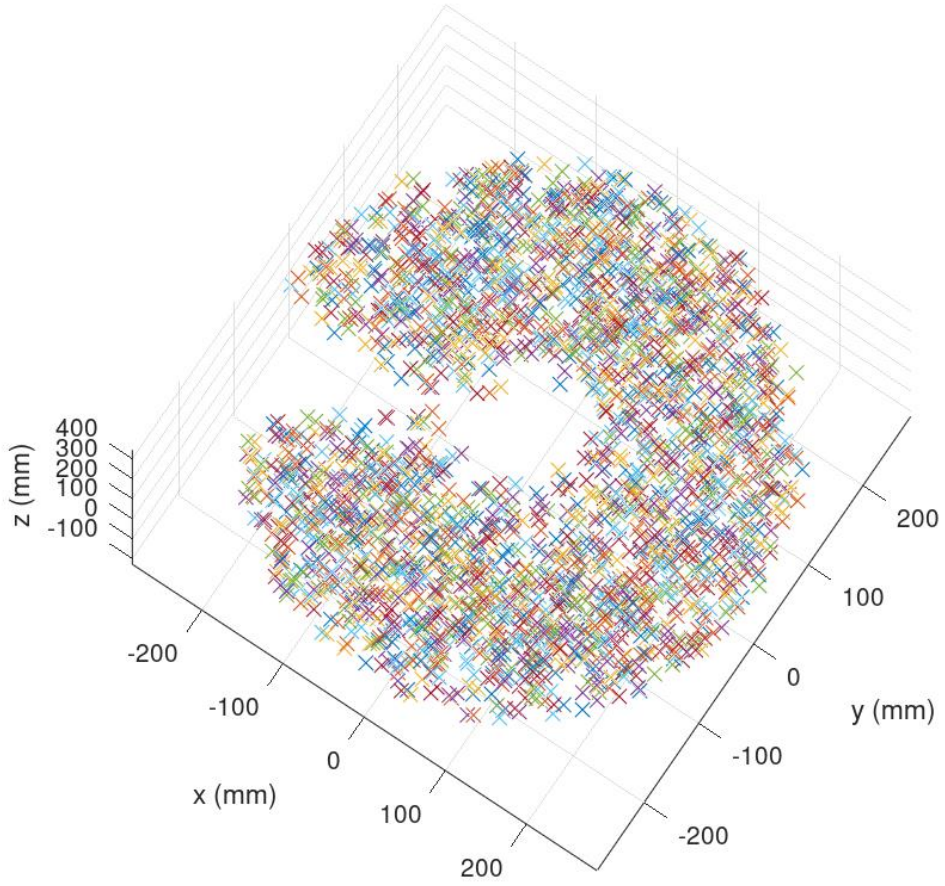

Figure 50: 3D Workspace simulation of single RobotArm.

The workspace simulation was run for 20000 achieved points in order to gather an in depth understanding of what working envelope is available for a single RobotArm. This means that a random point was generated, and the kinematic calculation performed to see if that desired point was achievable. If achievable, a mark was plotted. It can be seen from Figure 47: 3D Workspace simulation of single RobotArm - XZ plane. and Figure 48: 3D Workspace simulation of single RobotArm - YZ plane. that the side plane of the workspace is from a Z height of 0 to 300mm. This is consistent with the RobotArms dimensions.

From Figure 49: 3D Workspace simulation of single RobotArm - XY plane. there is a circular workspace of radius 300mm. Once again, this correlates with the physical dimensions of the RobotArm, as well as the results observed from the XZ and YZ planes.

The workspace generated was what was expected from investigation of the physical model. An incomplete annulus shape was because ThetaOne cannot perform a full 360-degree rotation.

5.3 3D Forward Kinematics and Singularities

In order to discover where the mathematics of the kinematics no longer gave reliable results, a singularity simulation was conducted in Python using the 3D FK and a Monte Carlo randomisation, like the workspace simulations.

In order to discover the singular points that are present within the RobotArm workspace, it was necessary to have the Jacobian matrix available. The Jacobian matrix relates the joint angles to the XYZ coordinate [81] [82]:

$$[Xdot] = J * [qdot] \quad \textit{Eq. 19}$$

$$[\dot{X}] = J * [\dot{q}] \quad \textit{Eq. 20}$$

A singularity occurs if the Jacobian is unable to be inverted to achieve the form:

$$[qdot] = J^{-1} * [Xdot] \quad \textit{Eq. 21}$$

$$[\dot{X}] = J^{-1} * [\dot{q}] \quad \textit{Eq. 22}$$

Therefore, in order to determine the singular points, one can find where the determinant of the Jacobian is equal to 0, i.e.:

$$\det(J) = 0 \quad \textit{Eq. 23}$$

5.3.1 3D Forward Kinematics:

The 3D FK equations were described as:

$$x = (L_2 * cos(\theta_2) + L_3 * cos(-\theta_3) + l) * cos(\theta_1) \quad \textit{Eq. 24}$$

$$y = (L_2 * cos(\theta_2) + L_3 * cos(-\theta_3) + l) * sin(\theta_1) \quad \textit{Eq. 24}$$

$$z = L_1 + L_2 * sin(\theta_2) + L_3 * sin(\theta_3) \quad \textit{Eq. 25}$$

The Python script used to perform the simulation is available in Appendix B.

5.3.2 Singularity Test One:

The first singularity test performed had the following conditions implemented:

$$0 < \theta_1 < 360$$

$$90 < \theta_2 < 180$$

$$90 < \theta_3 < 180$$

n = 50 000

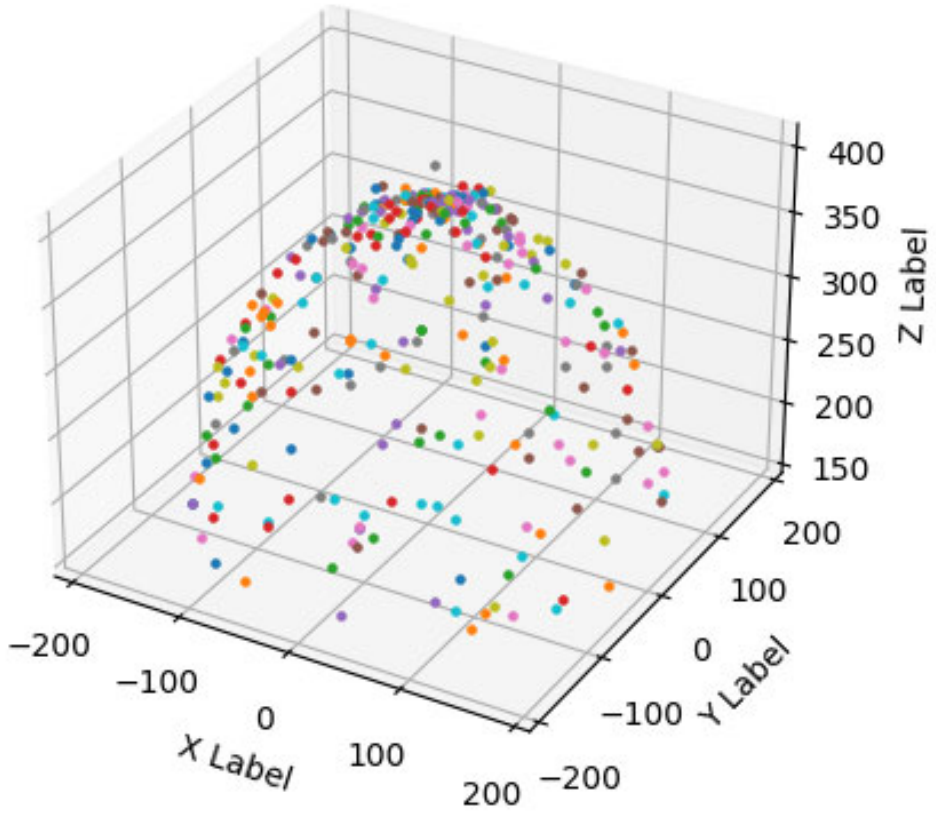

Figure 51: 3D plot of Singularities - test one.

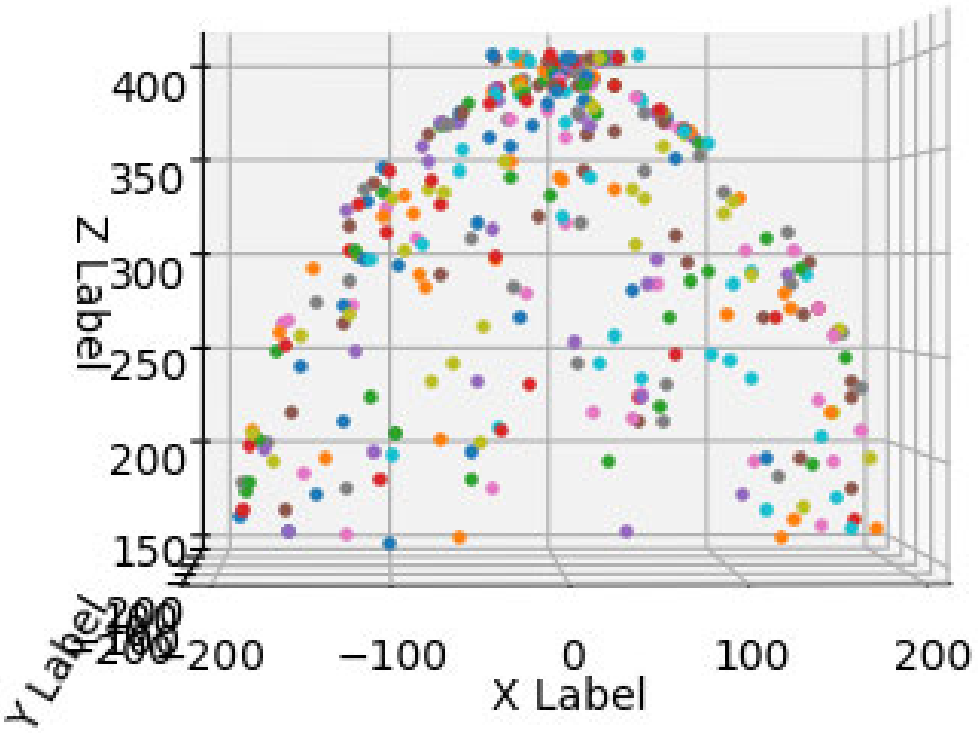

Figure 52: XZ plot of Singularities - test one.

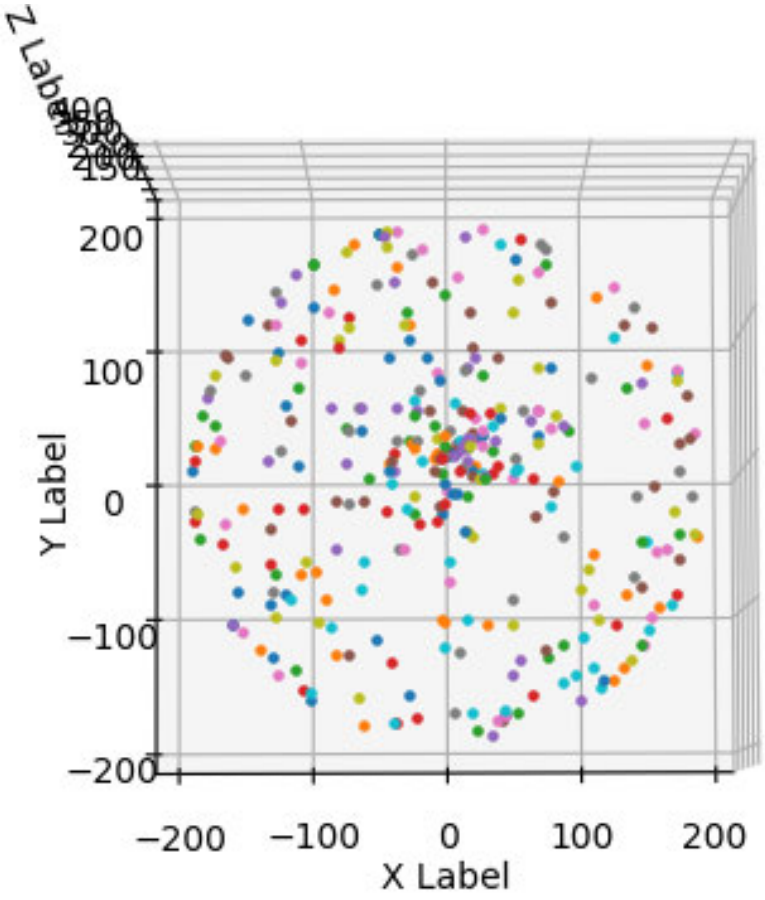

Figure 53: XY plot of Singularities - test one.

5.3.3 Singularity Test Two:

The second singularity test performed had the following conditions implemented:

$$1 < \theta_1 < 1$$

$$-90 < \theta_2 < 90$$

$$-90 < \theta_3 < 90$$

n = 50 000

This second test was essentially a one-degree section of the full rotational workspace, to illustrate in more detail the possible singularities present. It could be assumed that the remaining 359 degrees will have the same singularity profile as found below.

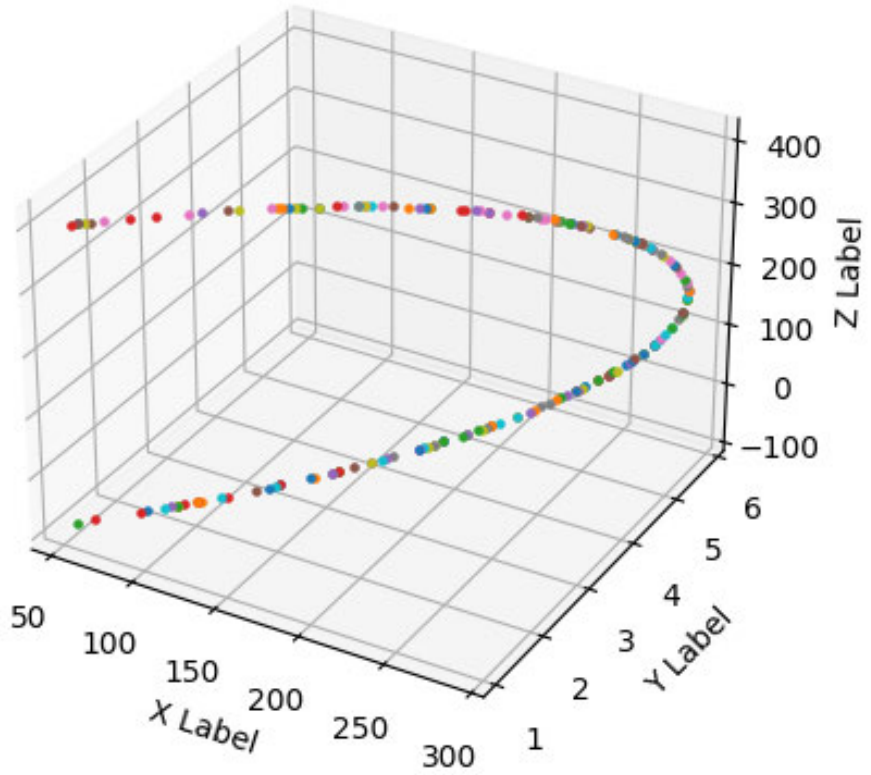

Figure 54: 3D plot of Singularities - test two.

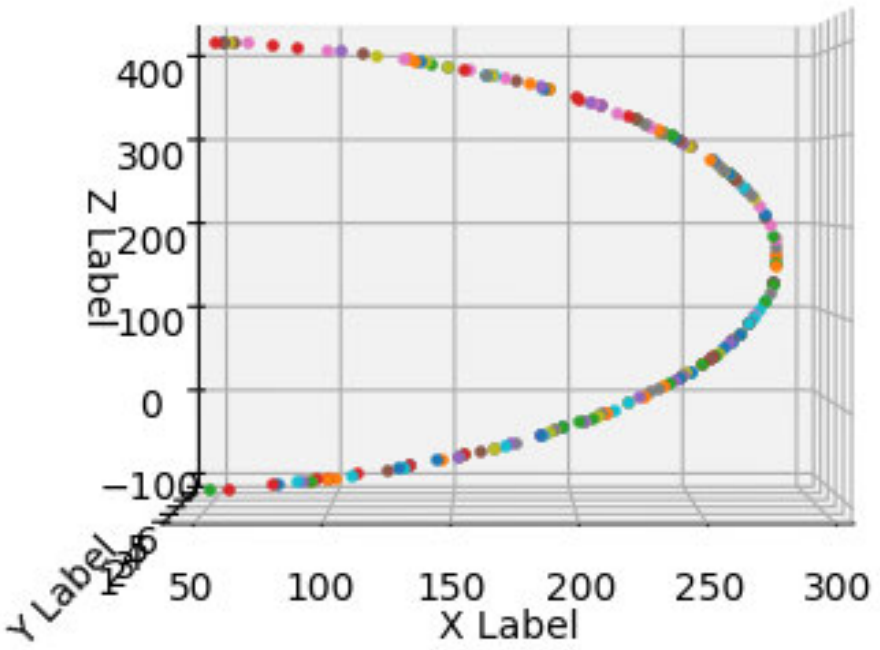

Figure 55: XZ plot of Singularities - test two.

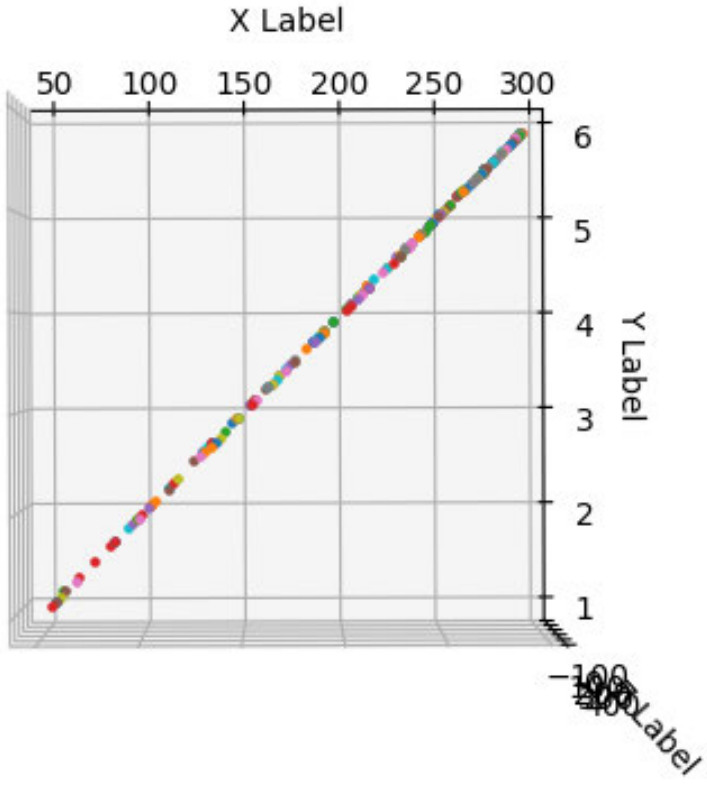

Figure 56: XY plot of Singularities - test two.

In the same methodology as the workspace simulation, 50000 points were randomly generated and parsed through the FK calculations in order to get a Jacobian matrix. The determinant of the Jacobian matrix was

then calculated and if this was equal to 0 a singular point was discovered and plotted. It can be seen from these singularity simulation plots that the only singular points available are that of boundary singularities [83]. These boundary singularities, although theoretically possible, are not actually present in the physical model due to the limitations of the mechanism caused by the nested parallelograms within the architecture.

It can be noted that the singular points discovered for the individual serial kinematic manipulator would be the same for the combined system. This is since the combined hybrid PKM consists of the same individual SKM. There would not be true PKM singularities as there is 9 actuating motors for 6 DOF.

5.4 Kinematic and Modelling Chapter Summary

Throughout this chapter, in-depth investigation is performed into the chosen quasi-serial RobotArm after the initial selection. The full 3D serial kinematic model was derived using a geometric vector approach. The full kinematic model allowed for a workspace simulation to be performed. This was done as a randomization scatter plot of valid points the kinematic model can achieve.

Finally with the use of the forward kinematics, a Jacobian matrix was determined. This Jacobian matrix was then utilized to solve for the singularities. It was found that the only singularities present within the system were that of boundary singularities. These prove to be theoretical due to the physical platform not being able to reach these points due to limitations within the physical architecture.

6. INVERSE KINEMATICS AND MODELLING OF A COMBINED HYBRID SKM-PKM PLATFORM

This chapter outlines the kinematic model of the optimised design proposed in the previous chapter, but extended into a parallel mechanism that has a common end effector.

6.1 Combined Hybrid Inverse Kinematics

When completing the hybrid kinematics, several steps need to be followed sequentially. The initial part of the inverse kinematic calculation was a pure PKM computation. The second part of the inverse kinematics was SKM, and flows through the full 3D serial IK of the single RobotArm shifted from the origin [84].

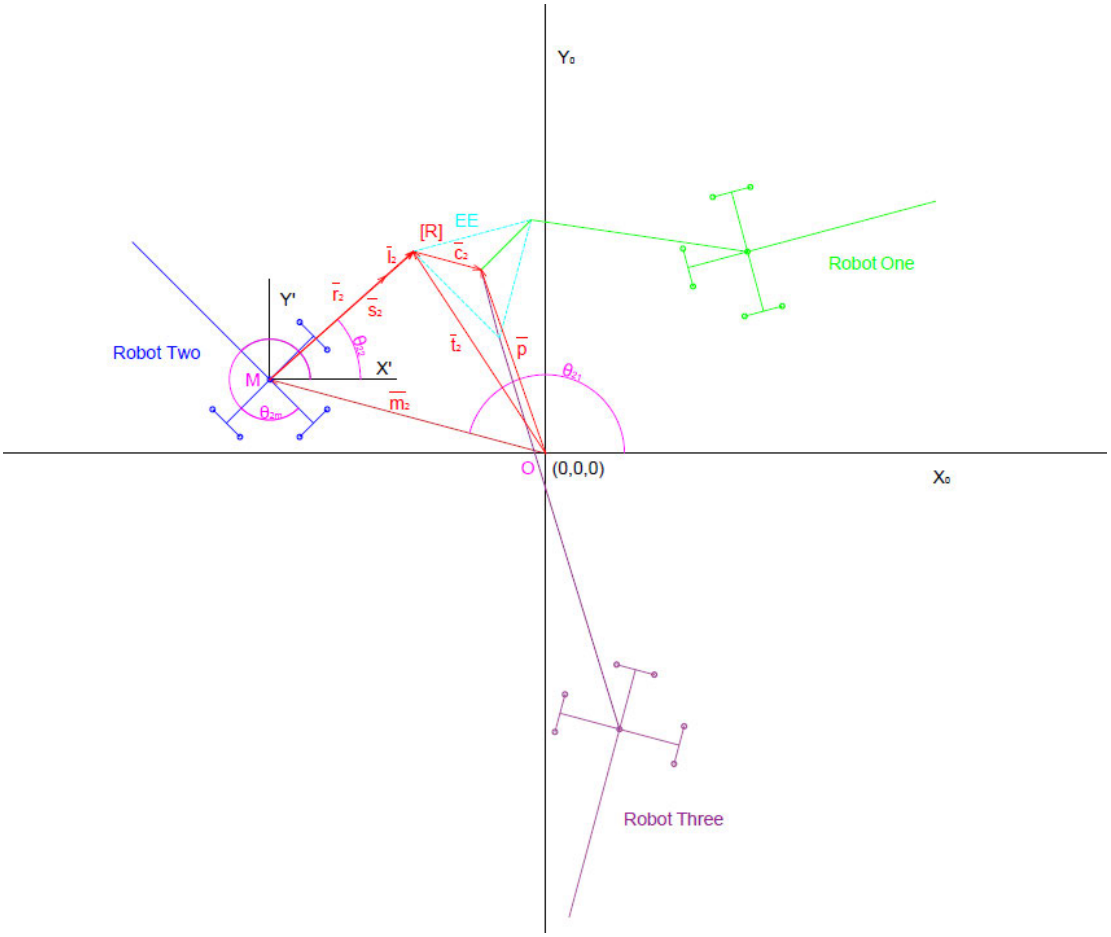

Figure 57: Combined Hybrid Kinematics: X-Y plane - used for PKM.

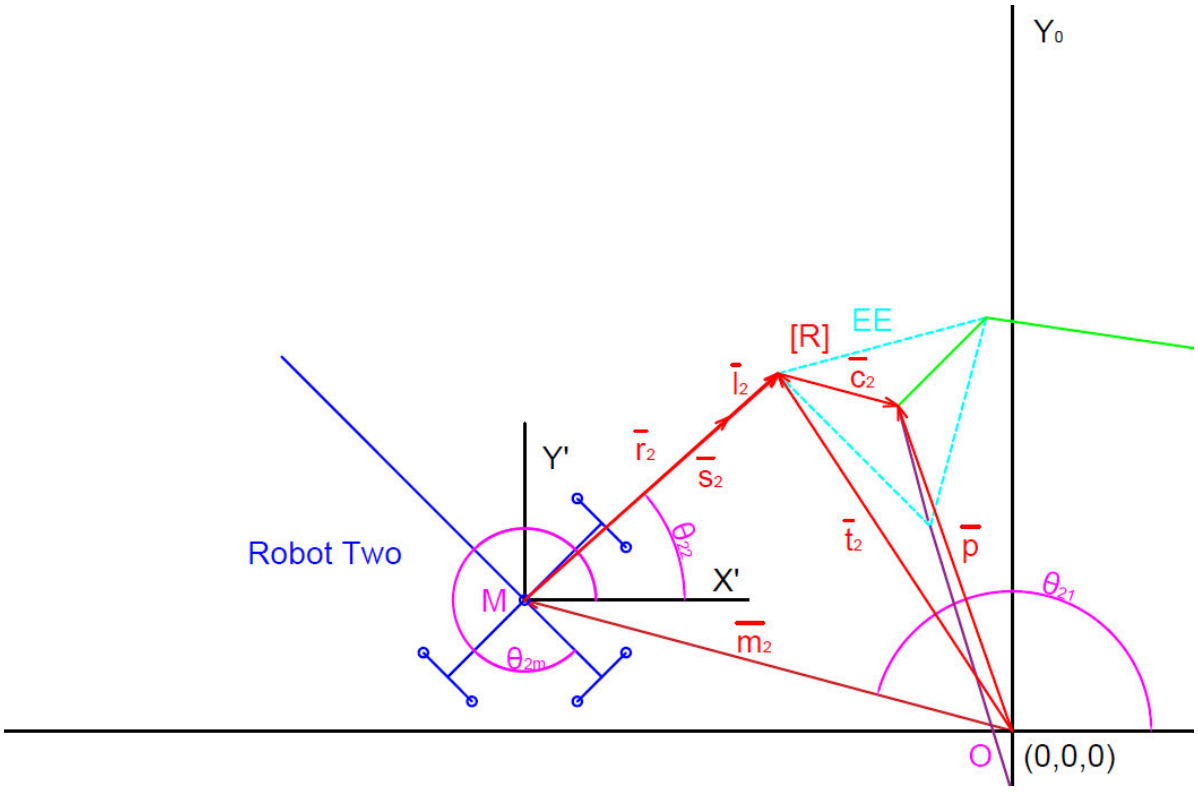

Figure 58: Combined Hybrid Kinematics: X-Y plane more detail - used for PKM.

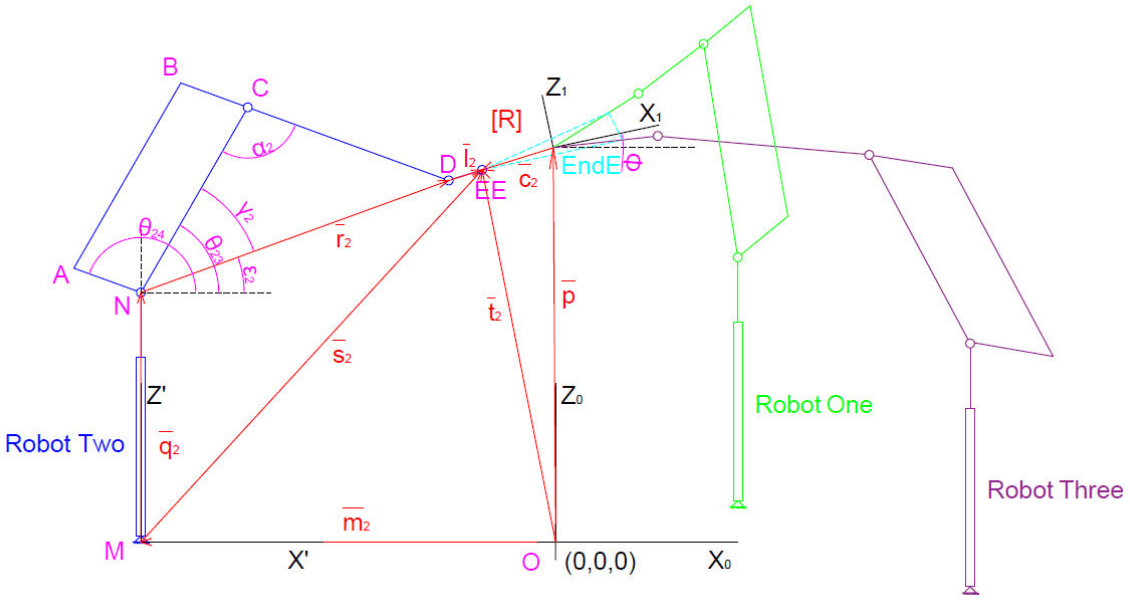

Figure 59: Combined Hybrid Kinematics: X-Z plane - used for PKM.

It can be seen from the combined kinematic images above; Figure 44: Collaborative Robots Kinematics: X-Y plane. to Figure 59: Combined Hybrid Kinematics: X-Z plane - used for PKM, that the setup is the same as a single robot outlined in 3D Inverse Kinematics of a RobotArm - Shifted from Origin however just more involved due to the introduction of the Rotation Matrix [R].

This rotation matrix needed to be included at this point as it was discovered that by linking several of the quasi-serial RobotArms onto a single end-effector; the hybrid platform was able to achieve an additional three degrees of rotation when compared to a single RobotArm. Therefore, the kinematic analysis needs to accommodate and compensate for the end-effectors position and overall rotations.

PKM IK:

$$p = vector\ made\ up\ from\ the\ X0Y0Z0\ origin\ \&\ X1Y1Z1\ origin\ (0,0,0).\ Centre\ of\ combined\ EE.$$

$$s = vector\ made\ up\ from\ base\ of\ RobotArm\ to\ target\ point\ EE.\ The\ centre\ of\ single\ EE.$$

In the case of a single arm at the origin, vector S = vector P.

$$\vec{p} = \begin{bmatrix} p_x \\ p_y \\ p_z \end{bmatrix} \qquad \textit{Eq. 26}$$

Rotation Matrix:

$$R_x = \begin{bmatrix} 1 & 0 & 0 \\ 0 & \cos(\theta_x) & -\sin(\theta_x) \\ 0 & \sin(\theta_x) & \cos(\theta_x) \end{bmatrix} \qquad \textit{Eq. 27}$$

$$R_y = \begin{bmatrix} \cos(\theta_y) & 0 & \sin(\theta_y) \\ 0 & 1 & 0 \\ -\sin(\theta_y) & 0 & \cos(\theta_y) \end{bmatrix}$$ *Eq. 28*

$$R_z = \begin{bmatrix} \cos(\theta_z) & -\sin(\theta_z) & 0 \\ \sin(\theta_z) & \cos(\theta_z) & 0 \\ 0 & 0 & 1 \end{bmatrix}$$ *Eq. 29*

$$[R_{xyz}] = R_x R_y R_z$$ *Eq. 30*

$$mounting\ distance = l + m$$ *Eq. 31*

$$\overrightarrow{m_n} = \begin{bmatrix} mounting\ distance * \cos(\theta_{n1}) \\ mounting\ distance * \sin(\theta_{n1}) \\ 0 \end{bmatrix}$$ *Eq. 32*

$$EEDistance = c$$ *Eq. 33*

$$\overrightarrow{c_n} = \begin{bmatrix} EEDistance * \cos(\theta_{n1}) \\ EEDistance * \sin(\theta_{n1}) \\ 0 \end{bmatrix}$$ *Eq. 34*

$$\overrightarrow{s_n} = \vec{p} + [R_{xyz}] \cdot \overrightarrow{c_n} - \overrightarrow{m_n}$$ *Eq. 35*

To offset the origin for the individual robot IK

$$\overrightarrow{t_n} = \overrightarrow{s_n} + \overrightarrow{m_n}$$ *Eq. 36*

We now take vector t as the input into a single offset RobotArm IK from 5.1 3D Inverse Kinematics of a RobotArm - Shifted from Origin.

6.2 Workspace Simulation – 3D Multiple RobotArms

The workspace of the combined hybrid platform was essentially the intersection of the three individual RobotArms; and hence the same approach was taken as the individual workspace. This time the three individual RobotArm workspaces were developed on the same plot that takes into consideration their mounting pattern and relative distances from one another.

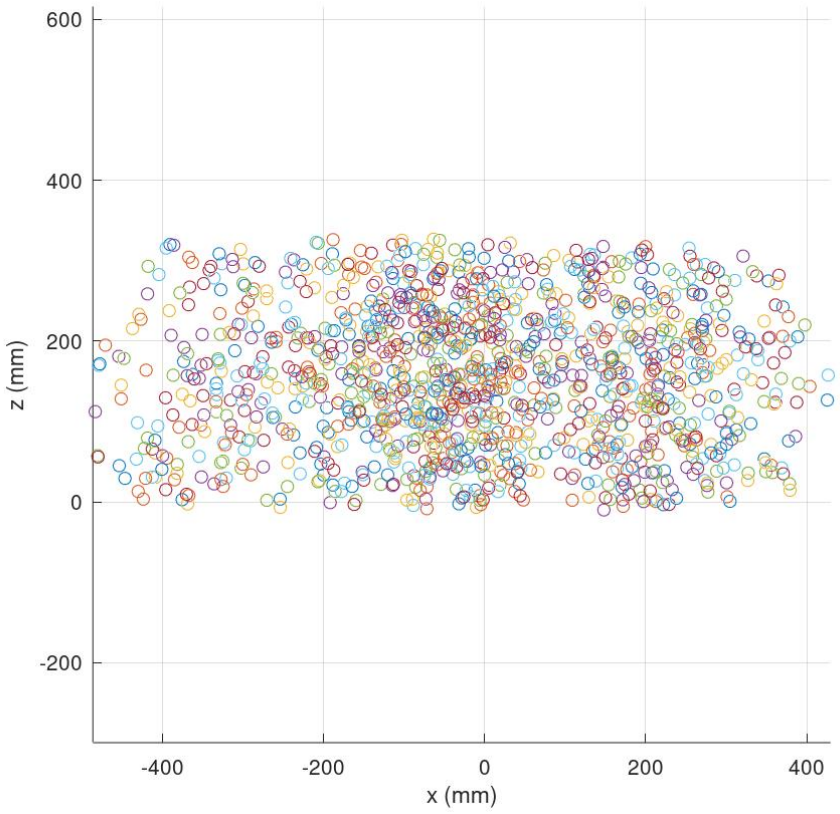

Figure 60: 3D Workspace simulation of combined RobotArm - XZ plane.

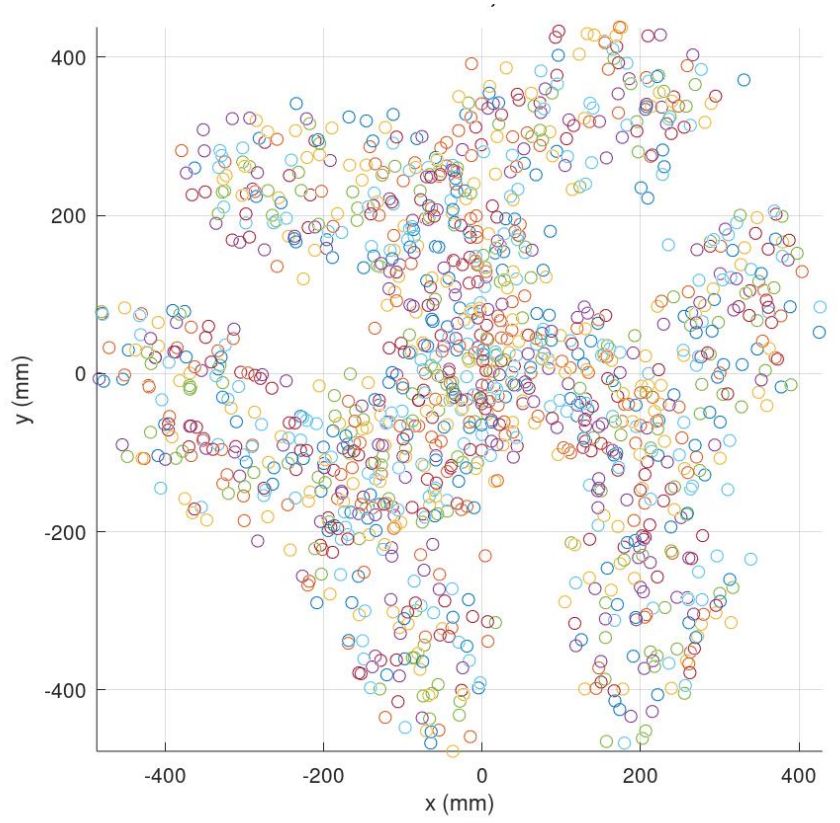

Figure 61: 3D Workspace simulation of combined RobotArm - XY plane.

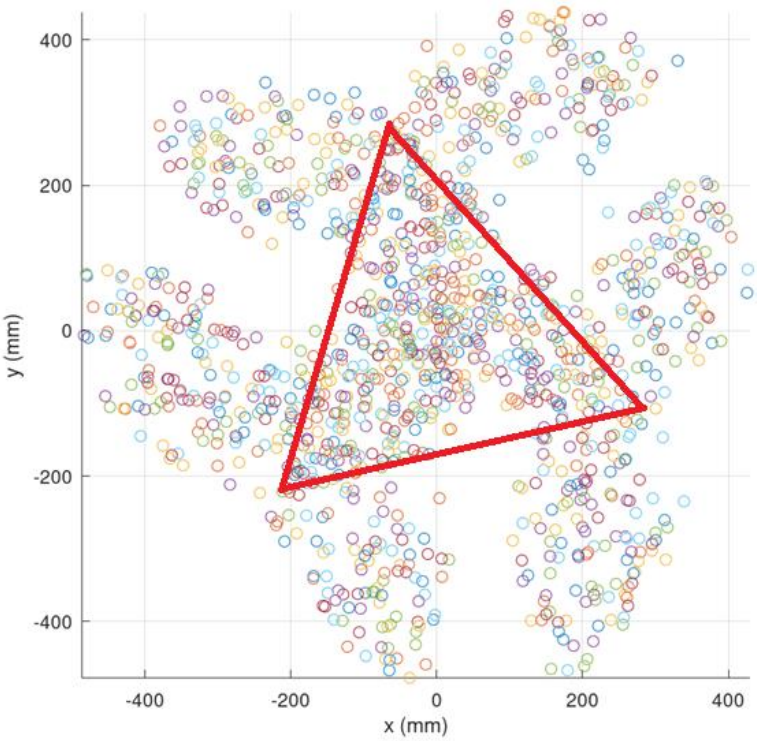

Figure 62: Hybrid kinematic platform workspace.

The red triangle was where the three individual RobotArm workspaces intersect and therefore represents the hybrid kinematic mechanisms available working envelope. As expected, this available working envelope of the PKM hybrid is smaller than the individual SKM workspaces. This corresponds with the parallel mechanism theory.

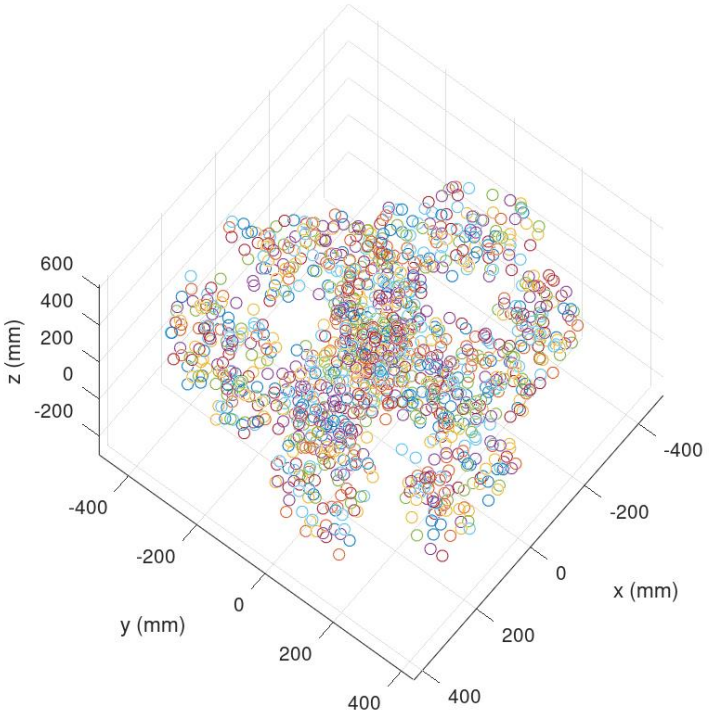

Figure 63: 3D Workspace simulation of combined RobotArm.

6.3 Inverse Kinematic and Modelling Chapter Summary

With the combination of several RobotArms into one combined mechanism, it was discovered that this manipulator has a parallel kinematic structure. This meant that a PKM derivation was necessary. This chapter therefore outlined the derivation of the parallel kinematic model that includes the rotation matrix.

The combination of three RobotArms into the same workspace, all shifted from the origin allowed for the simulation of the combined workspace. This allowed visualisation of the total available workspace to each RobotArm, as well as the intersection points in which they could collaborate or be one combined mechanism.

7. SOFTWARE

The control aspect of the research proved to be one of the most involved topics to master.

Initially, an approach to adapt a current control system was investigated, such as the very powerful open-source 3D printing control program Marlin. Initially it was considered to edit the Marlin software to be appropriate for the RobotArm. This proved to be a futile endeavour. The Marlin software was written and expanded upon so greatly, and hence all aspects of it are fully integrated throughout. It proved to be beyond grasp within the timeline to implement the RobotArm kinematics within the Cartesian specific Marlin software [85].

Research into other open-source control programs was performed. Software such as Mach3, Coppelia Sim, AR2, and more were investigated; however, all are limited to Cartesian or very specific examples of 5DOF/6DOF pre-made models of existing robotic manipulators, such as ABB.

A decision was made to write a custom control program from first principals. The control program grew with the capabilities of the robotic manipulator platform; however, the final control program has been outlined in the remainder of this chapter.

7.1 Code Overview Flowchart

The following depicts the logical flow of the control system, between the Python Graphical User Interface and the Arduino microcontroller program.

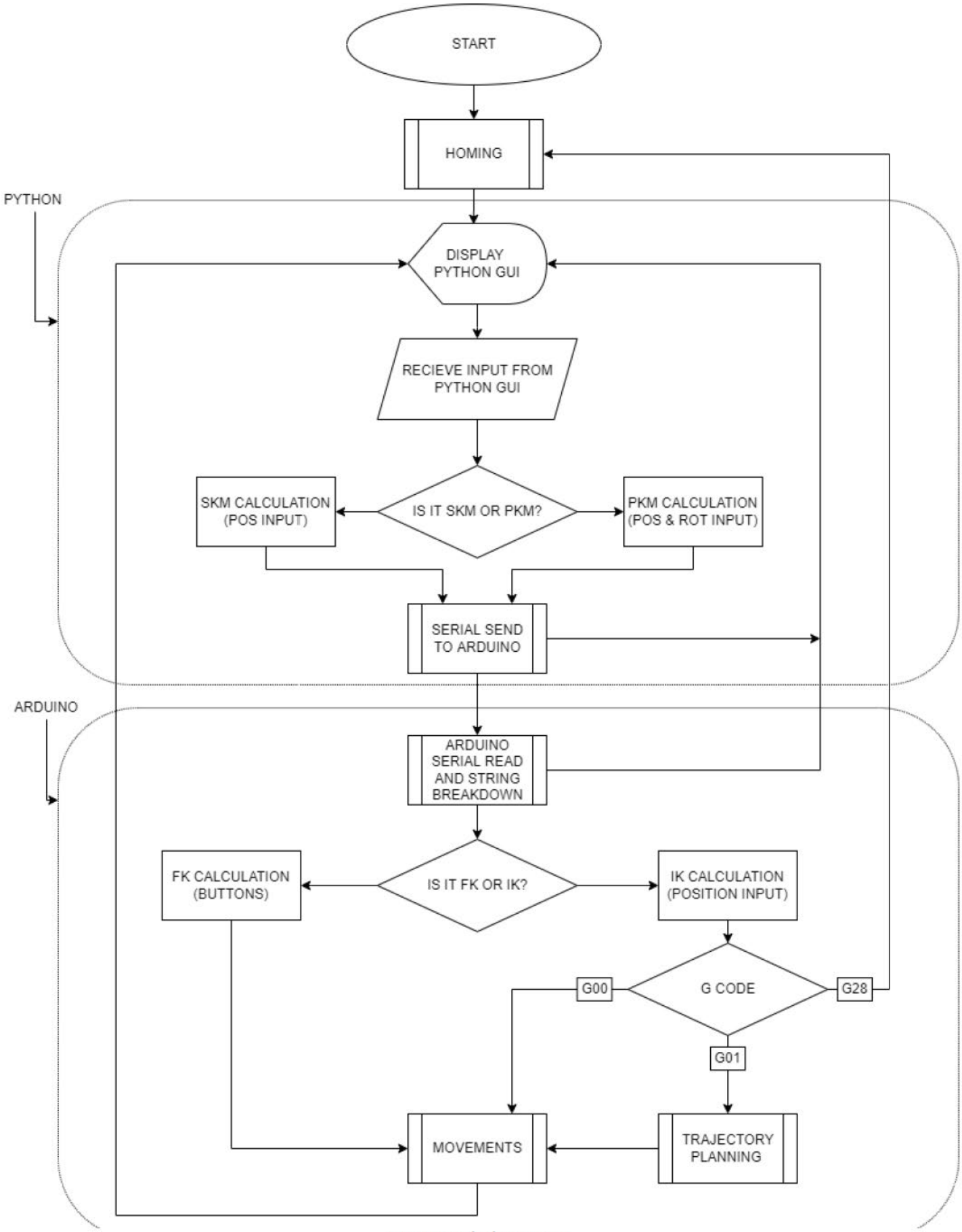

Figure 64: Code Flow Diagram.

7.2 Arduino Control

The initial control was written for a single RobotArm on the Arduino Integrated Development Environment (Arduino IDE). Arduino uses code in the format of C/C++ and hence was perfect for development via first principals.

The code developed for the Arduino microcontrollers was responsible for performing several tasks. These tasks are outlined as follows. The full Arduino code is available in A2. Appendix B.

7.2.1 Initialising and Setup:

This portion of the code was responsible for defining all variables and initialising them for the remainder of the program to reference. The setup of an Arduino code was only run through once on the initial start-up of the microcontroller.

- *Introduction of libraries to be referenced.*

The following libraries were used within the Arduino code:

1. AccelStepper.h
2. MultiStepper.h
3. Math.h
4. Ramp.h
5. String.h

- *Setup of pins and variables.*

Initially all pins and variables are defined and initiated. This included a section in which the specific RobotArm and mounting positions were able to be selected. All instances of the libraries were defined.

- *Homing*.

As the final stage of the setup, the homing procedure was run. The logic of the homing procedure was as follows:

1. Set all three steppers to run at constant speed in the direction of the limit switches.
2. When a limit switch is contacted, feedback tells the specific stepper to stop moving.
3. When all three limit switches have been contacted. The home position is updated through the kinematics to set a reference for the angle of each stepper and the XYZ cartesian co-ordinate of the end-effector.

7.2.2 Loop:

The loop is the main part of an Arduino program, in which the code is run through continuously whilst the microcontroller was powered, or no errors have occurred. The loop was responsible for all overall running inputs, calculations and outputs of the RobotArms.

- *Scan and receive serial inputs - recvWithStartEndMarkers():*

The code scans the serial input for a specific string command. The string was formatted in a manner that allows for the input of a G-Code with a RobotArm registry to ensure the correct RobotArm receives the intended command. The string was also formatted such that the beginning and end have unique markers that ensure the full string with all the information had been received from the Serial Input.

- *Parse data - parseData():*

If the string that had been received was appropriate, the code then deciphered the string and assigns the information to predefined variables. These variables were then used for several computations in the remainder of the program within the interpretation of the data flow.

- *Display data - showParsedData():*

The data that had been received and deciphered into their appropriate string and float variables were then displayed back to the Serial Monitor as reference.

- *Compute and perform movements - interpretData():*

The final multistage method being referenced by the main loop was that of interpretData(). This method referenced other methods sequentially to perform the kinematics, path planning and movements.

1. *interpretData()*

   The code was to decipher what G and M code had been requested. The programmed G-Codes were G00, G01, G28. The M codes were M03 and M04.

   Two new code functions were introduced, namely B and F. These were for the identification of button and file inputs respectively.

2. *IK()*

   When a G00 command was received, the code went directly to the inverse Kinematics method. This method included the following:

I. Local variable definition and initialising.
II. 3D Kinematic calculations
III. Degrees to steps
IV. Calling the movement method - moveit().

moveit() method had several functions to perform:

a) Local variable definition and initialising.
b) Checking that homing has been completed and that the point is within the workspace.
c) Ensuring the output from the IK() is a valid non infinite value.
d) Synchronising the three RobotArms.
e) Populating and calling the MultiStepper library.

3. Interpolation()

The interpolation method was called if a G01 command was received. The interpolation method was responsible for splitting up the vector between the current position and the desired position into segments via a parametric equation; and transferring each output point to the moveit() method.

4. HomingSequence()

If the G28 command was received, the homing sequence was initiated. The motors would run until the limit switches were activated.

During the programming of the kinematics of the different mounting positions of the RobotArms; it was challenging to create an all-encompassing function that can compute the Arctan calculations reliably. A semi-autonomous workaround was developed to identify the quadrant and map the 0 - PI output of the atan2 function to a -PI – PI or 0 – 2PI output.

Something that was discovered when the RobotArms were coupled together as a PKM, was that the execution of the movement of each RobotArm was different. This created a jerky movement of the combined end-effector.

It was discovered that the computational time of each RobotArm was a different length, and hence when one RobotArm would complete its computation, it would begin to move, however the other two were not synchronised. This caused the combined end-effector movement to pull and push the other RobotArms movements, and hence created an oscillating movement of the end-effector. As single RobotArms running SKM this was not apparent.

In order to solve this, timing would need to be introduced. To achieve this, each Arduino was connected to each other from Pin-Out to Pin-In. A method was then created within the Arduino control algorithm that

would be called during the PKM IK. This method was called after the completion of the individual motor steps calculation, but before initiating the movements.

Once the individual RobotArms had computed the required motor steps needed to execute the movement, it would flag the other two RobotArms, by setting the Pin-Out to high. The remaining two robots would read this high on the connected Pin-In. Only when all three Pin-Ins were reading high, would the movements be initiated.

This workaround proved to be successful for the continuation of testing; however, having a single control chip or microprocessor would prove more robust for real-world operations. Alternatively, the setting up of a CANBUS or I2C system could be used. In this way a common clock time could be referenced to synchronise the final movements.

7.3 Python GUI

The major visual part of the control program was the Graphical User Interface coded in Python, with the use of tkinter – a python plugin that allows for the creation of GUIs.

The Python portion of the control program can be thought of as the ‘’Main Brain” or frontend software and was responsible for connecting the multiple RobotArm Arduino microcontrollers together. The Python GUI has many duties to perform; namely:

- Organising all the inputs and outputs in a concise easy to use platform.
- Receiving robot specific inputs via G-code being typed in manually.
- Reading and receiving G-code from a file.
- Buttons as inputs to manually jog the RobotArms in all DOF.
- Creating the appropriate string, with start and end markers for each individual RobotArms Arduino microcontroller.
- To perform PKM calculations in the case of a coupled mechanism.
- Sending the information via Serial to each specific Arduino.
- Displaying information feedback from each Arduino.
- Displaying a live graphic visual of the positions of the combined mechanism.

An example of the string the Python GUI sends to the Arduino micro-controllers was as follows:

**ARD1, M, G00, X10, Y20, Z260,/*

The string consisted of a start (*) and end marker (/). The first part of the information is ARD1, which indicateed that the string was destined for the first robot, rather than the second or third robot. ARD1 is followed by either an M or a B, which indicates to the Arduino whether the input was from a coordinate for movement, or from a jogging button input. Following the Arduino reference was a G-code. Finally a set

of XYZ cartesian coordinates. All items within the string are seperated by commas to isolate them for variable seperation. The full Python code is available in A2. Appendix B.

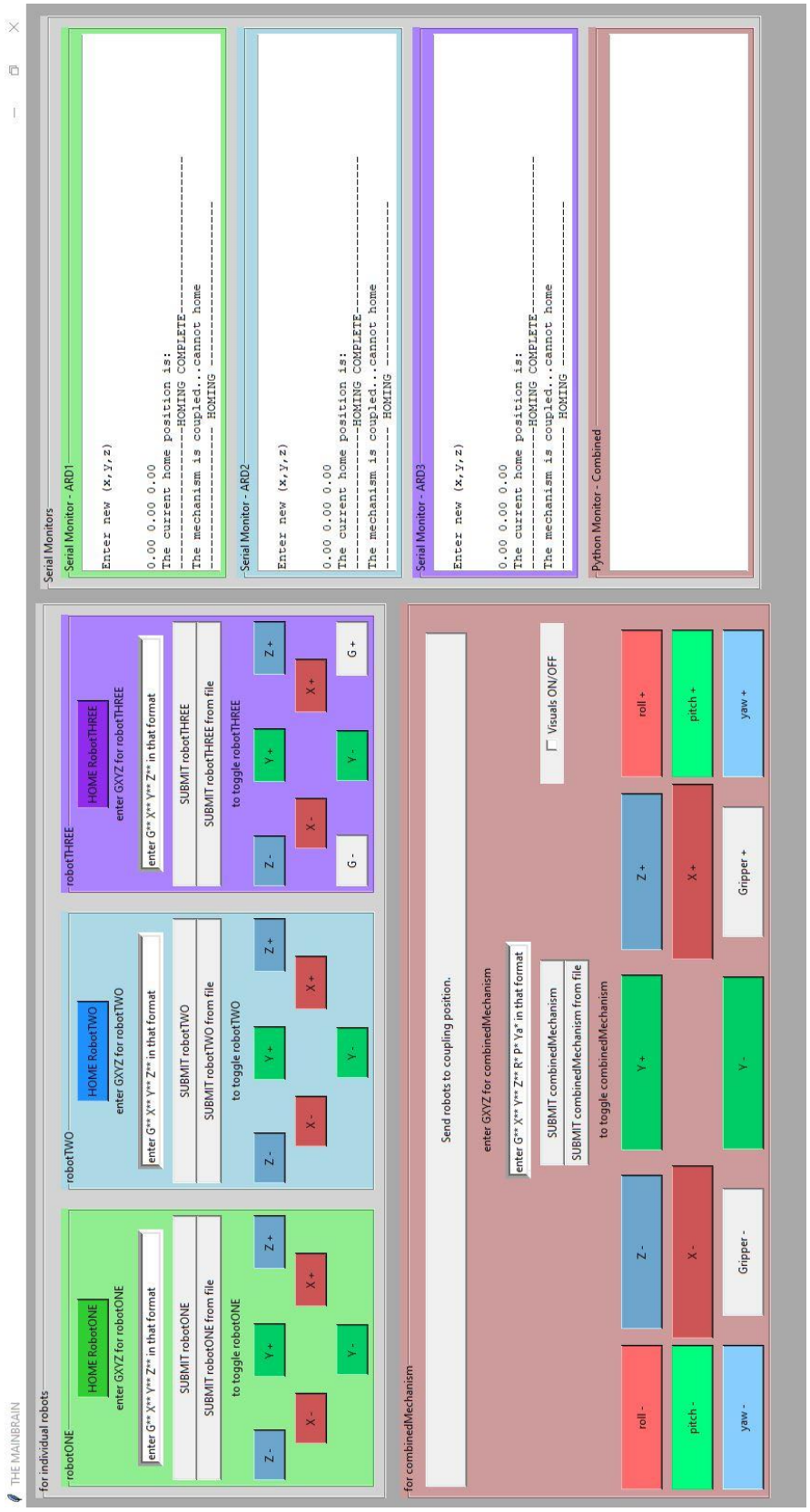

Figure 65: Full Python GUI.

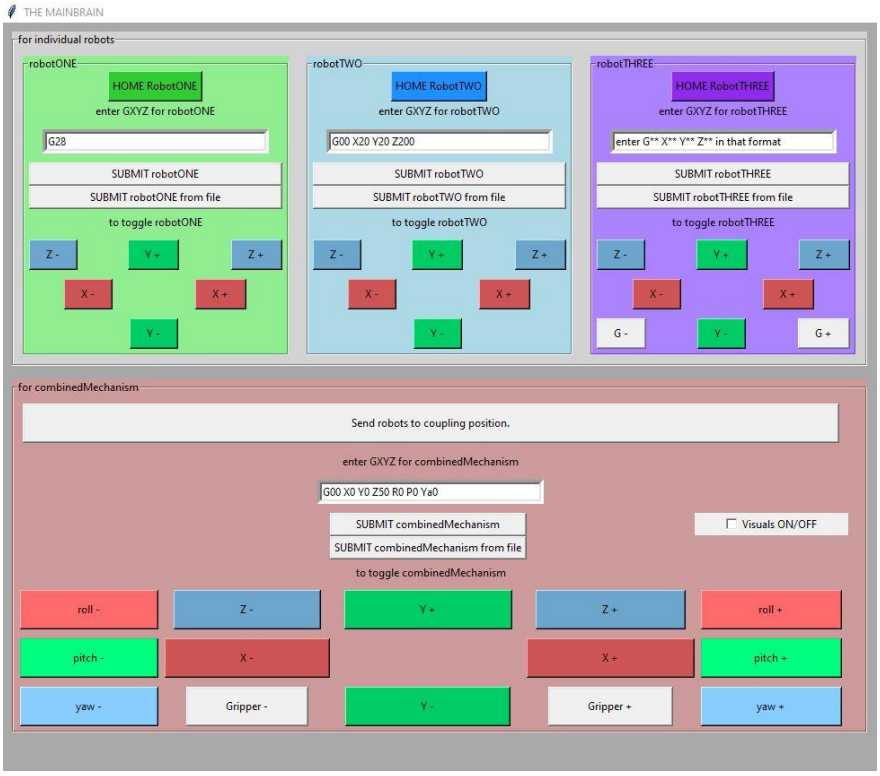

Figure 66: Python GUI input panel.

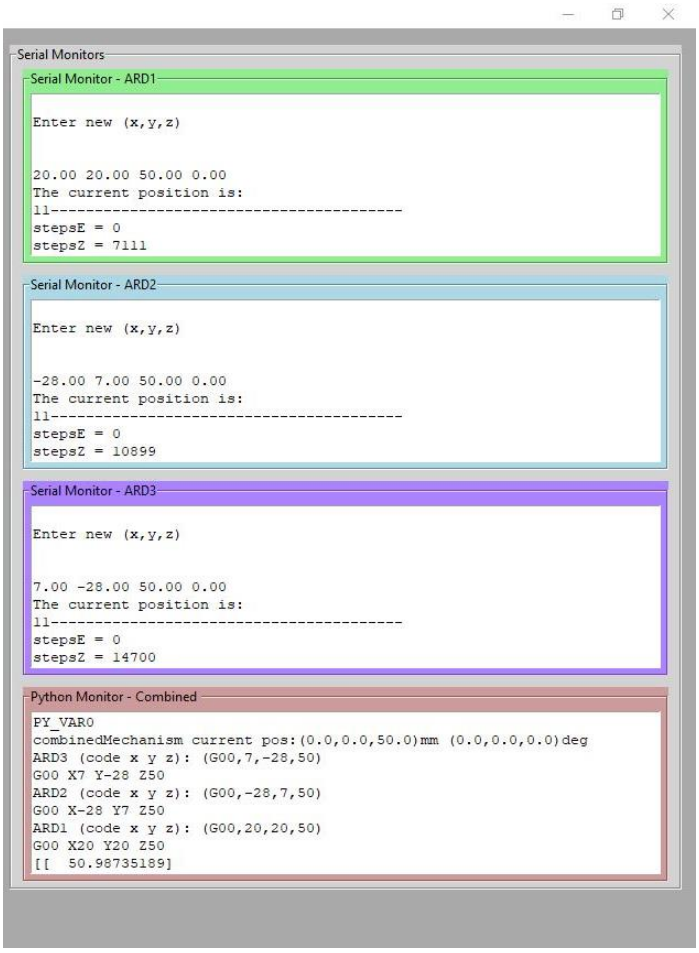

Figure 67: Python GUI output panel.

7.4 Software Chapter Summary

In order to get the robotic manipulators to perform tasks, a fully incorporated control system was required. This chapter outlines how the control was able to be achieved through the logic flowchart and scripted control methods.

The control consists of each individual RobotArm having an Arduino Mega 2560 microcontroller with kinematics and motor control logic. These individual Arduinos were then controlled serially via a common Python graphical user interface that could also perform PKM calculations for the combined hybrid kinematic manipulator.

8. TESTING AND EXPERIMENTATION

The following chapter outlines the tests performed on the RobotArms, both as individual platforms and as a combined mechanism.

Much of the testing focused on accuracy and repeatability of the platforms.

Initially, testing was performed upon the individual RobotArms working alone, in order to gauge a baseline performance. The testing then progresses to comparing the individual RobotArms to one another, while operating in the same workspace, as collaborative robots. These tests all relate to the overall construction and the control program. The kinematics in focus was the SKM IK.

The testing then moves to investigate the combined hybrid platform, in which the RobotArms are connected to a single common end-effector. In these cases, the same experiments are performed in order to discover how well the RobotArms work and a single unit.

The G-Code that has been used for these experiments is available in A4.1 Appendix D.

8.1 Robotic Platform Setup for Testing

The following are pictures and explanation of the physical set up of the three RobotArms mounted on the testing board with the selection of end-effectors used to perform the tests outlined in this chapter.

Further images relating to the physical platform is available in A6. Appendix F.

For the individual robot arm tests the RobotArms were mounted onto a laser cut and engraved board that has a Cartesian scale. The probe to be used in this experiment is a permanent marker attached to a custom end-effector, with a 3d printed cap that has a cone tip.

Figure 68: Individual RobotArm with marker - front view.

For the combined hybrid PKM the RobotArms were mounted 220mm away from the origin, at 120-degree intervals, on the laser cut board. This time the common end effector with probe is to be secured to each RobotArms mounting positions.

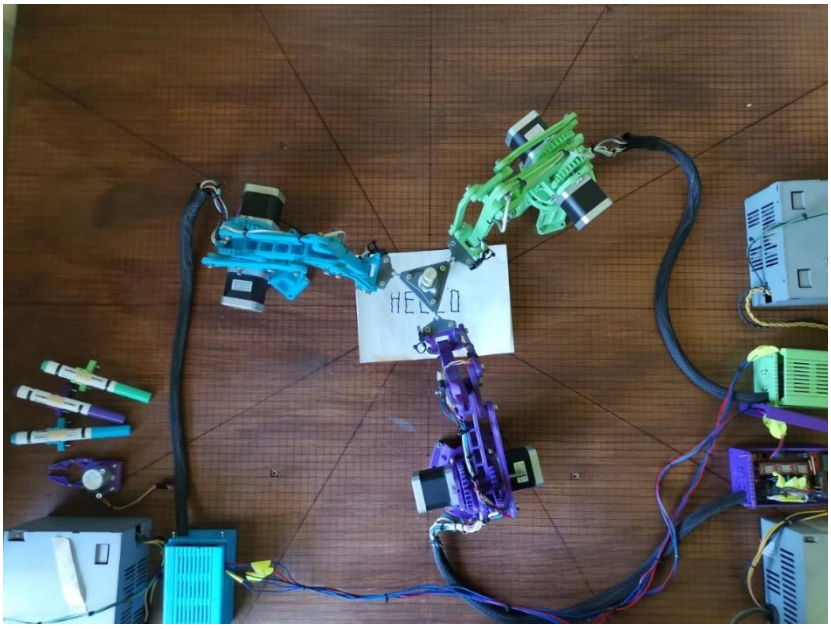

Figure 69: Combined RobotArms with marker pen - top view.

For the individual physical test, mount the RobotArms 220mm away from the origin, at 120-degree intervals, on the laser cut board as in 8.1. Jog the end effector to 0,0,260. Place the dial gauge under the end effector and apply the weight.

8.2 Individual RobotArm - Accuracy and Repeatability Test

8.2.1 Aim: Individual RobotArm - Accuracy and Repeatability Test

The aim of this experiment was to ascertain the accuracy and repeatability that can be achieved by the individual RobotArms in a shared XYZ Cartesian coordinate system.

8.2.2 Theory: Individual RobotArm - Accuracy and Repeatability Test

For the RobotArm to be successful at performing tasks in the real world, it should be able to achieve a desired coordinate point. The factors that are involved with the accuracy achieved by the RobotArm would be how accurately the components have been produced and coupled to one another. The accuracy that is achieved is highly dependent on the control program performing the kinematic calculations and executing the motor movements.

In order to investigate the accuracy that can be achieved by the RobotArm, a new end-effector needed to be produced that can hold a probe.

8.2.3 Setup: Individual RobotArm - Accuracy and Repeatability Test

Refer to 8.1 for set up.

8.2.4 Methodology: Individual RobotArm - Accuracy and Repeatability Test

1. Mount RobotArms onto laser cut board 220mm from the origin, 120 degrees apart.
2. Feed points via G-code to the RobotArms to achieve. Ensure that the desired XYZ points take into consideration the probe tool length. In this case the desired XY coordinate to be achieved is: (0,0,110), (30,30,110), (30,-30,110), (-30,30,110), (-30,30,110).
3. Measure and tabulate achieved XYZ coordinate position.
4. Run to each point 10 times in the same path plan, as outlined by ISO 9283 of 1998.
5. Repeat steps 3-5 using the second and third RobotArms.
6. Perform calculations to determine the AP and RP of each RobotArm.

The following equations are outlined by ISO 9283 of 1998 for calculating accuracy and repeatability:[86] [87] [88]

Pose Accuracy (AP):

$$AP = \sqrt{(\bar{x} - x_i)^2 + (\bar{y} - y_i)^2 + (\bar{z} - z_i)^2} \qquad \textit{eq. 38}$$

$$\bar{x} = \frac{1}{n}\sum_{j=1}^{n} x_j \qquad \textit{eq. 39}$$

Where,

$$x_i = command\ position \quad \textit{eq. 40}$$

$$x_j = achieved\ position \quad \textit{eq. 41}$$

$$n = number\ of\ measurements \quad \textit{eq. 42}$$

Pose Repeatability (RP):

$$RP = \bar{l} + 3 * S_l \quad \textit{eq. 43}$$

$$\bar{l} = \frac{1}{n}\sum_{j=1}^{n} l_j \quad \textit{eq. 44}$$

$$l_j = \sqrt{(x_j - \bar{x})^2 + (y_j - \bar{y})^2 + (z_j - \bar{z})^2} \quad \textit{eq. 45}$$

$$S_l = \sqrt{\frac{\sum_{j=1}^{n}(l_j - \bar{l})^2}{n-1}} \quad \textit{eq. 46}$$

Where:

S is Standard Deviation.

l is the distance between the attained pose and the barycentre of the attained poses.

8.2.5 Results: Individual RobotArm - Accuracy and Repeatability Test

The following tables and figures outline the results observed from this experiment in a summarised form. The remainder of the results and all the raw data is available in A4. Appendix D.

Table 3: AP vs RP summary of points 5 - 1 for Robot 1.

summary - robot 1		
point	**AP**	**RP**
5	1.257	2.853
4	2.283	2.461
3	2.112	2.481
2	2.492	3.115
1	1.578	3.109

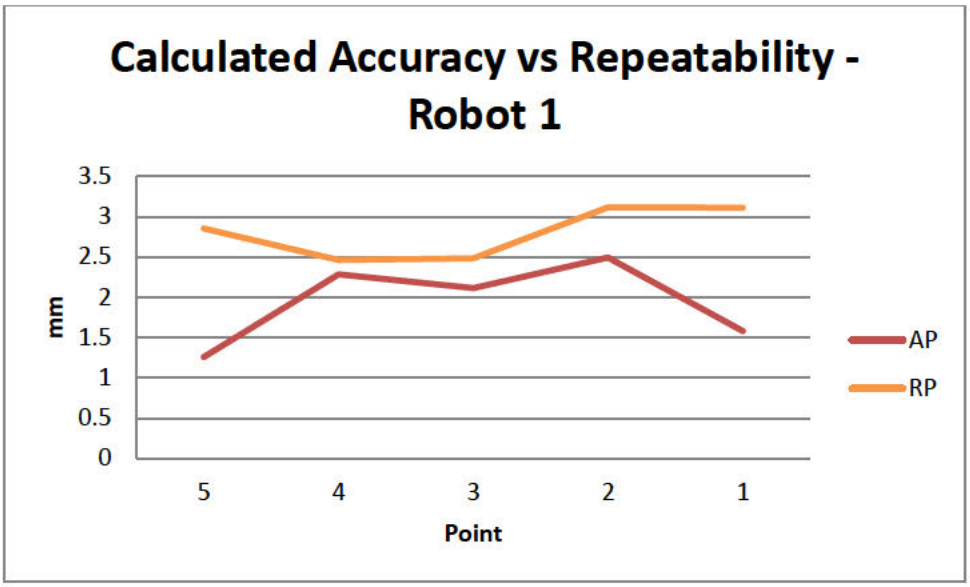

Figure 70: Graph of AP vs RP of points 5 - 1 for Robot 1.

Table 4: AP vs RP summary of points 5 - 1 for Robot 2.

summary - robot 2		
point	AP	RP
5	4.277	2.522
4	3.423	2.287
3	3.68	2.332
2	3.257	2.621
1	4.331	2.479

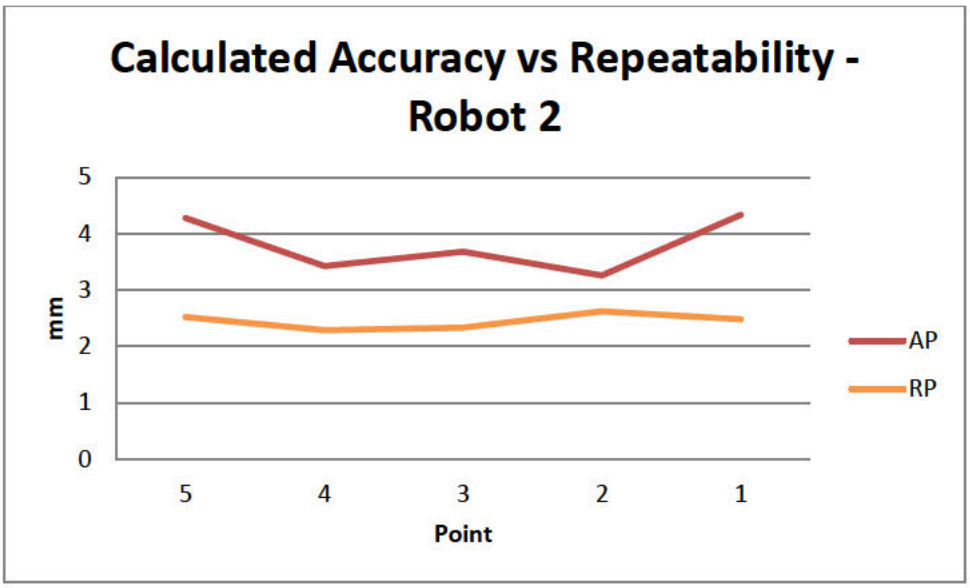

Figure 71: Graph of AP vs RP of points 5 - 1 for Robot 2.

Table 5: AP vs RP summary of points 5 - 1 for Robot 3.

summary - robot 3		
point	AP	RP
5	2.54	2.522
4	3.312	2.075
3	2.92	2.428
2	2.302	2.831
1	2.178	2.451

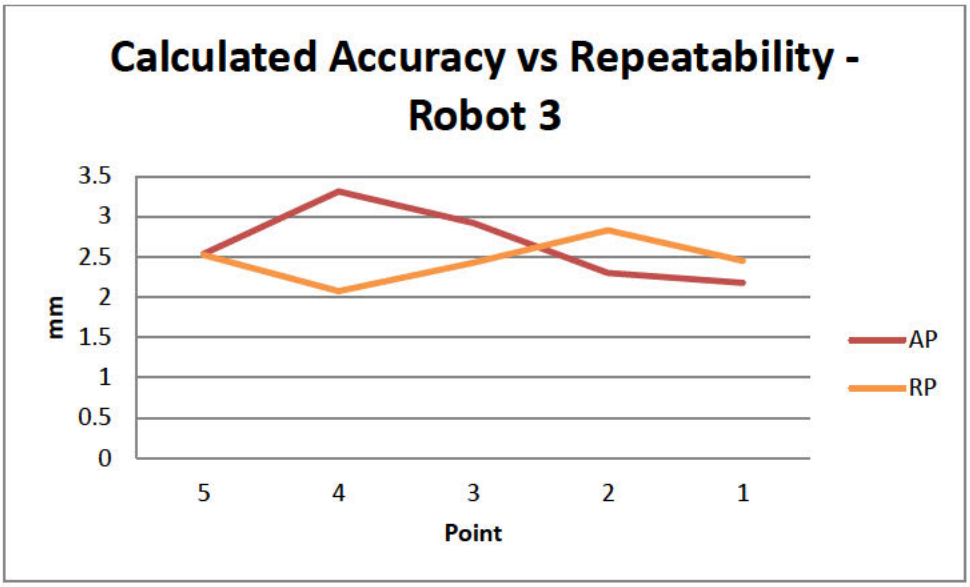

Figure 72: Graph of AP vs RP of points 5 - 1 for Robot 3.

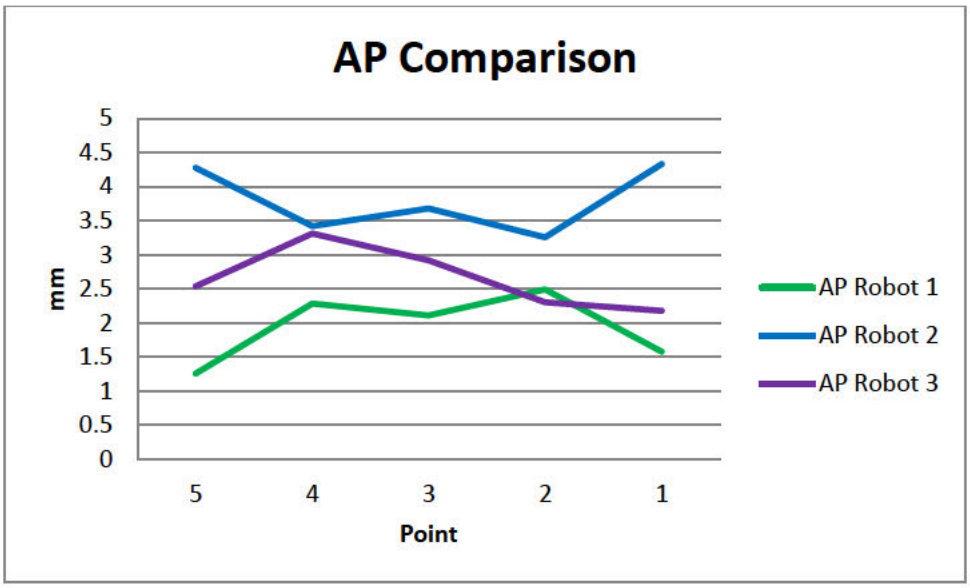

Figure 73: Graph of AP of points 5 - 1 for Robots 1 -3.

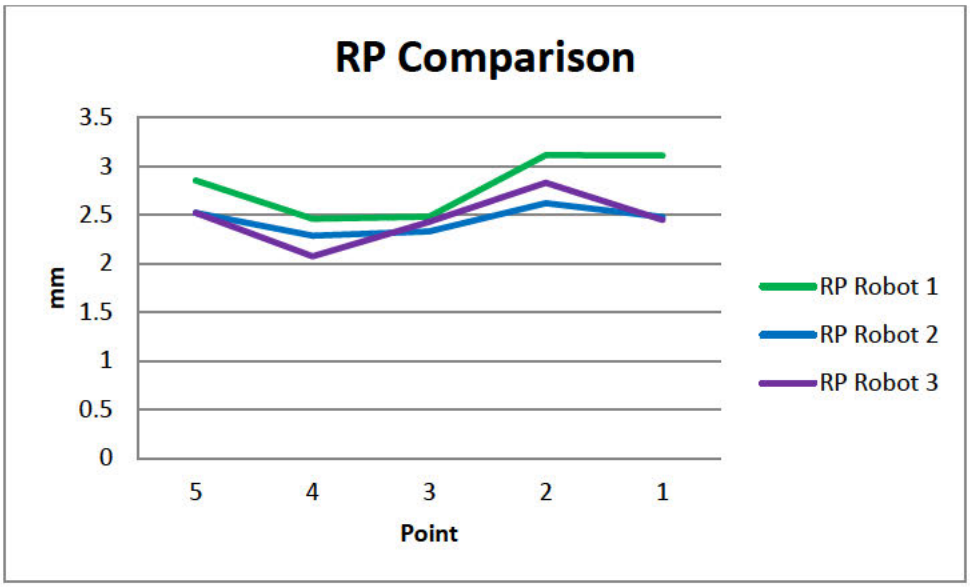

Figure 74: Graph of RP of points 5 - 1 for Robots 1 -3.

8.2.6 Discussion: Individual RobotArm - Accuracy and Repeatability Test

The RobotArms performed well, achieving the desired coordinate points within 2-4mm of the desired XY coordinate point, relative to the known laser cut coordinate. The average AP of the three robots for each point was 2.795mm, and the RP was 2.571mm. It can be noted that this accuracy level is not suitable for real world manufacturing; however, the source of the deviation from the known point was due to imperfect manufacture of the robot itself, as well as the mounting of the probe. It should be noted that the gear mesh being achieved by the 3D printed gears allowed for some backlash and play.

The distances between the achieved positions made by each RobotArm allows further insight into the consideration of whether the control program is the source of the deviation from the known desired point. Measuring from point (30,30) to point (30,-30) should produce a result of 60mm. This was accurate to approximately 1mm. This means that the control program was calculating the kinematics and executing the movements correctly – and further enhances the possibility that the production of the 3D printed robot arms are the cause of the deviation from the known to the desired points.

8.3 Combined RobotArms as a Hybrid Platform - Accuracy and Repeatability Test

8.3.1 Aim: Combined RobotArms as a Hybrid Platform - Accuracy and Repeatability Test

The aim of this experiment was to identify the accuracy and repeatability of the RobotArms when they are coupled with a common end-effector, working as a hybrid PKM.

8.3.2 Theory: Combined RobotArms as a Hybrid Platform - Accuracy and Repeatability Test

The theory is that when the RobotArms are coupled into a parallel mechanism the overall accuracy should increase due to increased stiffness. The PKM combination of the RobotArms should be able to mitigate the mechanical play that was experienced when the RobotArms were acting as individual SKM.

A new end-effector probe mount was produced, like the one used for the individual RobotArms, however this common end effector was able to link all three RobotArms into one combined hybrid mechanism. The probe is to be held by the common end-effector of the combined mechanism.

8.3.3 Setup: Combined RobotArms as a Hybrid Platform - Accuracy and Repeatability Test

Refer to 8.1 for set up.

8.3.4 Methodology: Combined RobotArms as a Hybrid Platform - Accuracy and Repeatability Test

1. Mount RobotArms onto laser cut board 220mm from the origin, 120-degrees apart from each other.
2. Couple the RobotArms with the common end-effector.
3. Feed points via G-code to the RobotArms to achieve. Ensure that the desired XYZ points take into consideration the probe length. In this case the desired XY coordinate to be achieved is: (0,0,95), (30,30,95), (30,-30,95), (-30,30,95), (-30,30,95).
4. Measure and tabulate the achieved XYZ coordinate position.
5. Run to each point 10 times in the same path plan, as outlined by ISO 9283 of 1998.
6. Repeat steps 3-5 using the second and third RobotArms.
7. Perform calculations to determine the AP and RP of the combined system using the same equations as 8.2.

8.3.5 Results: Combined RobotArms as a Hybrid Platform - Accuracy and Repeatability Test

The following results were produced from this experiment. The full set of raw data along with further calculations and graphs are available in A8. Appendix H.

Table 6: AP vs RP summary for combined platform.

summary - combined platform		
point	**AP**	**RP**
5	2.449	3.042
4	2.387	3.506
3	2.191	2.799
2	2.119	2.978
1	2.121	3.344

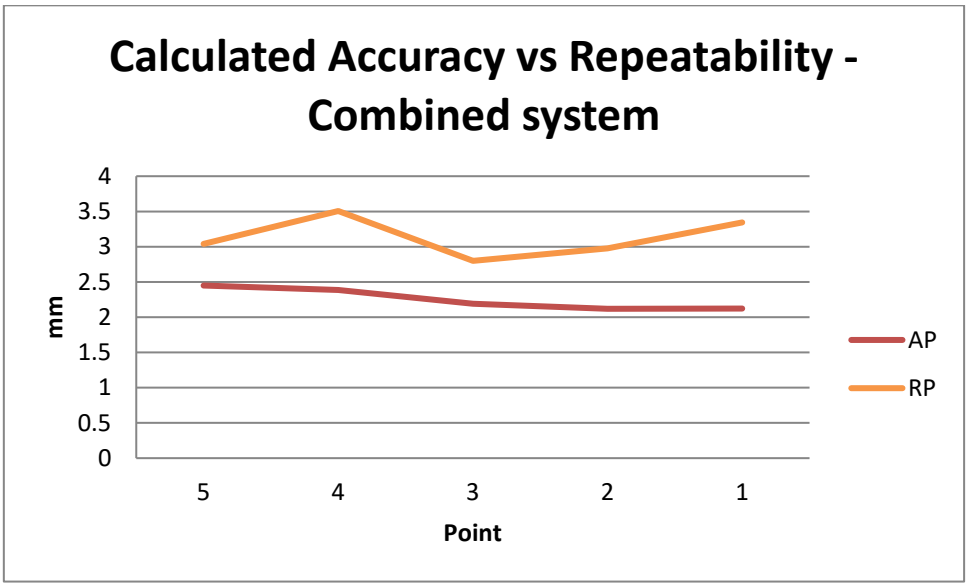

Figure 75: Graph of AP vs RP of points 5 - 1 for combined system.

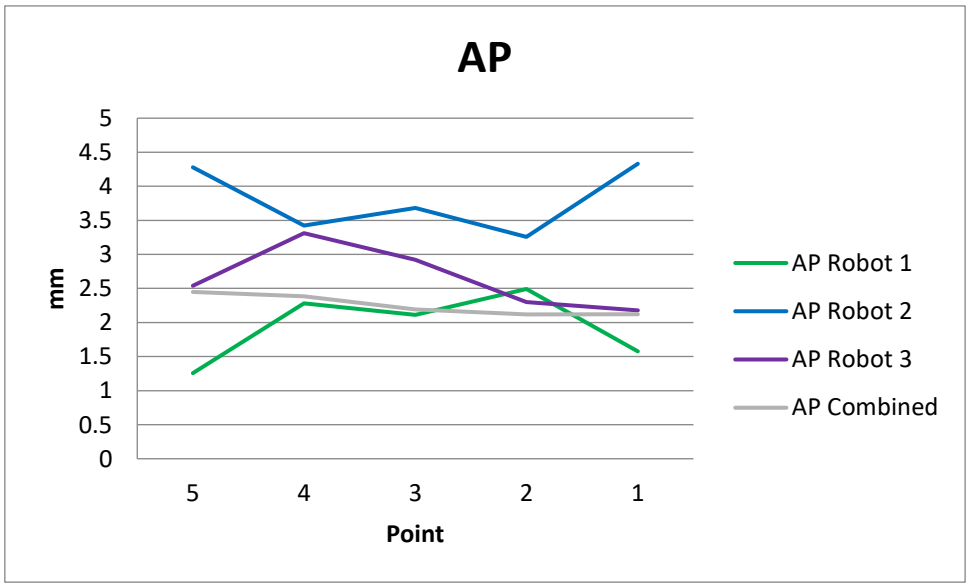

Figure 76: Graph of AP individual vs combined.

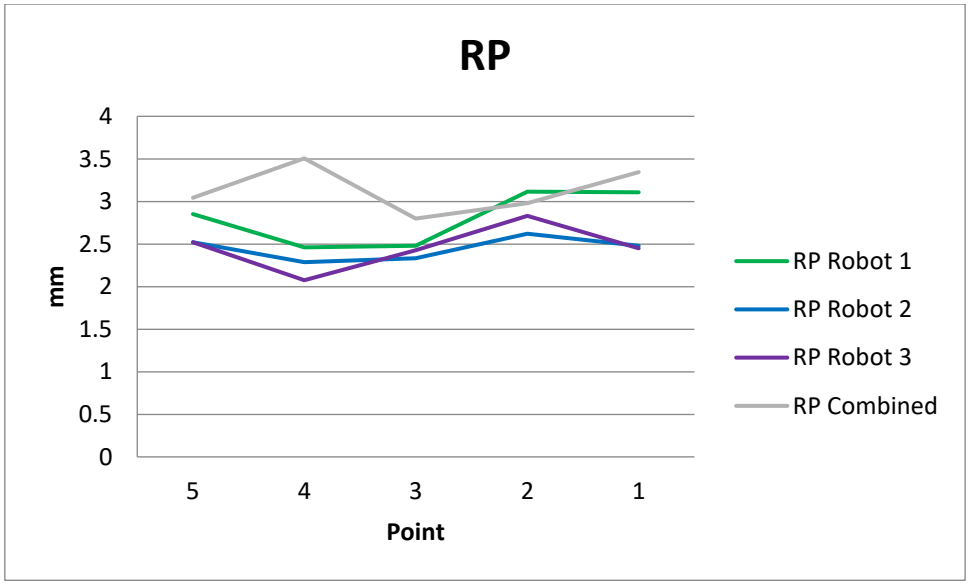

Figure 77: Graph of RP individual vs combined.

8.3.6 Discussion: Combined RobotArms as a Hybrid Platform - Accuracy and Repeatability Test

This test of combined accuracy was aimed at investigating the PKM IK and the associated control. The objective was to achieve desired points, the same as performed by the individual robots outlined in 8.2. however, it was proposed that the amount of deviation of the PKM should be less than that of the SKM.

The results produced by the combined hybrid platform acting as a PKM were slightly more accurate when compared to the individual RobotArms; with an average accuracy AP result of 2.253mm versus 2.795mm for the individuals. The RP of the hybrid was 3.134mm versus 2.571mm for the individuals. This meant that the hybrid system was more accurate but less repeatable than the individual RobotArms. The AP result confirms the theory that the combined mechanism is more mechanically rigid, and thus accommodates the mechanical tolerances in a more efficient manner. The hybrid platform was not as repeatable as the individual robot arm, this is due to the way in which the movements are performed and timed using three independent microcontrollers. The timing was not perfectly synchronous and therefore resulted in a push and pull between the RobotArms.

8.4 Combined RobotArms as a Hybrid Platform - Rotation Test

As individual RobotArms, they are each able to achieve 3DOF, namely XYZ translations. These translations have been thoroughly investigated in the afore outlined tests.

When 3 RobotArms are combined into the hybrid kinematic platform, the DOF able to be achieved increases to 6. In order to identify the overall articulation of the mechanism, isolated tests were performed on the rotational degrees of freedom.

The results obtained are directly proportional to the rotation matrix that is a part of the PKM kinematics, as well as the mechanical design of the common end effector and its joints.

8.4.1 Aim: Combined RobotArms as a Hybrid Platform - Rotation Test

The aim of the combined rotation test was to discover the amount of rotational freedom available within both the PKM kinematics, as well as the mechanical end effector.

8.4.2 Theory: Combined RobotArms as a Hybrid Platform - Rotation Test

Real world applications of robotic manipulators generally requires full articulation. Full articulation is achieved if all six degrees of freedom are available. Namely x-translation, y-translation, z-translation, x-rotation (roll), y-rotation (pitch) and z-rotation (yaw).

For the hybrid kinematic platform to be viable for industrial applications, full understanding of the rotational capabilities is required. The rotational capabilities of the robotic manipulator depend on several factors, which include the accuracy of the control algorithm, the joint freedoms, the mechanical limits that are present within the system and the overall workspace in which it can perform these operations.

Having a solid understanding of the capabilities of the robotic platform will allow the operator to program operation to the manipulator's full potential; without damaging the mechanism.

8.4.3 Setup: Combined RobotArms as a Hybrid Platform - Rotation Test

Refer to 8.1 for set up.

8.4.4 Methodology: Combined RobotArms as a Hybrid Platform - Rotation Test

1. Mount RobotArms onto laser cut board.
2. Couple the RobotArms with the common end-effector.
3. From a neutral rotation position, increase the roll value through the control program until the physical limit is reached.
4. Measure the angle achieved of the end-effector.
5. Compare the physical angle to the value input into the control program.

6. Repeat 3 - 5 with the pitch and yaw rotations.

8.4.5 Results: Combined RobotArms as a Hybrid Platform - Rotation Test

At (X0, Y0, Z200) the following roll, pitch and yaw range was established to be possible.

ROLL: -130° to 130°

PITCH: -85° to 85°

YAW: -90° to 90°

The following figures illustrated the results produced from this experiment.

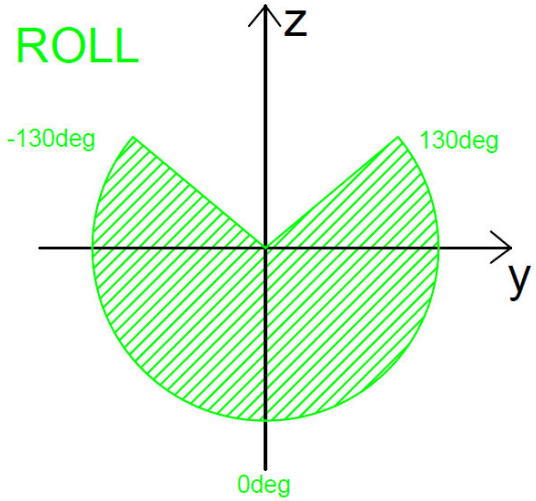

Figure 78: Graph of Roll range.

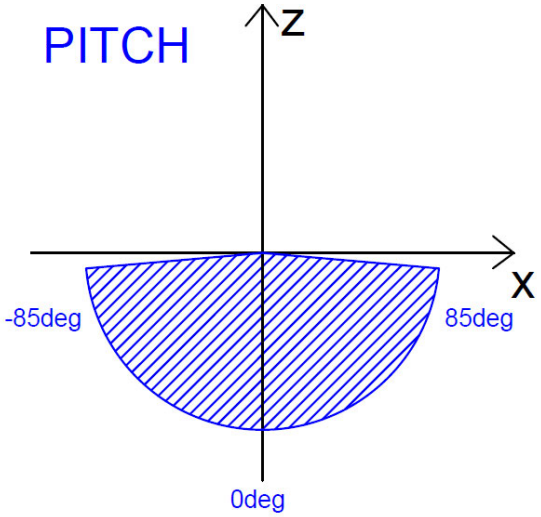

Figure 79: Graph of Pitch range.

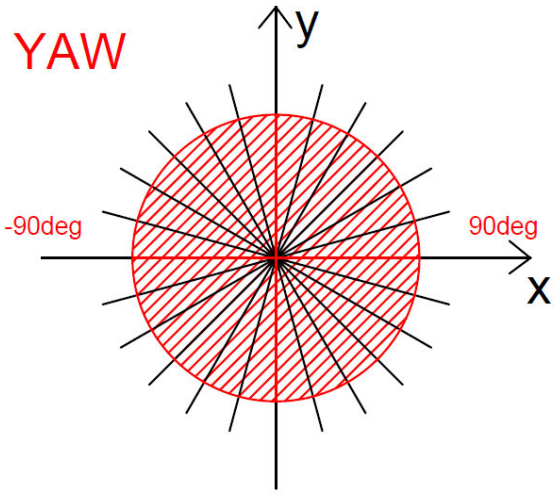

Figure 80: Graph of Yaw range.

8.4.6 Discussion: Combined RobotArms as a Hybrid Platform - Rotation Test

The test was designed to determine the amount of roll pitch and yaw rotation that is available as a maximum. This was achieved by jogging to the mechanical limit from a neutral position with the end effector placed at the origin at a height of 260mm, as outlined in 8.1.

It was found that the robot could achieve 260 degrees of roll, 170 degrees of pitch and 180 degrees of yaw.

8.5 Static Deflection Test

It had been hypothesised and proposed that there would be an increase in rigidity and therefore the amount of force that can be translated through the manipulator as a hybrid system when compared to an individual robotic arm. This test is designed to compare the theoretical and actual static deflection of an individual robot arm versus the combined hybrid mechanism.

8.5.1 Aim: Static Deflection Test

The aim of the static deflection test was to compare the actual and theoretical amount of deviation that occurs at the end effector of the individual arm versus the combined system, when placed at the same XYZ coordinate, and loaded with the same weight.

8.5.2 Theory: Static Deflection Test

Serial kinematic robotic manipulators are known to have poor rigidity when compared to their parallel counterparts. The serial kinematic chain has compounding errors through the combination of end-to-end limbs. This tends to amplify the error of each joint to the end effector. This results in a large deflection at the end effector tip.

A parallel mechanism has greater potential for rigidity due to having multiple limbs joined to the base and the end effector simultaneously. This means the errors of each joint do not compound to cause a large deflection at the end effector.

The theoretical approach via the use of Free Body Diagrams (FBD), indicates that the rigidity should increase proportionally to the number of manipulators included in the hybrid mechanism.

8.5.3 Setup: Static Deflection Test

Refer to 8.1 for set up. For the combined physical test, the common end effector to be secured to each RobotArm and jogged to 0,0,260. The dial gauge placed under the end effector and the weight applied.

8.5.4 Methodology: Static Deflection Test

1. Mount RobotArms onto laser cut board.
2. Move to 0,0,260
3. Insert dial gauge below the end-effector and zero.
4. Note gauge start value.
5. Apply weight.
6. Note gauge end value.
7. Repeat 3 times.
8. Couple the RobotArms with the common end-effector.
9. Move to 0,0,260.
10. Repeat steps 3-7.

8.5.5 Results: Static Deflection Test

8.5.1.1 Theoretical

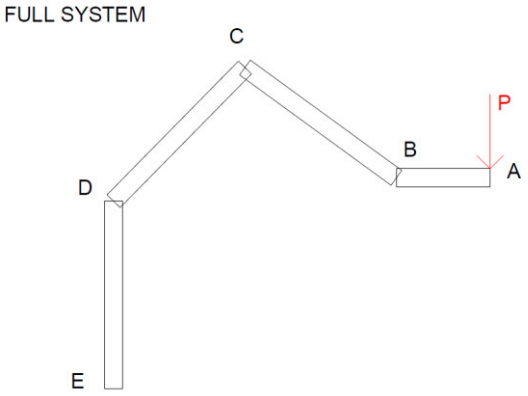

Figure 81: FBD - full system

$$\sum F = 0 \qquad \textit{eq. 47}$$

$$\sum M = 0 \qquad \textit{eq. 48}$$

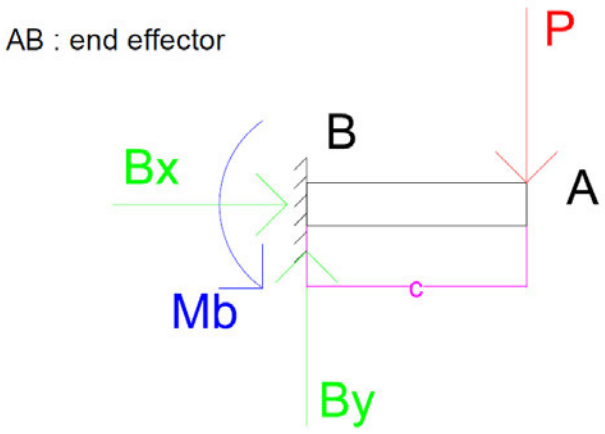

Figure 82: FBD - Link AB

$$\sum F = 0 \qquad \textit{eq. 49}$$

$$\therefore B_y = F \qquad \textit{eq. 50}$$

$$\sum M = 0 \qquad \textit{eq. 51}$$

$$-M_b + F * c = 0 \qquad \textit{eq. 52}$$

$$\therefore M_b = F * c \qquad \textit{eq. 53}$$

BC : third link

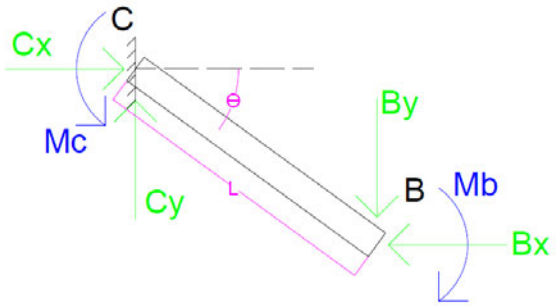

Figure 83: FBD - Link BC

$$\sum F = 0 \qquad \textit{eq. 54}$$

$$C_x = B_x \qquad \textit{eq. 55}$$

$$C_y = B_y = F \qquad \textit{eq. 56}$$

$$\sum M = 0 \qquad \textit{eq. 57}$$

$$M_b = M_c \qquad \textit{eq. 58}$$

$$\therefore F * c \; = \; B_y \cos(\theta) * L + \; B_x \sin(\theta) * L \qquad \textit{eq. 59}$$

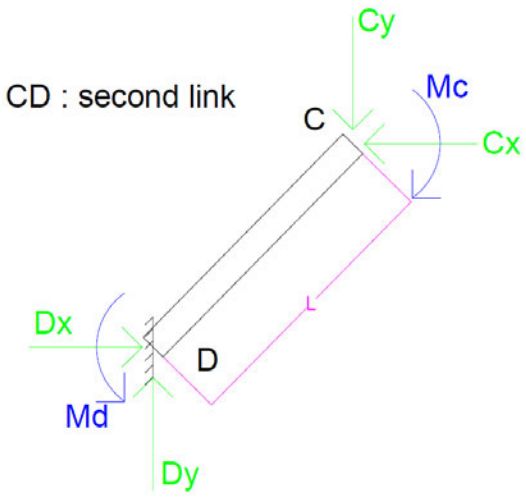

Figure 84: FBD - Link CD

$$\sum F = 0 \qquad \textit{eq. 60}$$

$$D_x = C_x = B_x \qquad \textit{eq. 61}$$

$$D_y = C_y = B_y = F \qquad \textit{eq. 62}$$

$$\sum M = 0 \qquad \textit{eq. 63}$$

$$M_b = M_c = M_d \qquad \textit{eq. 64}$$

$$\therefore F * c = B_y cos(\theta) * L + B_x sin(\theta) * L \qquad \textit{eq. 65}$$

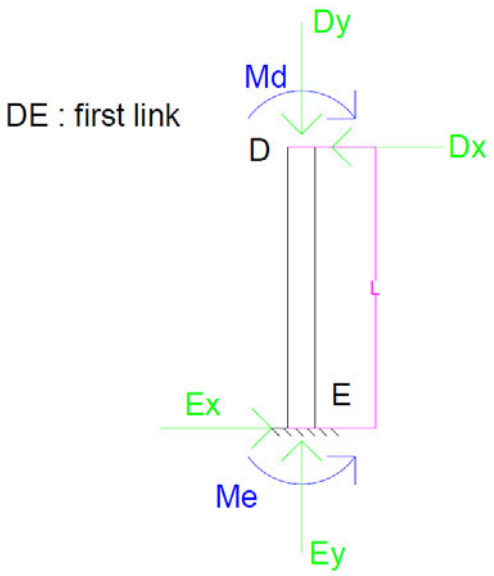

Figure 85: FBD - Link DE

$$\sum F = 0 \qquad \textit{eq. 66}$$

$$E_x = D_x = C_x = B_x \qquad \textit{eq. 67}$$

$$E_y = D_y = C_y = B_y = F \qquad \textit{eq. 68}$$

$$\sum M = 0 \qquad \textit{eq. 69}$$

$$M_b = M_c = M_d = M_e \qquad \textit{eq. 70}$$

$$\therefore F * c = B_y \cos(\theta) * L + B_x \sin(\theta) * L \qquad \textit{eq. 71}$$

8.5.1.2 Physical

For a common applied mass of 254.43g. This was the maximum weight a single robot holding torque could handle.

Table 7: Individual Static Deflection Results.

INDIVIDUAL	Test 1	Test 2	Test 3
Start Reading	2.0	2.0	2.0
End Reading	6.14	6.22	4.16
Deflection (mm)	4.14	4.22	4.16
Average Individual Deflection (mm)	4.1733		

Table 8: Combined Static Deflection Results.

COMBINED	Test 1	Test 2	Test 3
Start Reading	2.0	2.0	2.0
End Reading	3.31	3.18	3.38
Deflection (mm)	1.31	1.18	1.38
Average Combined Deflection (mm)	1.29		

$$Delta = \frac{Average\ Individual\ Deflection\ (mm)}{Average\ Combined\ Deflection\ (mm)}$$

$$\Delta = \frac{4.1733}{1.29}$$

$$\therefore \Delta = 3.235$$

8.5.6 Discussion: Static Deflection Test

The test was designed to determine the deflection that occurs at the end-effector of the individual RobotArms compared to the combined hybrid kinematic platform, for the same applied mass. The individual and combined end-effectors were loaded with the same mass when positioned in the same position, and it was discovered that the average deflection of the individual serial RobotArms was 4.1733mm versus 1.29mm for the combined hybrid platform.

Initially it was hypothesised that the combined hybrid system should be more rigid due to the increased number of motors and their holding torques, but also due to the reconfiguration from being a cantilevered serial configuration to that of a closed loop parallel system. The results confirm the hypothesis, with the combined system deflecting 3.235 times less than the individual serial RobotArms.

8.6 Maximum Lifting Load

8.6.1 Aim: Maximum Lifting Load

The aim of this experiment was to determine and compare the maximum lifting potential of the individual RobotArms versus the combined hybrid PKM.

8.6.2 Theory: Maximum Lifting Load

Theoretically the combined hybrid PKM should have roughly three times the capability to lift a load, and therefore be able to lift 3 times the amount when compared to a single RobotArm. It can be noted that although there are three serial arms that combine to make the hybrid PKM, this may not result in purely three times the lifting capability. There are geometric changes that should be taken into consideration when comparing a single serial arm versus a parallel combination. The parallel combination may result in more than three times the lifting potential.

8.6.3 Setup: Maximum Lifting Load

Refer to 8.1 for set up. For the tests, the end effector is to be jogged to 0,0,260, and then perform a pure vertical lift.

8.6.4 Methodology: Maximum Lifting Load

1. Mount RobotArms onto laser cut board.
2. Move to 0,0,260
3. Connect the weight via a cord.
4. Increase the Z value to lift the weight.
5. Increase weight until it cannot be lifted to determine the maximum.
6. Repeat with all 3 RobotArms.
7. Couple the RobotArms with the common end-effector.
8. Move to 0,0,260.
9. Repeat steps 3-6.

8.6.5 Results: Maximum Lifting Load

For a common applied weight of 254.43g. This was the maximum weight a single robot holding torque could handle.

Table 9: Individual Max Lifting Results.

INDIVIDUAL	Robot 1	Robot 2	Robot 3
Max Mass (g)	222	232	224
Average Max Mass (g)	226		

Table 10: Combined Max Lifting Results.

COMBINED	Test 1	Test 2	Test 3
Max Mass (g)	730	726	728
Average Max Mass (g)	728		

$$Delta = \frac{Average\ Combined\ Mass\ (g)}{Average\ Individual\ Mass\ (g)}$$

$$\Delta = \frac{728}{226}$$

$$\therefore \Delta = 3.221$$

8.6.6 Discussion: Maximum Lifting Load

The test was designed to determine the maximum lifting potential of the individual serial RobotArms versus the combined hybrid system. Like the static deflection test, the hypothesis was that the combined system should have approximately three times the lifting potential.

It was discovered that the average mass that the individual serial RobotArms could lift was 226 grams, when compared to the combined hybrid platform which was able to lift a mass of 728 grams. This resulted in the combined hybrid platform being able to lift 3.221 times the individual serial RobotArms. This result could be attributed to the potential increase in strength properties achieved through the reorientation from a serial configuration to that of a parallel system.

8.7 Testing and Experimentation Chapter Summary

To prove the validity of the research performed to this point the final chapter looked at physical testing of the individual and combined manipulators.

Initially the individual RobotArms were tested for accuracy and repeatability. It was found that although there was some deviation from the desired points, it was likely due to the mechanical construction of the RobotArms and not the kinematic models or associated control systems implemented. This hypothesis was confirmed in the mechanical tolerance test, that has been outlined in A3. Appendix C.

Testing then progressed onto the combined hybrid kinematic platform, which was also tested for accuracy and repeatability. It was found that although there were some difficulties synchronising the movements, the accuracy results obtained were better than the individual arms, however there was a reduction in the repeatability when compared to the individual RobotArms.

Further tests performed were to establish how much rotational range was possible for the combined manipulator. As well as static deflection and maximum lifting of the individual serial RobotArms versus the combined hybrid platform. In both of those tests, the combined hybrid platform performed more than three times better than the individual.

9. DISCUSSION

Manufacturing has transitioned into and become largely dependent on automation. There is strong evidence that the manufacturing output a country can achieve is dependent on the amount of automation available within industry. Many countries, including the BRICS collaboration, currently have a small automation footprint. For these countries to be able to compete with larger GDP countries such as USA and China, greater flexibility needs to become available within their current automation potential. Industry 4.0, in which the factory of the future has developed into, allows for a large amount of flexible automation to occur. Industry 4.0 however has been utilized by countries that have a large pre-existing automation footprint within their industry. For countries with a lower automation footprint to still be able to compete on a global market, the ability to achieve greater flexibility from their current level of automation is essential.

The topic of research performed throughout this dissertation was based around the question of *"Can simple serial kinematic chains be incorporated in parallel to create a hybrid robotic system? Subsequently, how would such a system be automated and controlled?"*. The combined hybrid platform should combine the advantageous properties of serial kinematic manipulators and of parallel kinematic manipulators.

The aim of the research was to perform investigation and develop a scaled prototype of a multipurpose, hybrid platform. The platform consisted of multiple low degree of freedom serial kinematic robotic manipulators that have the potential to operate as individuals, collaboratively, within the same workspace; as well as a single combined hybrid platform that could operate as a unified manipulator with greater potential when compared to the individual. The investigation was to be performed via the use of low-cost desktop models with focus on the reconfigurability while presenting a unified control approach to allow for combined operation.

The initial objective of the research was to become familiar with the current state-of-the-art of industrial kinematic platforms, including the current serial, parallel and combined or hybridized mechanisms available. This initial literature review portion was the foundation on which the remainder of the research would be based upon.

It was found that there was a wide array of industrial robotic manipulators implemented into industry for specific tasks and applications. It was found that most of the robotic manipulators can be grouped into three major categories, dependant on several factors. One of the major factors that dictate the application a specific mechanism can take was that of degrees of freedom (DOF). Full articulation is achieved in a platform that can achieve six degrees of freedom (6 DOF) – namely translation and rotation in the X, Y and Z axes.

In order to achieve the degrees of freedom, several combinations of joint types and actuation methods are coupled together. It was found that although there are a wide variety of combinations, the majority stick to a few distinct methods. Most joints used in industrial applications are prismatic and revolute joints. Each type of joint has a corresponding level of stiffness that can be achieved. In general, the highest level of

stiffness is desired for industrial applications. The combinations of these degrees of freedom, joint types and methods of actuation define the naming of that robotic manipulator.

Cartesian style CNC machines are widely used in applications such as machining, due to their simple design and rigid construction. These robotic platforms make use of three to five degrees of freedom, generally in a combination of prismatic and revolute joint types; actuated electrically via motors. Examples of such machines are that of milling centres, laser cutters, lathes and alike. These types of mechanisms, although hugely useful in industrial applications, are not suitable for hybridization within the scope of this research.

Serial robotic manipulators are classified as such due to their combination of joints linked one after another in a serial manner. These types of manipulators generally have a combination of revolute joints linked one after another; actuated via electric motors. It was found that the number of actuated joints in the serial chain dictate the degrees of freedom that can be achieved. A defining characteristic of serial manipulators are that they can achieve a great amount of flexibility with the trade-off of stiffness, due to the poor dynamic properties associated with having only one fixed point. It was found that any errors or inaccuracies are compounded through the serial chain of joints. Several different types of serial manipulators were explored, and their advantageous properties investigated.

Parallel platforms, like serial manipulators, are defined as such due to their combination of joints. Parallel platforms have several joint types, and actuation methods, available to them however are classified as such since each joint is coupled both to the base and the working end. This orientation of links allows parallel platforms to be extremely rigid and accurate, but with the trade-off of having a large form factor and limited articulation capabilities. Several well documented and implemented parallel platforms were investigated, including the two most popular – the Steward-Gough and the Delta platforms.

At this point it was clear the direction the research needed to continue in – exploring a combination of serial and parallel attributes into one hybrid mechanism. Therefore, investigation into current hybrid platforms was performed. Unfortunately, many of such platforms were discovered to be made up of a parallel base coupled with a serial end effector. These options, including the Tricept and Tri-variant, although somewhat hybridised, do not adequately take advantage of the positive properties of the serial and parallel formations.

A specific type of serial manipulator was discovered - the quasi-serial manipulator. Essentially a serial manipulator that had been designed with parallel mechanisms imbedded into the joint links. Quasi-serial manipulators are currently implemented in industry specifically as pick and place mechanisms due to their serial articulation and parallel strength properties. The trade-off of having parallel links embedded as nested four-bar mechanisms is that the degrees of freedom had been reduced to three purely translational freedoms.

Methods of collaboration and combined platforms were investigated, with the most notable being that of the transformable serial to parallel manipulator and that of the Puma combined system, in which two serial manipulators followed the same trajectory whilst sandwiching a part between their end-effectors. This method is the closest the literature came to combining several low DOF serial manipulators into one hybrid system.

With a firm understanding of the different classifications of industrial manipulators had been achieved, a research concept was developed determining the potential increase in functionality of the hybrid platform. Several hypothesised advantages of combining several low DOF serial manipulators into a combined hybrid mechanism were outlined.

The first potential increase that would become available via the combined hybridization of several low DOF serial manipulators was that of the overall DOF available. It was hypothesised that with the increased number of manipulators and their motors, there would be an increase in DOF. 6 DOF would allow the combined hybrid platform to achieve full articulation.

The second hypothesised advantage from the hybridisation was that of the increase in rigidity, or reduction on deflection. The research concept of combining several low DOF serial manipulators in parallel to create a combined hybrid kinematic platform has some interesting advantages for the stiffness properties. It was outlined in the literature review that serial kinematic chains have poor stiffness properties since it is a serial link with only one rigid base connection. All the subsequent joints are cantilevered from the base, which causes a compounding of errors through each joint to the end-effector. However, when these serial manipulators are combined into a parallel architecture, the advantageous effects of a parallel architecture become relevant. With more than one rigidly connected base link, and no cantilever effect through the joints to the end-effector, a parallel platform is more rigid, and therefore would deflect less during loading.

Another proposed advantage due to hybridisation was that of increased working envelope. Having several serial architectures working in an overlapping workspace, there would be an increase in the overall envelope. These individual serial robots have to potential to pass objects between one another and therefore access a larger working envelope than a single serial manipulator could. A trade-off from this concept was that of the combined hybrid systems workspace. The combined system would not be able to access all this workspace. As outlined in the literature review, parallel systems have a smaller workspace available to them. However, having the ability to work as independent serial manipulators as well as a combined hybrid parallel system, the full workspace was still available to the mechanism. The individual serial manipulators can bring components from a wider reach into the overlapping portion of the workspace. From here the manipulator could be combined into the hybrid system and work as a parallel mechanism to perform tasks that require more accuracy or rigidity, such as a machining operation.

The final research concept advantage due to hybridisation was that of increased force potential. As mentioned, serial manipulators have cantilevered joints, and therefore do not have the same potential of the parallel counterparts. Once again, when several low DOF serial manipulators are combined into a parallel system, the parallel architectures advantageous properties become available. The combined hybrid system is hypothesised to have more lifting potential, due to the parallel combination and the increase in motors.

The second objective outlined was to research, design and construct low DOF serial kinematic robots that could be implemented into larger parallel systems. Initially a QFD was performed in order to establish the driving factors that would dictate the design process. The key factors discovered were that of the adaptability of the hybrid platform, ease of use and the precision. These driving factors are dependant largely on the control methodology of the system. Cost was not ranked as a priority because the goal of

the system would be to utilize already implemented systems, in which the large capital outlay has already been made.

It was decided that a quasi-serial style manipulator would be the most suitable platform to try extending into a hybrid mechanism. A fantastic model, RobotArm, by Florin Tobler was discovered and available via the Creative Commons Licence through Thingyverse.com. This model was then 3D printed using a Creality Ender 3, and PLA+ filament.

The hardware involved for control per robot was three NEMA 17 stepper motors, three A4988 stepper drivers, an Arduino Mega 2560, and a RAMPS 1.4 breakout board.

With the initial design having been proven as a solid starting point, some updates were required. The initial design did not accommodate limit switches for homing. These were added into the design and would be implemented into the control code. The design required an updated end-effector that would be more efficient in orientation, as well as lighter for better dynamic properties. The wiring and electronics case were also updated from the original supplied with the design from Florin Tobler.

Once the robotic manipulator was in its final form, a full kinematic model was required. This meant deriving the kinematics in 3D via a geometric approach with the use of vectors. It was known that the RobotArm would be linked with two other RobotArms within the same workspace, therefore the kinematics were derived with additional vectors included that allow each RobotArm to be mounted away from the origin, at a specific rotational orientation. The rotational orientation was required due to the limited rotational availability of the first revolute joint. Each RobotArm would be oriented slightly differently to ensure that the limitation of rotation of the first joint did not hinder the overall movements and achievable workspace.

With the full 3D inverse kinematic model available, the 3D workspace of each RobotArm could be simulated. The workspace was simulated via a Monte-Carlo randomization technique. The technique creates a random point in XYZ space and then runs through the inverse kinematic model. If the IK can achieve the solution that point is plotted in a point cloud. The simulation was run with 20 000 iterations.

The kinematics of robotic manipulators had a major consideration – singularities. Singular points are points within the workspace where the mathematics don't work. If the platform is moved to such a position, several undesirable results can occur. Essentially, a singular point has an undefined solution. This could lead to several different combinations of joint positions to achieve the same point, or it could lead to a loss of one of the joint actuations/DOF, or it could cause the robot to try and achieve a point that is not within its working envelope.

Singular points need to be known and avoided. In order to discover the singular points that were present within the platforms being researched, a full 3D forward kinematic model would be required. The forward kinematic model was derived using the same methodology as the inverse kinematic model. Therefore, the forward kinematic model was derived. Having the forward kinematic model available allowed for the Jacobian matrix to be investigated. The Jacobian matrix is the point in which the joint angles translate to the XYZ coordinate. In order to discover the singular points, a simulation was performed using a Monte-Carlo randomization in which a random set of joint angles were produced. These joint angles were then fed through the forward kinematic model, in which the Jacobian matrix is inverted to achieve a solution. A

singular point is such when the Jacobian matrix fails to be inverted. At such a position, a point was plotted in a point cloud.

It was discovered through this simulation that the singularities present within the system were that only of boundary singularities. This can be considered a good result, and more than likely due to the nested parallelograms within the RobotArm architecture. Something to note with the singularities, although only to be found on the boundary, these positions would never be able to be achieved physically due to the limitations of rotation within the quasi-serial architecture. This means, the RobotArms do not have any physical singular points within its achievable working envelope. A great success for industrial applications.

The next objective was to integrate the individual serial robots into a combined parallel system, and hence with a fully defined individual RobotArm, the remaining two RobotArms could be manufactured. The next two RobotArms were manufactured in the same manner as the initial one, via 3D printing rapid prototyping. The final two RobotArms were manufactured to be the same as the updated design of the initial RobotArm.

With three RobotArms available, collaboration and hybridization could be further researched. Initially collaboration was explored via suitable mounting of each RobotArm within the same workspace. This meant that each RobotArm could work independently with an overlapping workspace, which allowed for the transfer of items between them.

In order to perform hybridization, or the coupling of the three individual RobotArms into one mechanism, a new end-effector needed to be designed and manufactured. This end-effector should allow the individual RobotArms to be coupled together in a manner that allows free movement. A keynote when combining the RobotArms into one mechanism was the addition of three rotational degrees of freedom. These rotational degrees of freedom were not available to the individual RobotArms which could only produce pure translational movements.

With the common end-effector available, the RobotArms were coupled together into one mechanism. The new mechanism that was produced was of a parallel kinematic nature. The next objective of researching and developing the inverse kinematic model for the hybrid system could be outlined. This meant that a new parallel kinematic model would need to be derived. Once again, a geometric vector method was followed. The parallel kinematic model was more involved when compared to the individual serial kinematic model due to the additional rotational degrees of freedom.

With all three RobotArms fully defined as individuals as well as a single combined mechanism, a full workspace could be simulated.

The next objective was to design and implement a suitable electronic system for the low DOF serial and combined hybrid platform, that included the implementation of the kinematic models previously derived. After all the mechanical aspects of the serial individual and parallel hybrid platform had been finalized, it was necessary to have one all-encompassing control method available. The control would need to be able to perform several tasks, including the mechanical actuation of the joints, receiving feedback from sensors and be powerful enough to perform all kinematic calculations timeously. The control would also need a

method of receiving information from the operator. Generally industrial robotic manipulators have proprietary control software, and hence for the remainder of the research a custom control algorithm would need to be developed. The aim of the research topic was to keep the costs to a minimum, and therefore it became apparent that hobbyist control hardware would be the most suitable. The control would revolve around an Arduino microcontroller and cheap hardware. The benefit of the Arduino was that it is a low-cost version of the popular PLC methodology widely implemented into industry.

At this point each RobotArm had their individual Arduino microcontroller coupled to them. The serial inverse kinematic model of each RobotArm was implemented on the individual Arduinos. The Arduino algorithm was responsible for controlling the individual RobotArms. This meant and initial homing sequence was performed on startup. The control then allows for the input of an XYZ coordinate via a string input. The string input was set up such that it has start and end markers, with a G-code or M-code command in the middle. The G-code commands that were integrated into the system were that of G28 for homing, G00 for rapid movement, and a G01 command that would create a linear interpolation, resulting in a linear movement. The M-codes integrated consisted of a M03 and M04 commands which relate to the end-effector opening and closing. The control would then calculate the required joint angles needed to achieve that coordinate. The joint angles were then converted into motor specific steps, scaled with the appropriate gear ratios and micro-stepping available.

These steps were then fed to a stepper control library, MultiStepper. This library would be responsible for the interpretation and simultaneous movement of each stepper to the required step count. This individual control proved to work well.

It was found that there was a limitation within the method of the kinematics. It was discovered that with the individual robot arms being mounted around the origin, each arm was in a different quadrant, and therefore the arctan calculation had limitations. It was found that the output of the atan2 function was between 0 and PI, but it was required to have the output between 0 and 2PI, or -PI to PI. A semi-autonomous workaround was implemented to map this output; however, a more suitable approach could be investigated in future work.

In order to combine the three Arduinos into one hybrid platform and accommodate the parallel kinematic model, a centralized node would be required. This central hub would need to be able to take inputs from the operator and simultaneously communicate with the individual Arduinos coupled to the RobotArms. It was decided that the most suitable method to achieving this would be to create a Python GUI that could receive robot specific commands, as well as combined commands. The backend of the Python GUI would be responsible for calculating the parallel kinematics for the hybrid mechanism, and then feed the required XYZ coordinate to the individual RobotArm Arduinos. The GUI should also be able to receive information back from the individual Arduinos for troubleshooting.

Something that was discovered through this Python centralized node was that the movements of the individual RobotArms were not synchronized. In order to work around this, each Arduino was connected, and a flag command generated when each RobotArm was ready to perform the movement. Only when all three RobotArms had flagged they were ready would the movements take place. This method proved to work satisfactorily; however, it should be noted that in future research, having a single more powerful control method would be more suitable. Having one control platform would allow for specific timing to

occur via the on-board clock. Having a common clock would also allow for more accurate speed control to become available.

The final objective was to develop and perform tests on the individual low DOF serial manipulators and the combined hybrid kinematic platform and analyse the data. In order to determine how well the individual and combined hybrid system can perform, a series of tests were designed and conducted. The first set of tests focused on the individual RobotArms, the second set of tests focused on the combined system.

Initially the individual RobotArms were tested for overall accuracy and repeatability by jogging them to known points on the mounting board. Once the RobotArms were at the desired location, a measurement was made from the achieved position to the desired position. It was found that there were some inaccuracies with the achieved points. The individual RobotArms achieved marks had an average accuracy of 2.795mm, and the repeatability was 2.571mm, as calculated by the ISO 9283 of 1998 standard.

In order to determine if the inaccuracies were present due to the control, or mechanical construction, a mechanical tolerance test was performed. This consisted of moving the RobotArms to the desired locations and then physically moving them around in order to establish how much mechanical play was present within the system. The mechanical play present in the system could be attributed to several things. Firstly, the fact that the RobotArms were manufactured from 3D printed components that do not have a great deal of tolerance or stiffness. Secondly the individual RobotArms were acting as serial manipulators, which as the theory illustrates, do not have the rigidity of a parallel mechanism.

This test resulted in determining the acceptable amount of inaccuracy that can be expected from further tests. It was determined that the mechanical play results in an acceptable range of approximately 5mm radius from the desired point. This result meant that the initial accuracy and repeatability was within the known error amount, and hence it could be assumed that the control system, including the kinematic model, were operating as they should.

It was discovered that the robots performed well, however it can be noted that the achieved position of each robot was off by the same error distance, but in different directions. Generally, the error achieved by each RobotArm was in the direction of their base. It was later discovered that the possible reason for such a consistent error was due to the mounting of the permanent marker pens, which had a taper to their design and hence were not perfectly perpendicular to the mounting board.

The next phase of testing was aimed at the combined hybridized platform, in which all three RobotArms were coupled together and acting as a combined hybrid single parallel mechanism. It was hypothesised ahead of these tests that the results obtained should be more accurate than the individual RobotArms due to the increased rigidity of the parallel mechanism. This hypothesis was confirmed in the results obtained from the combined accuracy test, in which the marks made were had an accuracy result of 2.253mm versus 2.795mm for the individuals. The repeatability of the hybrid was 3.134mm versus 2.571mm for the individuals. The reduction in repeatability of the combined hybrid system when compared to the individual could be due to the synchronisation of the movements between the three independent Arduinos. The kinematic calculations of each RobotArm had different durations, therefore a work around was implemented to time the beginning of the movement. This work around worked to gather results, however future work should implement a single unified control methodology in one microcontroller with a single

clock or look at combining several microcontrollers over I2C that share a common clock to allow for greater synchronisation and timing of movements.

The next test performed was to establish the amount of rotational freedom available within the combined system. At the origin it was established that the end effector had 260 degrees of roll, 170 degrees of pitch and 180 degrees of yaw.

The final tests performed were that of the static deflection and the maximum lifting load. It was hypothesised originally that the combined system should be able to have three times the potential when compared to the individual serial manipulators. In both the static deflection and the maximum lifting load tests performed, it was found that the combined hybrid platform had in excess of three times the capabilities of a single serial RobotArm. The static deflection of the combined hybrid platform was 3.235 times less than the individual. The maximum lifting load of the combined hybrid system was 3.221 times that of a single serial manipulator. These results show great potential for the hybridised system, as it was able to achieve results greater than the sum of the individual parts. It can be assumed that the reason for these results is due to the reorientation from serial to parallel configurations.

The results obtained from all the tests bode well for the overall design and implementation of the control and hybrid platform as a viable industrial solution.

10. CONCLUSION

The research question of whether several low degree of freedom serial arms could be incorporated into a hybrid parallel mechanism, and how such a platform would be controlled was investigated and documented throughout the research.

The aim of developing a low-cost desktop model to perform hybridization of serial to parallel kinematics was to be produced and investigated. This led to the selection of a quasi-serial kinematic model to be chosen as the central architecture for the research. The aim of how to control such a mechanism was developed and hence a control structure that could calculate the kinematics and move the motors accordingly was achieved. The objectives outlined in the initial stages of the research were followed and resulted in the identifying of the current industrial robots and their modes of reconfigurability. The production of several low degree of freedom serial manipulators were implemented; and hence the investigation into different methods of hybridization of these serial manipulators was performed. The different methods of performing kinematic derivations were followed and outlined until an all-encompassing control algorithm was produced. The final objective was to develop tests to indicate the level of success achieved throughout the research and develop tangible factors to the success.

In order to flow through the objectives outlined and ultimately achieve the desired aims of the research question the initial research was performed on the current state-of-the-art industrial robotic platforms, of both the serial and parallel design, and outlined. It was found that the final mechanism should be of a combination of several quasi-serial mechanisms. This then led to the production of several low-cost desktop models via rapid prototyping methods; that were then incorporated into a hybridized kinematic platform. It can be concluded that to aid in further research, the rapid prototyping aspect should have an iterative approach to ensure that the overall gear meshing is satisfactory, as it was found later through the testing that a major aspect of the inaccuracies was due to mechanical backlash.

The kinematics of such a platform was then derived and implemented into an electronic system and control algorithm via Arduino microcontrollers and a Python centralized GUI. It can be concluded that the closed loop vector methods utilized to derive both the forward and inverse kinematic models proved a valid method for manipulators of this architecture. It was discovered that although this method of control integration proved to be successful, future work should focus on the use of a single microcontroller that has a single clock to allow for exact synchronisation of movements.

The kinematic models allowed for the investigation into the workspace and singularities of said mechanism. The workspace and singularity analysis performed was done via a Monte-Carlo randomisation method, this proved to be a robust analysis tool for such investigations. It was discovered that the quasi-serial robotic architecture has only boundary singularities present, however, due to the nested parallelograms within its structure, these singularities would never physically be possible to achieve. This means for this class of robot architecture; no singularities are within the working envelope.

Finally, to validate the research several tests were then performed on the platform to determine how suitable it would be for industry. The tests focused on accuracy and repeatability as the two major performance parameters. It can be concluded that the accuracy and repeatability were good, with the errors that were present due to the mechanical construction of the platform.

Since all the aims and objectives outlined were able to be achieved and hence the research question answered, it can be considered a success.

REFERENCES

[1] "Animated Chart of the Day: World's Top Ten Manufacturing Nations, 1970 ...." 05 Jul. 2019," in *Google*, ed. https://www.aei.org/carpe-diem/animated-chart-of-the-day-worlds-top-ten-manufacturing-nations-1970-to-2017/: AEI, 2019.

[2] "South Africa's ratio of industrial robots to employees amongst the global top 40," in *Google* N. o. i. r. b. country, Ed., ed. Consultancy.co.za, 2018.

[3] M. Calì and G. Presidente, "Automation and manufacturing performance in a developing country," 2021.

[4] N. Sharif and Y. Huang, "Industrial automation in China's "workshop of the world"," *The China Journal,* vol. 81, no. 1, pp. 1-22, 2019.

[5] F. Carbonero, E. Ernst, and E. Weber, "Robots worldwide: The impact of automation on employment and trade," 2020.

[6] H. Besada, K. Winters, and E. Tok, "South Africa in the BRICS: Opportunities, challenges and prospects," *Africa insight,* vol. 42, no. 4, pp. 1-15, 2013.

[7] Z. Pandilov and V. Dukovski, "COMPARISON OF THE CHARACTERISTICS BETWEEN SERIAL AND PARALLEL ROBOTS," *Acta Technica Corviniensis-Bulletin of Engineering,* vol. 7, no. 1, 2014.

[8] L.-W. Tsai, *Robot analysis: the mechanics of serial and parallel manipulators*. John Wiley & Sons, 1999.

[9] J. Barnfather, M. Goodfellow, and T. Abram, "Positional capability of a hexapod robot for machining applications," *The International Journal of Advanced Manufacturing Technology,* vol. 89, pp. 1103-1111, 2017.

[10] A. Changela and K. Hirpara, "Geometric Approach for Inverse Kinematics Solution: 3-PSU Parallel Kinematic Manipulator," *International Journal of Engineering Research and Technology,* vol. 1, no. 2, 2012.

[11] A. Karim and A. Verl, "Challenges and obstacles in robot-machining," in *IEEE ISR 2013*, 2013: IEEE, pp. 1-4.

[12] J. Wang, H. Zhang, and T. Fuhlbrigge, "Improving machining accuracy with robot deformation compensation," in *2009 IEEE/RSJ International Conference on Intelligent Robots and Systems*, 2009: IEEE, pp. 3826-3831.

[13] U. Schneider, J. D. Posada, M. Drust, and A. Verl, "Position control of an industrial robot using an optical measurement system for machining purposes," in *International Conference on Manufacturing Research (ICMR)*, 2013, pp. 307-312.

[14] Y. Chen and F. Dong, "Robot machining: recent development and future research issues," *The International Journal of Advanced Manufacturing Technology,* vol. 66, no. 9-12, pp. 1489-1497, 2013.

[15] S. M. Sackey and A. Bester, "Industrial engineering curriculum in Industry 4.0 in a South African context," *South African Journal of Industrial Engineering,* vol. 27, no. 4, pp. 101-114, 2016.

[16] M. Hermann, T. Pentek, and B. Otto, "Design principles for industrie 4.0 scenarios—paper presented at the 49th Hawaii international conference on system sciences," *IEEE Computer Society, DOI,* vol. 10, 2016.

[17] R. Drath and A. Horch, "Industrie 4.0: Hit or hype? IEEE Ind Electron Mag 8: 56–58," ed, 2014.

[18] S. Engines. "Industry 4.0 and how smart sensors make the difference." Spectral Engines. https://www.spectralengines.com/articles/industry-4-0-and-how-smart-sensors-make-the-difference (accessed 2023).

[19] X. Yao and Y. Lin, "Emerging manufacturing paradigm shifts for the incoming industrial revolution," *The International Journal of Advanced Manufacturing Technology,* vol. 85, pp. 1665-1676, 2016.
[20] J. Iqbal, R. U. Islam, S. Z. Abbas, A. A. Khan, and S. A. Ajwad, "Automating industrial tasks through mechatronic systems–A review of robotics in industrial perspective," *Tehnički vjesnik,* vol. 23, no. 3, pp. 917-924, 2016.
[21] L. E. Jörg Tertünte. "Switching from robot systems to Cartesian handling systems." Festo Marketing Concepts. https://www.linearmotiontips.com/switching-robot-systems-cartesian-handling-systems/ (accessed 20/3, 2018).
[22] K. Sawai, Y. Nomaguchi, and K. Fujita, "Fundamental framework toward optimal design of product platform for industrial three-axis linear-type robots," *Journal of Computational Design and Engineering,* vol. 2, no. 3, pp. 157-164, 2015/07/01/ 2015, doi: https://doi.org/10.1016/j.jcde.2015.03.002.
[23] R. Vaughn and N. Charlotte, "The Difference between Cartesian, Six-Axis, and SCARA Robots," *Machine Design,* 2013.
[24] J. Pandremenos, C. Doukas, P. Stavropoulos, and G. Chryssolouris, "Machining with robots: a critical review," *Proceedings of DET2011,* pp. 1-9, 2011.
[25] A. Yeshmukhametov, M. Kalimoldayev, O. Mamyrbayev, and Y. Amirgaliev, "Design and kinematics of serial/parallel hybrid robot," in *Control, Automation and Robotics (ICCAR), 2017 3rd International Conference on*, 2017: IEEE, pp. 162-165.
[26] J. Pettersson. "Seminarium med fokus på begreppet ”Industry 4.0”." PackNews. http://www.packnyheter.se/default.asp?id=11312&show=more (accessed 21/3, 2018).
[27] R. M. Crowder. "ROBOT GEOMETRY." Automation and Robotics. http://www.soton.ac.uk/~rmc1/robotics/argeometry.htm (accessed 20/3, 2018).
[28] X. Wang and L. Baron, *Topology and Geometry of Serial and Parallel Manipulators*. 2008.
[29] N. Bajaj, A. Spiers, and A. M. Dollar, "State of the Art in Prosthetic Wrists: Commercial and Research Devices," presented at the ICORR, Singapore, 2015, 2015. [Online]. Available: file:///C:/Users/user/Downloads/Bajaj_ICORR2015.pdf.
[30] C. M. Gonzalez, "What’s the Difference Between Industrial Robots?," *Machine Design,* no. December 2016, pp. 1-4, 2016. [Online]. Available: http://www.machinedesign.com/datasheet/what-s-difference-between-industrial-robots-pdf-download.
[31] M. S. N. Kale. Fundamental of Robotic Manipulator [Online] Available: https://www.slideshare.net/snkalepvpit/fundamental-of-robotic-manipulator
[32] A. Robots, "Spherical Robots," vol. 2018, ed. AllOnRobots.com, 2013.
[33] LabAutopedia. "Robotic Sample Transport." http://www.labautopedia.org/mw/Robotic_Sample_Transport (accessed 20/3, 2018).
[34] C. Dumas, S. Caro, M. Chérif, S. Garnier, and B. Furet, "A methodology for joint stiffness identification of serial robots," in *2010 IEEE/RSJ International Conference on Intelligent Robots and Systems*, 18-22 Oct. 2010 2010, pp. 464-469, doi: 10.1109/IROS.2010.5652140.
[35] Z. Pandilov and V. Dukovski, "Parallel kinematics machine tools: Overview-from history to the future," *Annals of the Faculty of Engineering Hunedoara,* vol. 10, no. 2, p. 111, 2012.
[36] L. Romdhane, "Design and analysis of a hybrid serial-parallel manipulator," *Mechanism and Machine Theory,* vol. 34, no. 7, pp. 1037-1055, 1999.
[37] M. Carricato and V. Parenti-Castelli, "Singularity-Free Fully-Isotropic Translational Parallel Mechanisms," *The International Journal of Robotics Research,* vol. 21, no. 2, pp. 161-174, 2002, doi: 10.1177/027836402760475360.
[38] J.-P. Merlet, *Parallel robots*. Springer Science & Business Media, 2006.
[39] A. A. Shaik, "Design, modelling and simulation of 2 novel 6 DOF hybrid machines," University of KwaZulu-Natal, Durban, 2012.

[40] B. Dasgupta and T. S. Mruthyunjaya, "The Stewart platform manipulator: a review," *Mechanism and Machine Theory,* vol. 35, no. 1, pp. 15-40, 2000/01/01/ 2000, doi: https://doi.org/10.1016/S0094-114X(99)00006-3.

[41] B. R. Hopkins and R. L. Williams, "Kinematics, design and control of the 6-PSU platform," *Industrial Robot: An International Journal,* vol. 29, no. 5, pp. 443-451, 2002.

[42] M. A. Laribi, L. Romdhane, and S. Zeghloul, "Analysis and dimensional synthesis of the DELTA robot for a prescribed workspace," *Mechanism and Machine Theory,* vol. 42, no. 7, pp. 859-870, 2007/07/01/ 2007, doi: https://doi.org/10.1016/j.mechmachtheory.2006.06.012.

[43] A. Fair. "ABB Robotics Pack Expo 2013 exhibit highlights new 8 kg IRB 360 FlexPicker and comprehensive palletizing portfolio." https://www.automation-fair.com/2013/09/23/abb-robotics-pack-expo-2013-exhibit-highlights-new-8-kg-irb-360-flexpicker-and-comprehensive-palletizing-portfolio/ (accessed 5 May, 2023).

[44] Y. Li and Q. Xu, "Stiffness analysis for a 3-PUU parallel kinematic machine," *Mechanism and Machine Theory,* vol. 43, no. 2, pp. 186-200, 2008/02/01/ 2008, doi: https://doi.org/10.1016/j.mechmachtheory.2007.02.002.

[45] L. Wang, H. Xu, and L. Guan, "Optimal design of a 3-PUU parallel mechanism with 2R1T DOFs," *Mechanism and Machine Theory,* vol. 114, pp. 190-203, 2017/08/01/ 2017, doi: https://doi.org/10.1016/j.mechmachtheory.2017.03.008.

[46] V. Poppeova, J. Uricek, and V. Bulej, "The development of mechanism based on hybrid kinematic structure," *Development,* no. 228/229, 2011.

[47] H. T. Liu, T. Huang, X. M. Zhao, J. P. Mei, and D. G. Chetwynd, "Optimal design of the TriVariant robot to achieve a nearly axial symmetry of kinematic performance," *Mechanism and Machine Theory,* vol. 42, no. 12, pp. 1643-1652, 2007/12/01/ 2007, doi: https://doi.org/10.1016/j.mechmachtheory.2006.12.001.

[48] T. Huang, M. Li, X. M. Zhao, J. P. Mei, D. G. Chetwynd, and S. J. Hu, "Conceptual design and dimensional synthesis for a 3-DOF module of the TriVariant-a novel 5-DOF reconfigurable hybrid robot," *IEEE Transactions on Robotics,* vol. 21, no. 3, pp. 449-456, 2005, doi: 10.1109/TRO.2004.840908.

[49] P. TRICEPT. "Tricept T9000." http://www.pkmtricept.com/productos/index.php?id=en&Nproduct=1238061426 (accessed 28/8, 2018).

[50] Y. Y. Wang, T. Huang, X. M. Zhao, J. P. Mei, D. G. Chetwynd, and S. J. Hu, "Finite Element Analysis and Comparison of Two Hybrid Robots-the Tricept and the TriVariant," in *2006 IEEE/RSJ International Conference on Intelligent Robots and Systems*, 9-15 Oct. 2006 2006, pp. 490-495, doi: 10.1109/IROS.2006.282522.

[51] Y. Jin *et al.*, "Kinematic analysis and dimensional synthesis of exechon parallel kinematic machine for large volume machining," *Journal of Mechanisms and Robotics,* vol. 7, no. 4, p. 041004, 2015.

[52] J. Zhang, H. Fang, and T. Tang, *Two comprehensive indices–based static performance evaluation for the tripod parallel kinematic machine*. 2017, p. 168781401773411.

[53] A. A. Shaik, N. S. Tlale, and G. Bright, "A new hybrid machine design for a 6 DOF industrial robot arm," 2012.

[54] L. Sun and L. Fang, "An approximation method for stiffness calculation of robotic arms with hybrid open-and closed-loop kinematic chains," *Advances in Mechanical Engineering,* vol. 10, no. 2, p. 1687814018761297, 2018.

[55] A. Klimchik, E. Magid, S. Caro, K. Waiyakan, and A. Pashkevich, "Stiffness of serial and quasi-serial manipulators: comparison analysis," in *MATEC Web of Conferences*, 2016, vol. 75: EDP Sciences, p. 02003.

[56] FANUC. "M-410iB/450." https://www.fanuc.eu/bg/en/robots/robot-filter-page/m-410-series/m-410ib-450 (accessed 20/11, 2018).

[57] T. K. Tanev, "Kinematics of a hybrid (parallel–serial) robot manipulator," *Mechanism and machine theory,* vol. 35, no. 9, pp. 1183-1196, 2000.
[58] X. Liu, C. Qiu, Q. Zeng, and A. Li, "Kinematics analysis and trajectory planning of collaborative welding robot with multiple manipulators," *Procedia Cirp,* vol. 81, pp. 1034-1039, 2019.
[59] X. Liu, C. Qiu, Q. Zeng, A. Li, and N. Xie, "Time-energy optimal trajectory planning for collaborative welding robot with multiple manipulators," *Procedia Manufacturing,* vol. 43, pp. 527-534, 2020.
[60] C. Y. Lai, D. E. Villacis Chavez, and S. Ding, "Transformable parallel-serial manipulator for robotic machining," *The International Journal of Advanced Manufacturing Technology,* vol. 97, pp. 2987-2996, 2018.
[61] H. Shen, L. Pan, and J. Qian, "Research on large-scale additive manufacturing based on multi-robot collaboration technology," *Additive Manufacturing,* vol. 30, p. 100906, 2019.
[62] K. Afsari, S. Gupta, M. Afkhamiaghda, and Z. Lu, "Applications of collaborative industrial robots in building construction," in *54th ASC Annual International Conference Proceedings*, 2018, pp. 472-479.
[63] D. Kragic, J. Gustafson, H. Karaoguz, P. Jensfelt, and R. Krug, "Interactive, Collaborative Robots: Challenges and Opportunities," in *IJCAI*, 2018, pp. 18-25.
[64] K. G. Gim, J. Kim, and K. Yamane, "Design of a serial-parallel hybrid leg for a humanoid robot," in *2018 IEEE International Conference on robotics and automation (ICRA)*, 2018: IEEE, pp. 6076-6081.
[65] S. Kumar, H. Wöhrle, J. de Gea Fernández, A. Müller, and F. Kirchner, "A survey on modularity and distributivity in series-parallel hybrid robots," *Mechatronics,* vol. 68, p. 102367, 2020.
[66] G. Montemayor and J. T. Wen, "Decentralized collaborative load transport by multiple robots," in *Proceedings of the 2005 IEEE International Conference on Robotics and Automation*, 2005: IEEE, pp. 372-377.
[67] T. Sugar, J. P. Desai, V. Kumar, and J. P. Ostrowski, "Coordination of multiple mobile manipulators," in *Proceedings 2001 ICRA. IEEE International Conference on Robotics and Automation (Cat. No. 01CH37164)*, 2001, vol. 3: IEEE, pp. 3022-3027.
[68] L. Chaimowicz, T. Sugar, V. Kumar, and M. F. M. Campos, "An architecture for tightly coupled multi-robot cooperation," in *Proceedings 2001 ICRA. IEEE international conference on robotics and automation (cat. no. 01CH37164)*, 2001, vol. 3: IEEE, pp. 2992-2997.
[69] N. Emissary. "What is Pitch, Roll and Yaw." https://emissarydrones.com/what-is-roll-pitch-and-yaw (accessed 19/3, 2018).
[70] C. Dumas, S. Caro, M. Cherif, S. Garnier, and B. Furet, "Joint stiffness identification of industrial serial robots," *Robotica,* vol. 30, no. 4, pp. 649-659, 2011, doi: 10.1017/S0263574711000932.
[71] Robot-Welding. "Robot Types." http://www.robot-welding.com/robots.htm (accessed 20/3, 2018).
[72] J. Terninko, *Step-by-step QFD: customer-driven product design*. Routledge, 2018.
[73] F. Tobler. "RobotArm." https://www.thingiverse.com/thing:1718984 (accessed 15/9/2018, 2018).
[74] N. Shahrubudin, T. C. Lee, and R. Ramlan, "An overview on 3D printing technology: Technological, materials, and applications," *Procedia Manufacturing,* vol. 35, pp. 1286-1296, 2019.
[75] B. Kelly, J. Padayachee, and G. Bright, "Quasi-serial Manipulator for Advanced Manufacturing Systems," in *ICINCO (2)*, 2019, pp. 300-305.
[76] D. ELECTRONICS. https://www.diyelectronics.co.za/store/ (accessed 4/8/2023, 2023).
[77] B. Kelly, J. Padayachee, and G. Bright, "Quasi-Serial Manipulator-Inverse Kinematics and Workspace Analysis for Industrial Automation," in *2020 International SAUPEC/RobMech/PRASA Conference*, 2020: IEEE, pp. 1-6.
[78] V. Smutný, "Forward and Inverse Kinematics of Serial Manipulators," in *Robotics*, ed: Czech Technical University in Prague, 2012.

[79] A. Ghosal, "Kinematics of serial manipulators," *Department of Mechanical Engineering, Indian Institute of Science, Bangalore., 2015,* 2015.
[80] M. Aboelnasr, H. M. Bahaa, O. J. J. o. M. E. Mokhiamar, and Sciences, "Novel use of the Monte-Carlo methods to visualize singularity configurations in serial manipulators," vol. 15, no. 2, pp. 7948-7963, 2021.
[81] M. Spong and M. Vidyasagar, "VELOCITY KINEMATICS–THE MANIPULATOR JACOBIAN," *Robot dynamics and control. Wiley India Pvt. Limited,* pp. 99-100, 2008.
[82] R. Y. Abdolmalaki, "Geometric Jacobians derivation and kinematic singularity analysis for smokie robot manipulator & the Barrett WAM," *arXiv preprint arXiv:1707.04821,* 2017.
[83] K. M. Lynch and F. C. Park, *Modern robotics*. Cambridge University Press, 2017.
[84] P. Lambert and J. Herder, *Parallel robots with configurable platforms: Fundamental aspects of a new class of robotic architectures*. 2015.
[85] M. W. Spong, S. Hutchinson, and M. Vidyasagar, *Robot Modeling and Control*. ProQuest Information and Learning Company, 2005.
[86] *Manipulating industrial robots performance criteria and related test methods,* ISO9283, 1998.
[87] C.-V. Lidholm and V. Runnquist, "Accuracy and Repeatability of a Robotic Arm," ed, 2021.
[88] I. Kuric, V. Tlach, Z. Ságová, M. Císar, and I. Gritsuk, "Measurement of industrial robot pose repeatability," in *MATEC web of conferences*, 2018, vol. 244: EDP Sciences, p. 01015.

A1. APPENDIX A: QFD

A1.1 QFD

Legend		
⊙	Strong Relationship	9
O	Moderate Relationship	3
▲	Weak Relationship	1
++	Strong Positive Correlation	
+	Positive Correlation	
−	Negative Correlation	
▼	Strong Negative Correlation	
▼	Objective Is To Minimize	
▲	Objective Is To Maximize	
X	Objective Is To Hit Target	

Figure 86: QFD Legend.

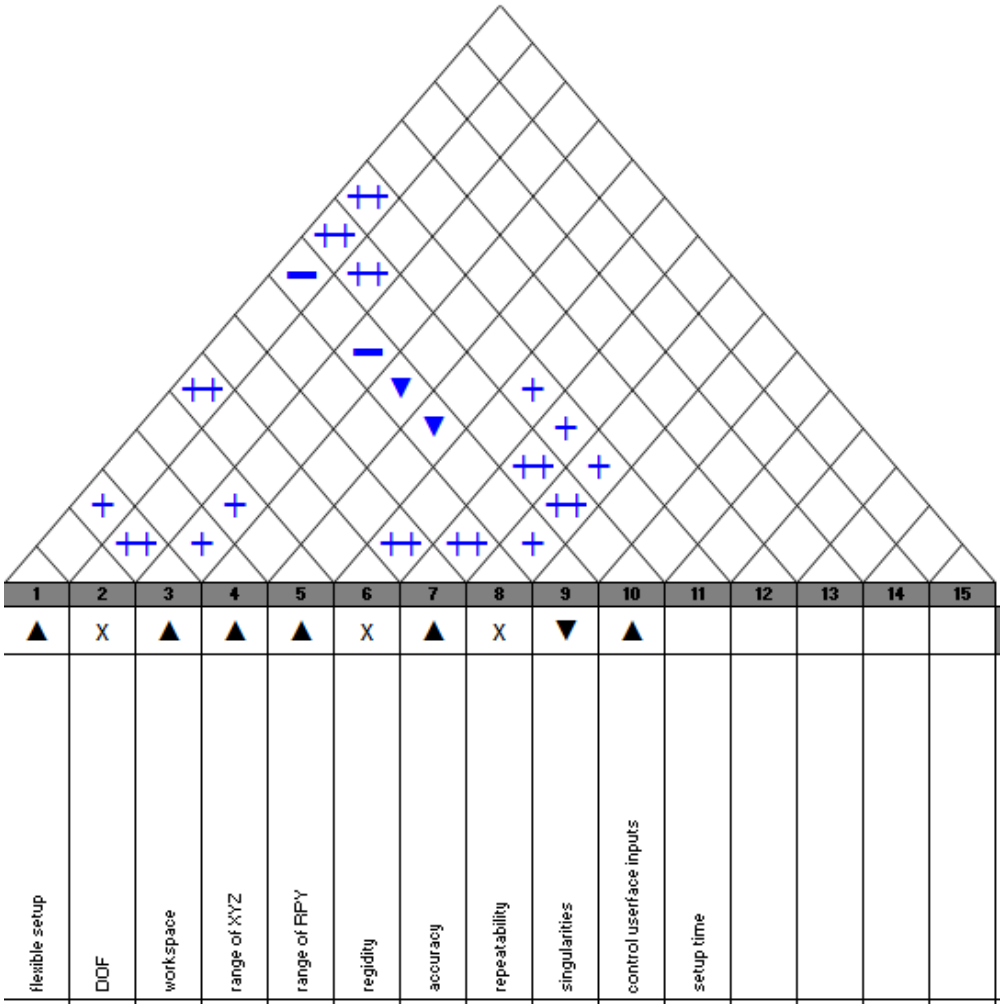

Figure 87: QFD Attic.

Column #		1	2	3	4	5	6	7	8	9	10	11	12	13	14	15
Direction of Improvement: Minimize (▼), Maximize (▲), or Target (x)		▲	X	▲	▲	▲	X	▲	X	▼	▲					
Row #	Max Relationship Value in Row	Relative Weight	Weight / Importance	Demanded Quality (a.k.a. "Customer Requirements" or "whats") \ Quality Characteristics (a.k.a. "Functional Requirements" or "Hows")												
1	9	19.1	9.0	ease of use	○	○	○					◎				
2	9	17.0	8.0	adaptable to many applications	◎	◎	○	○	◎	○	○	○				
3	9	17.0	8.0	low cost			○	○	○		◎	○				
4	9	17.0	8.0	high precision	◀		○	◎	◎	◎	○					
5	9	14.9	7.0	XYZ travel	○	◎	○	◎			○					
6	9	14.9	7.0	RPY rotation	○	◎	○		◎		○					
7																
8																
9																
10																

Figure 88: QFD Customer Requirements.

Target or Limit Value		multiple configurations	6	400mm^3	400mm	120deg	less than 1mm backlash	2mm & 2deg	2mm & 2deg	0	6	10 min					
Difficulty (0=Easy to Accomplish, 10=Extremely Difficult)		8	9	5	5	5	7	7	7	9	8	6					
Max Relationship Value in Column		9	9	9	9	9	9	9	9	9	9	9					
Weight / Importance		317.0	478.7	300.0	185.1	185.1	255.3	204.3	255.3	568.1	427.7	223.4					
Relative Weight		9.3	14.1	8.8	5.4	5.4	7.5	6.0	7.5	16.7	12.6	6.6					

Figure 89: QFD Target Specifications.

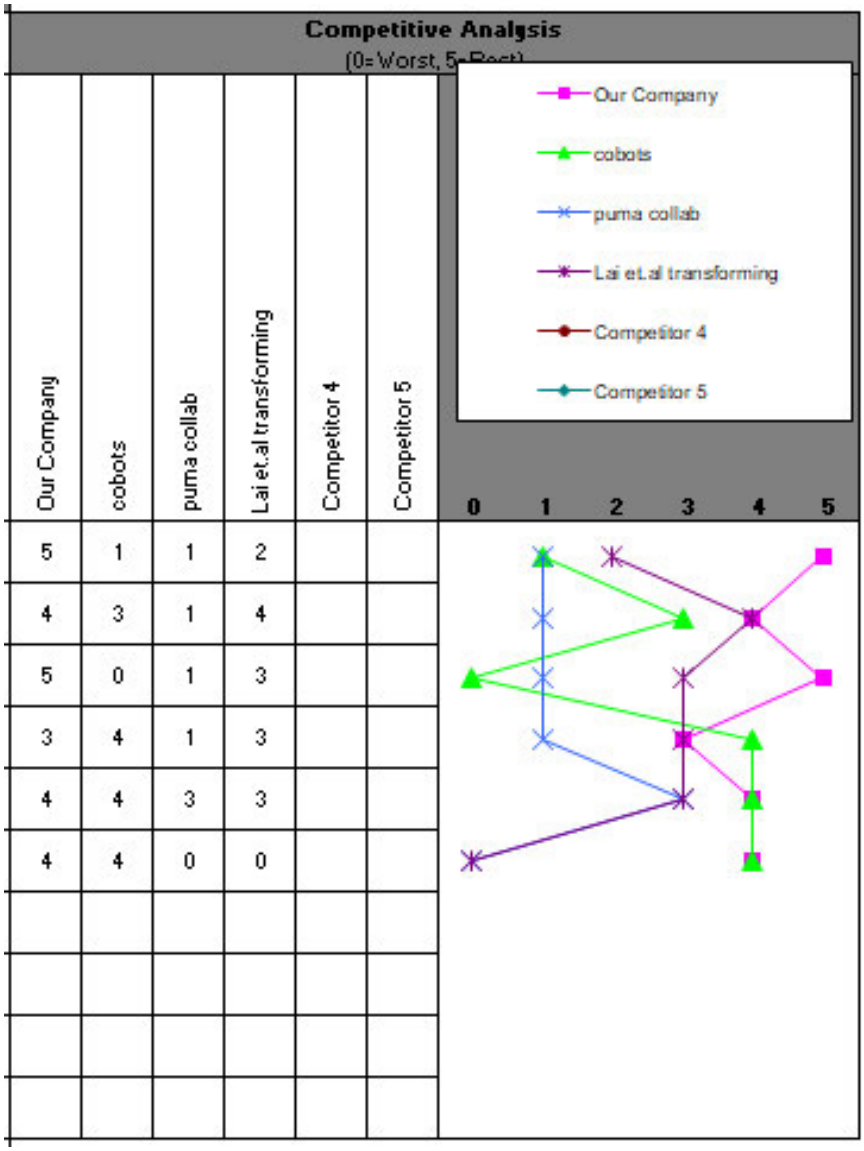

Our Company	cobots	puma collab	Lai et.al transforming	Competitor 4	Competitor 5
5	1	1	2		
4	3	1	4		
5	0	1	3		
3	4	1	3		
4	4	3	3		
4	4	0	0		

Figure 90: QFD Competitors.

A2. APPENDIX B: LINKS

The following links give access to the Arduino and Python code used for control; as well as the Octave and Python scripts used to perform the workspace and singularity simulations via the Monte-Carlo randomisation technique.

https://stuukznac-my.sharepoint.com/personal/212501838_stu_ukzn_ac_za/_layouts/15/onedrive.aspx?view=0

The following is a link to a video demonstration of the operational platform.

https://www.youtube.com/watch?v=2aIEhKJOjO4

A3. APPENDIX C: TESTING

A3.1 Individual RobotArm – Control Resolution Investigation

A3.1.1 Aim: Individual RobotArm – Control Resolution Investigation

Calculate the theoretical control resolution and movement resolution that is available to the robotic platform and establish a benchmark for absolute accuracy and repeatability.

A3.1.2 Theory: Individual RobotArm – Control Resolution Investigation

The control resolution is a function of the microcontroller that has been utilised to perform the kinematic calculations, as well as a function of the gear ratios that have been introduced within the physical system. It is important to understand what the system is theoretically possible of, in order to establish whether future inaccuracies are due to a poor available resolution or rather if there are other factors influencing the results.

A3.1.3 Methodology: Individual RobotArm – Control Resolution Investigation

1. Establish the bits available to the microcontroller.
2. Establish the microstepping of the motor controllers.
3. Establish the gear ratios and link lengths.
4. Range of motion
5. Tabulate findings.
6. Perform calculations.

Use the following equations to establish the control resolution:

$$CR = \frac{range\ of\ motion}{2^n} \qquad \textit{eq. 72}$$

A3.1.4 Results: Individual RobotArm – Control Resolution Investigation

The following tables and calculations outline the results observed from this investigation.

Table 11: Control resolution values.

ITEM	VALUE
Microcontroller	8 bit
Microstepping	16
Gear Ratio	3.56

Link length	120mm
Range of motion	300 deg

$$CR1 = \frac{300}{2^8} \quad \textit{eq. 73}$$

$$CR1 = 1.17\ deg/bit \quad \textit{eq. 74}$$

$$\therefore CR = \frac{2 * \pi * 120 * 1.17 * 3200 * 3.56}{360} \quad \textit{eq. 75}$$

$$\therefore CR = 0.000215\ mm/step \quad \textit{eq. 76}$$

A3.1.5 Discussion: Individual RobotArm – Control Resolution Investigation

In order to have a firm understanding of the capabilities of the robotic platform when performing further analysis and investigation, it was required to understand how much resolution was available through the control system. If the control resolution was found to be a large value, it would open possibilities that future inaccuracies were due to the control being incapable of achieving the positions accurately.

With the 8-bit microcontroller coupled with 1/16th microstepping and a 3.56:1 gear ratio it was calculated that the overall linear resolution available was 0.000215mm/step. Meaning theoretically the control system can move 2.15µm per controllable step. This finding allows the assumption that the control setup has extremely fine resolution available.

With the extremely fine control resolution discovered, a benchmark for future tests has been established. Any inaccuracies discovered in the subsequent testing are due to other factors over and above the control resolution available.

A3.2 Individual RobotArm - Mechanical Tolerance Test

A3.2.1 Aim: Individual RobotArm - Mechanical Tolerance Test

The aim of this experiment was to determine how much mechanical play is apparent within the construction of the RobotArms.

A3.2.2 Theory: Individual RobotArm - Mechanical Tolerance Test

It has been discovered that there is a deviation of the desired coordinate position to the actual achieved position. In order to isolate the problem, the control portion of the previous experiments was to be made redundant. This will allow us to find the true deviation that is acceptable for the desktop versions of the RobotArms.

3D printing has many factors and thus allows for irregular or poor tolerances in construction. It was required to find how much mechanical play is coming into effect to be able to further enhance the mechanical design, or to establish whether the kinematics and control portion was inaccurate.

If it was discovered that there is a minimal amount of play within the mechanical construction, then further work needs to be done to the kinematics and overall control algorithm in place.

A3.2.3 Setup: Individual RobotArm - Mechanical Tolerance Test

Refer to 8.1 for set up.

A3.2.4 Methodology: Individual RobotArm - Mechanical Tolerance Test

At each coordinate point, the operator should physically move the end of the probe about while the RobotArm keeps a fixed position. If the marker can make several, or larger dots on the page it can be assumed that most of the inaccuracies discovered in the previous experiment are in fact due to mechanical play.

1. Mount RobotArms onto laser cut board.
2. Secure blank page within the XY workspace.
3. Feed points via G-code to the RobotArms to achieve. Ensure that the desired XYZ points take into consideration the permanent marker tool length. In this case the desired XY coordinate to be achieved is:
   (0,0), (30,30), (30,-30), (-30,30), (-30,30).
4. Place a dot on the paper with the use of the permanent marker mounted into the end-effector.
5. Physically move the tip of the permanent marker around to see how much mechanical play there is.
6. Repeat steps 3 - 5 using the second and third RobotArms.

A3.2.5 Results: Individual RobotArm - Mechanical Tolerance Test

The following figure illustrated the results produced from this experiment.

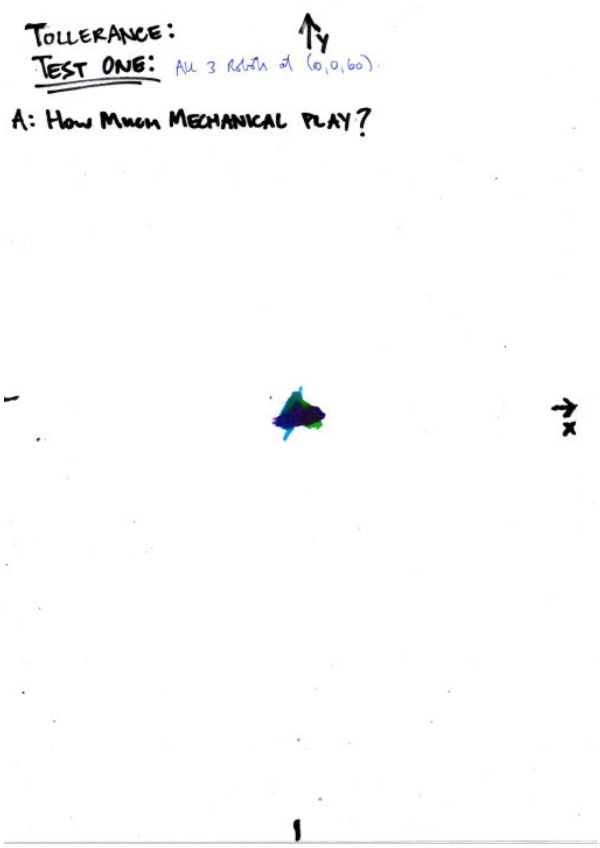

Figure 91: All robots – tolerance.

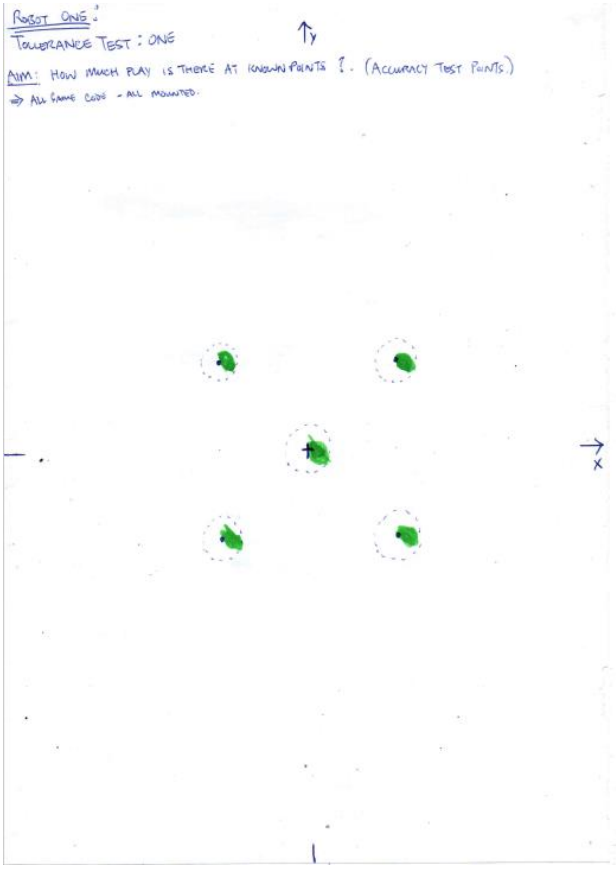

Figure 92: Robot one – tolerance.

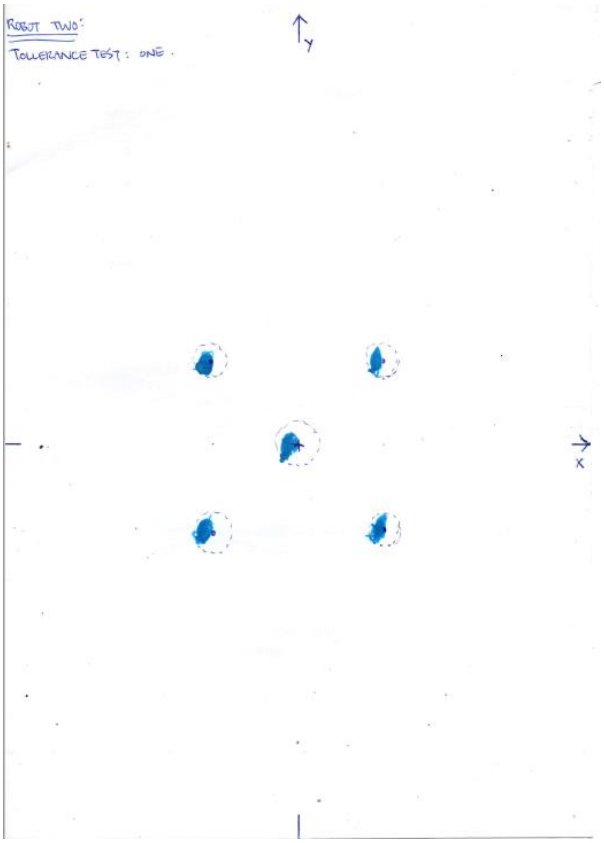

Figure 93: Robot two – tolerance.

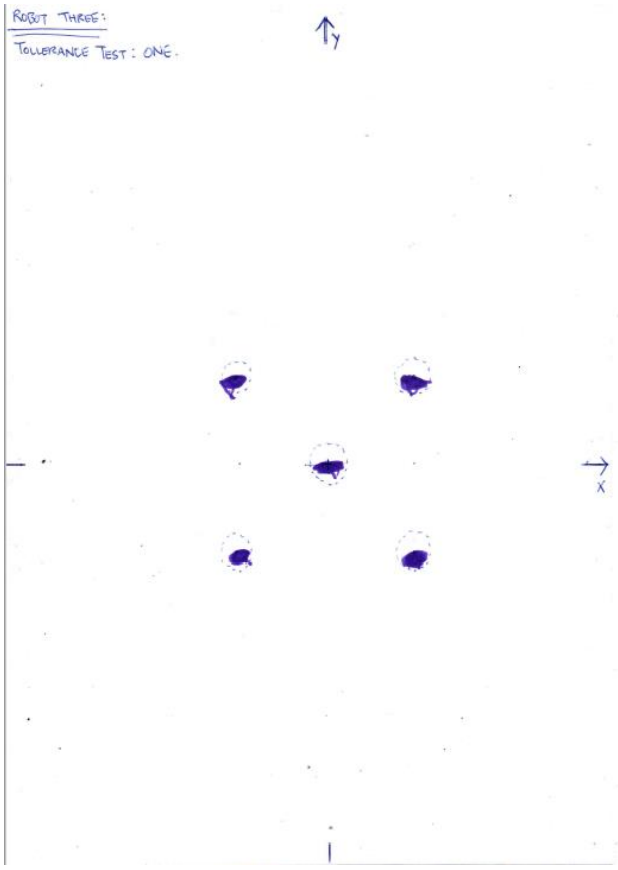

Figure 94: Robot three – tolerance.

A3.2.6 Discussion: Individual RobotArm - Mechanical Tolerance Test

It has become apparent through this experiment that there is a considerable amount of mechanical play that is coming through the construction of the RobotArms.

While the RobotArms are at a fixed position, the permanent marker tip was able to move around a considerable amount – in the region of 5 – 10mm. This may be exaggerated somewhat passed the physical operations of the RobotArms due to human interaction with the desktop models. The holding torque of the motors and stiffness of the 3D printed components can be overcome by the operator's interaction with the permanent marker tip. Nevertheless, there is mechanical play within the construction.

The experiment can be considered a success, as it was hypothesised through the previous experiments that the inaccuracies was most likely due to mechanical play. The results also offer an insight into what is acceptable as a standard deviation for these desktop model RobotArms.

With the known mechanical issues discovered and a baseline accuracy window achieved, further investigation into the repeatability of the RoboArms could be performed.

A4. APPENDIX D: INDIVIDUAL ACCURACY AND REPEATABILITY DATA

A4.1 Accuracy and Repeatability for Individual G-Code:

```
G00 X0 Y0 Z270
G00 X0 Y0 Z110
G00 X30 Y30 Z110
G00 X30 Y-30 Z110
G00 X-30 Y-30 Z110
G00 X-30 Y30 Z110
G00 X0 Y0 Z110
G28
G00 X0 Y0 Z270
```

A4.2 Raw Data for Each Robot at Each Point

Table 12: Individual Accuracy Data - Robot 1.

individual accuracy - ROBOT ONE															
	GOAL - i														
	5			4			3			2			1		
	xi	yi	zi	xi	yi	zi	xi	yi	zi	xi	yi	zi	xi	yi	zi
	30	30	110	30	-30	110	-30	-30	110	-30	30	110	0	0	110
j															
1	30	28	111	32	-32	111	-28	-31	111	-29	27	111	1	-1	111
2	31	30	111	31	-31	111	-28	-31	111	-29	28	111	1	-1	111
3	32	31	111	31	-32	111	-29	-32	111	-28	27	111	1	-1	111
4	31	31	111	32	-31	111	-28	-31	111	-29	28	111	1	0	111
5	29	30	111	32	-32	111	-30	-32	111	-29	29	111	1	-1	111
6	30	29	111	31	-31	111	-29	-31	111	-29	28	111	1	0	111
7	32	31	111	32	-31	111	-30	-33	111	-30	29	111	1	-1	111
8	31	29	111	31	-32	111	-30	-32	111	-29	28	111	1	-1	111
9	31	29	111	31	-31	111	-29	-31	111	-29	29	111	1	0	111
10	30	29	111	32	-31	111	-28	-31	111	-28	27	111	1	-1	111
TOT	307	297	1110	315	-314	1110	-289	-315	1110	-289	280	1110	10	-7	1110

Table 13: Individual Accuracy Data - Robot 2.

individual accuracy - ROBOT TWO															
	GOAL - i														
	5			4			3			2			1		
	xi	yi	zi	xi	yi	zi	xi	yi	zi	xi	yi	zi	xi	yi	zi
	30	30	110	30	-30	110	-30	-30	110	-30	30	110	0	0	110
j															
1	27	26	112	28	-32	112	-32	-32	112	-30	26	112	-2	-3	112
2	28	26	112	27	-31	112	-34	-32	112	-31	27	112	-2	-4	112
3	28	29	112	27	-32	112	-33	-31	112	-30	28	112	-3	-3	112
4	28	28	112	27	-31	112	-32	-32	112	-30	27	112	-2	-2	112
5	27	26	112	28	-31	112	-33	-32	112	-31	28	112	-3	-2	112
6	27	26	112	28	-32	112	-32	-30	112	-30	28	112	-2	-3	112
7	28	27	112	28	-31	112	-32	-31	112	-31	28	112	-2	-3	112
8	29	28	112	27	-32	112	-33	-32	112	-30	27	112	-3	-3	112
9	28	28	112	28	-30	112	-34	-32	112	-31	27	112	-2	-4	112
10	27	26	112	28	-32	112	-32	-31	112	-32	29	112	-3	-3	112
TOT	277	270	1120	276	-314	1120	-327	-315	1120	-306	275	1120	-24	-30	1120

Table 14: Individual Accuracy Data - Robot 3.

individual accuracy - ROBOT THREE															
	GOAL - i														
	5			4			3			2			1		
	xi	yi	zi	xi	yi	zi	xi	yi	zi	xi	yi	zi	xi	yi	zi
	30	30	110	30	-30	110	-30	-30	110	-30	30	110	0	0	110
j															
1	28	28	108	31	-32	108	-28	-32	108	-29	28	108	-1	-1	108
2	29	29	108	32	-33	108	-28	-30	108	-29	29	108	0	-1	108
3	30	29	108	32	-31	108	-28	-30	108	-31	30	108	0	-1	108
4	29	28	108	31	-32	108	-29	-31	108	-29	30	108	0	0	108
5	28	30	108	32	-33	108	-28	-32	108	-29	29	108	-1	0	108
6	28	29	108	32	-31	108	-29	-32	108	-28	30	108	-1	-1	108
7	29	31	108	31	-33	108	-28	-32	108	-29	30	108	0	-1	108
8	28	28	108	32	-31	108	-28	-31	108	-28	29	108	-1	-1	108
9	28	30	108	31	-32	108	-29	-33	108	-29	29	108	-1	0	108
10	29	31	108	32	-33	108	-29	-31	108	-30	29	108	0	-1	108
TOT	286	293	1080	316	-321	1080	-284	-314	1080	-291	293	1080	-5	-7	1080

A4.3 Graphs of Achieved Positions

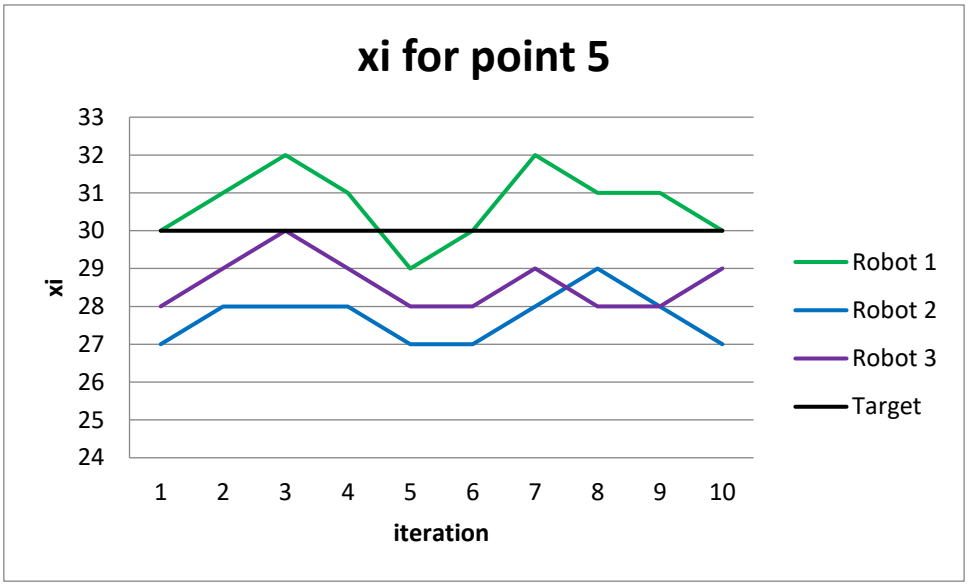

Figure 95: Graph of xi for point 5 for each robot.

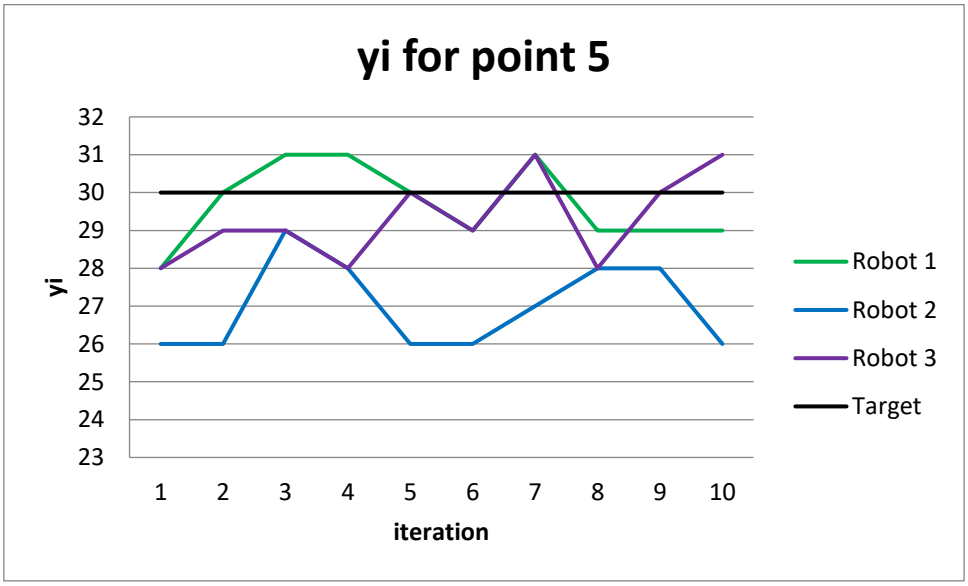

Figure 96: Graph of yi for point 5 for each robot.

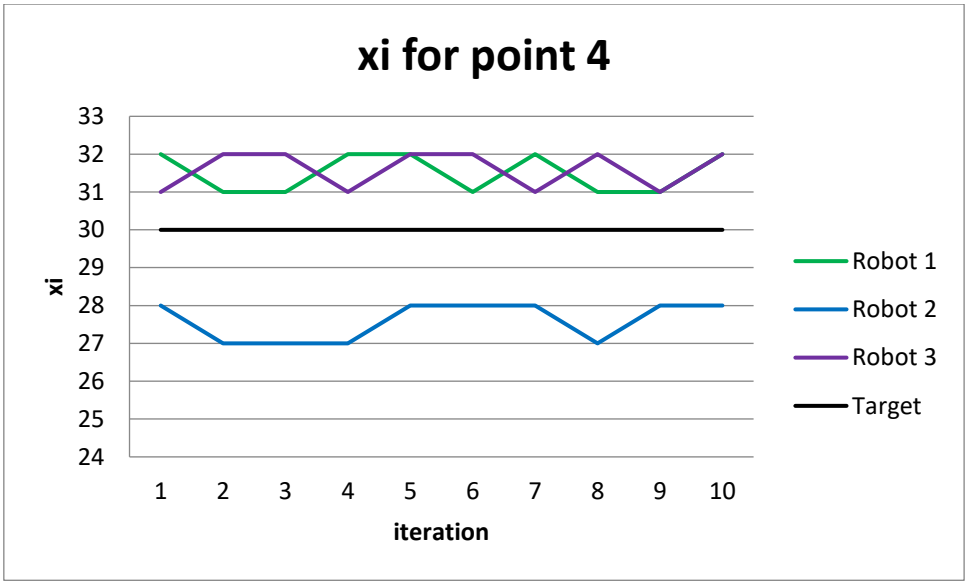

Figure 97: Graph of xi for point 4 for each robot.

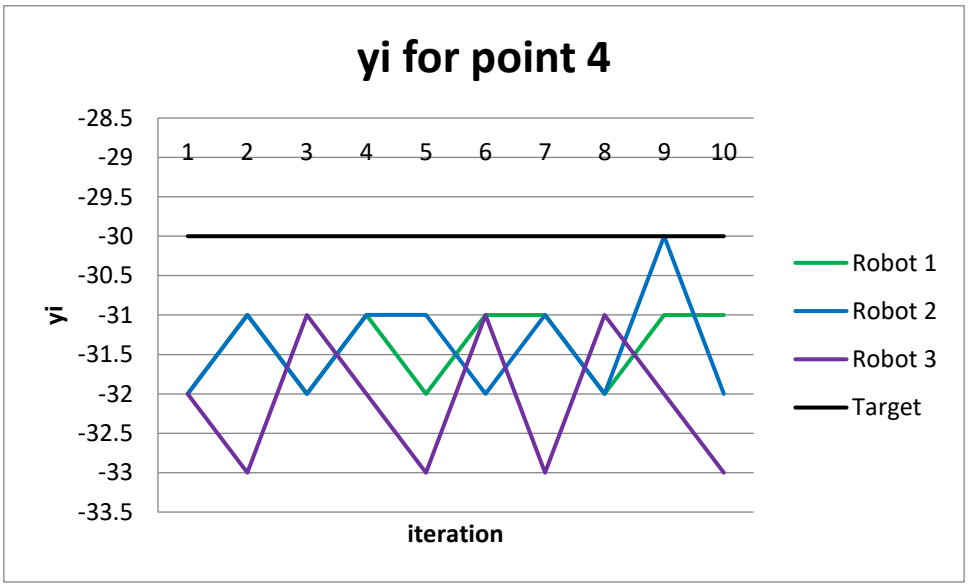

Figure 98: Graph of yi for point 4 for each robot.

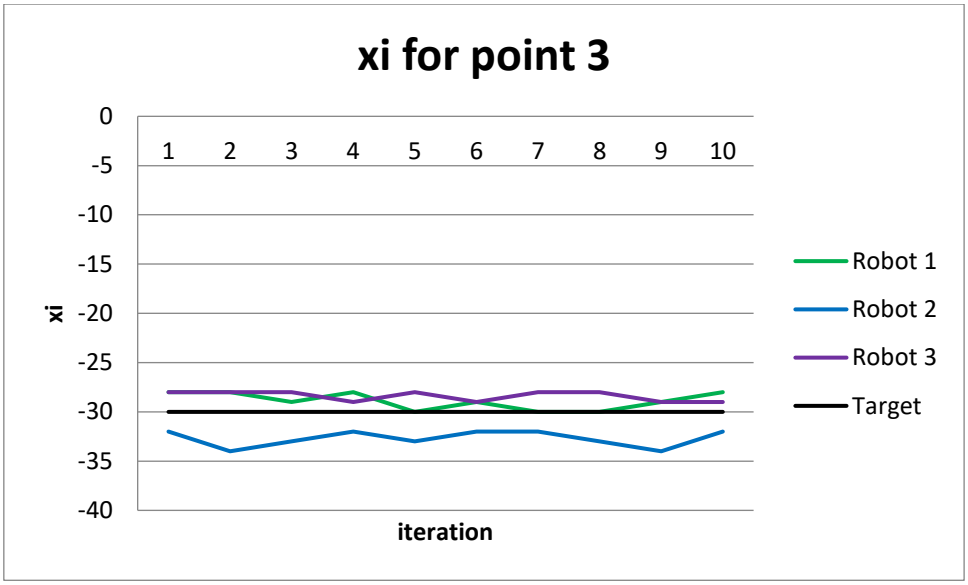

Figure 99: Graph of xi for point 3 for each robot.

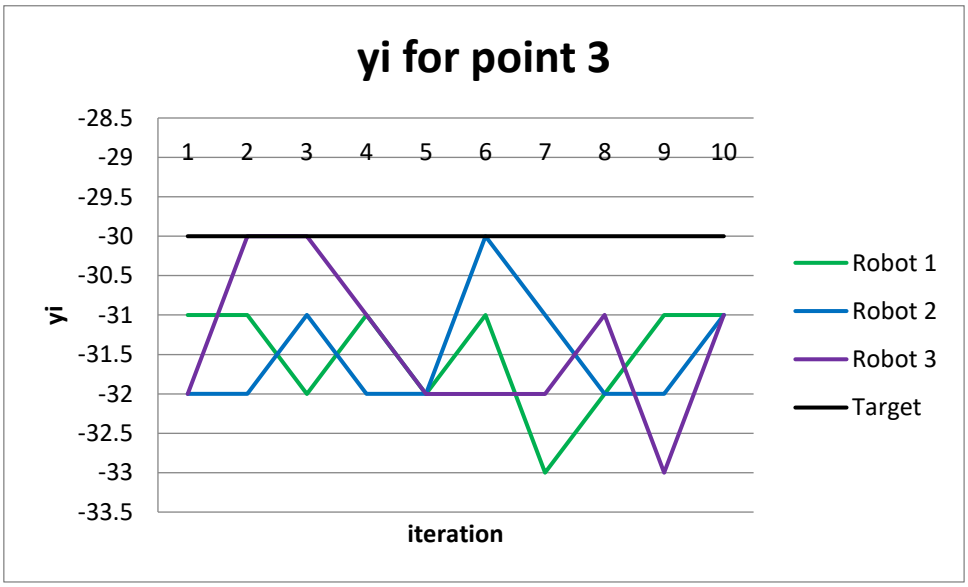

Figure 100: Graph of yi for point 3 for each robot.

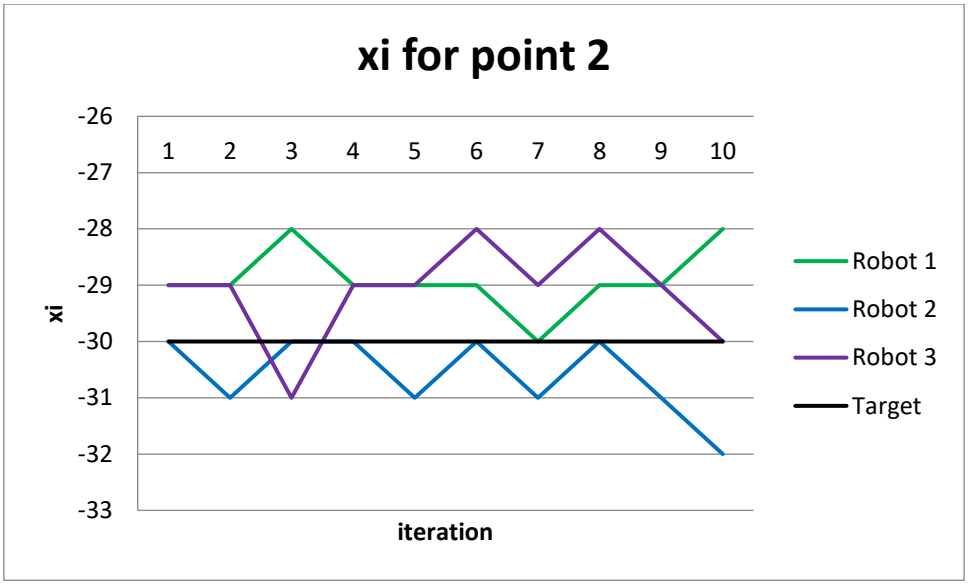

Figure 101: Graph of xi for point 2 for each robot.

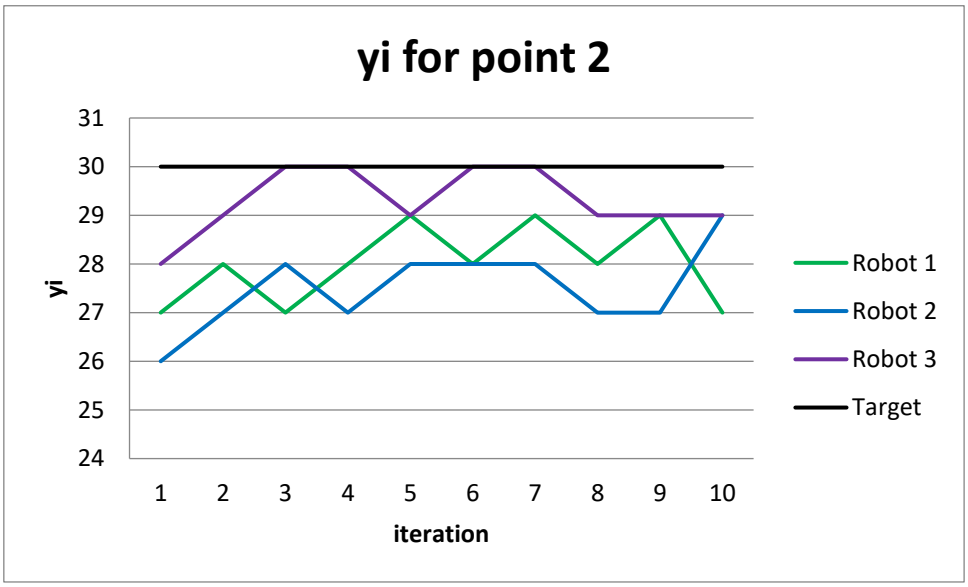

Figure 102: Graph of yi for point 2 for each robot.

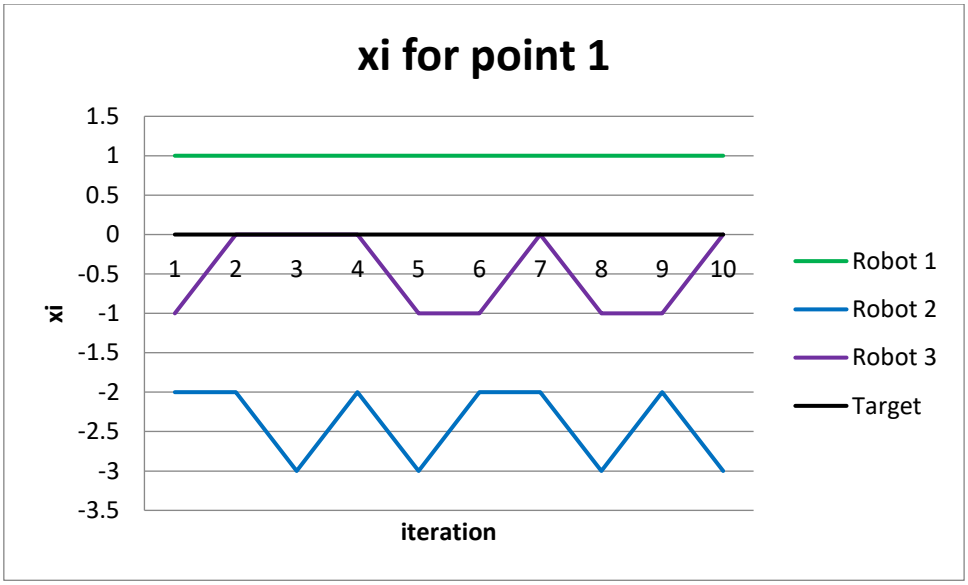

Figure 103: Graph of xi for point 1 for each robot.

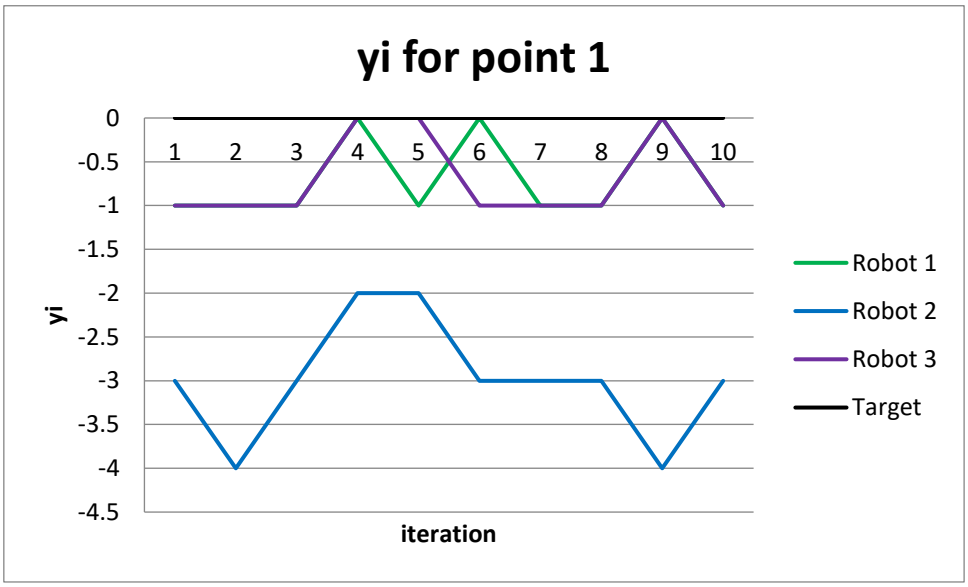

Figure 104: Graph of yi for point 1 for each robot.

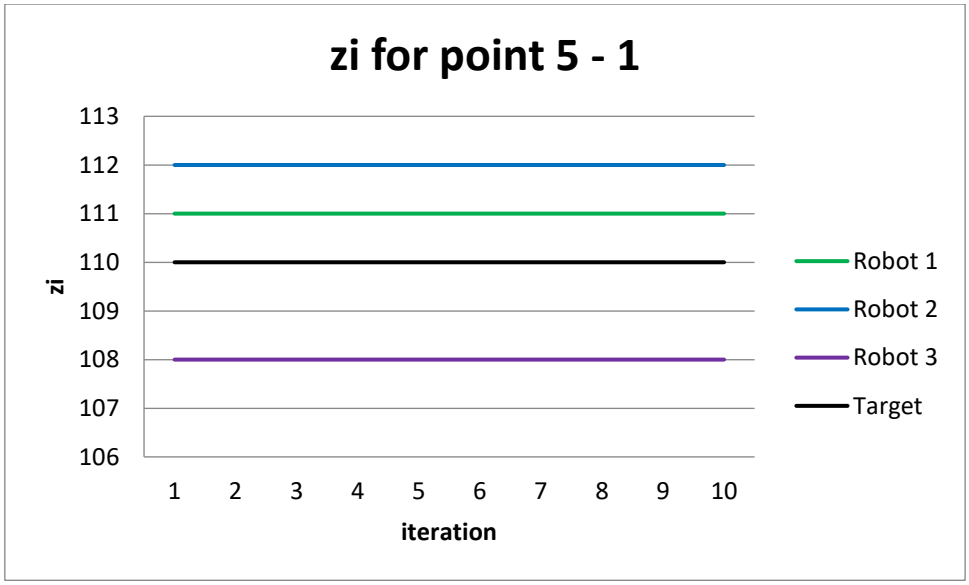

Figure 105: Graph of zi for point 5-1 for each robot.

A4.4 Accuracy and Repeatability – Robot 1

The following is the resultant accuracy (AP) and repeatability (RP) that was calculated from the achieved x (xi), y (yi) and z (zi) positions at each point.

A4.4.1 Point 5: Accuracy and Repeatability – Robot 1

Table 15: Accuracy Data - Point 5 - Robot 1.

accuracy	point 5
xbar	30.7
ybar	29.7
zbar	111
AP	1.256981

Table 16: Repeatability Data Calculations - Point 5 - Robot 1.

	repeatability	POINT 5	
j	**lj**	**lj - lbar**	**(lj - lbar)^2**
1	1.838477631	0.588159168	0.345931207
2	0.424264069	-0.826054394	0.682365862
3	1.838477631	0.588159168	0.345931207
4	1.334166406	0.083847944	0.007030478
5	1.72626765	0.475949187	0.226527629
6	0.989949494	-0.260368969	0.067792
7	1.838477631	0.588159168	0.345931207
8	0.761577311	-0.488741152	0.238867914
9	0.761577311	-0.488741152	0.238867914
10	0.989949494	-0.260368969	0.067792

Table 17: Repeatability Data - Point 5 - Robot 1.

lbar	1.250318463
Sl	0.534065895
RP	2.852516147

A4.4.2 Point 4: Accuracy and Repeatability – Robot 1

Table 18: Accuracy Data - Point 4 - Robot 1.

accuracy	point 4
xbar	31.5
ybar	-31.4
zbar	111
AP	2.282542

Table 19: Repeatability Data Calculations - Point 4 - Robot 1.

	repeatability	POINT 4	
j	**lj**	**lj - lbar**	**(lj - lbar)^2**
1	0.781024968	-0.469293495	0.220236385
2	0.640312424	-0.610006039	0.372107368
3	0.781024968	-0.469293495	0.220236385
4	0.640312424	-0.610006039	0.372107368
5	0.781024968	-0.469293495	0.220236385
6	0.640312424	-0.610006039	0.372107368
7	0.640312424	-0.610006039	0.372107368
8	0.781024968	-0.469293495	0.220236385
9	0.640312424	-0.610006039	0.372107368
10	0.640312424	-0.610006039	0.372107368

Table 20: Repeatability Data - Point 4 - Robot 1.

lbar	0.696597441
Sl	0.588178898
RP	2.461134135

A4.4.3 Point 3: Accuracy and Repeatability – Robot 1

Table 21: Accuracy Data - Point 3 - Robot 1.

accuracy	point 3
xbar	-28.9
ybar	-31.5
zbar	111
AP	2.111871

Table 22: Repeatability Data Calculations - Point 3 - Robot 1.

	repeatability	POINT 3	
j	**lj**	**lj - lbar**	**(lj - lbar)^2**
1	1.029563014	-0.220755449	0.048732968
2	1.029563014	-0.220755449	0.048732968
3	0.509901951	-0.740416511	0.54821661
4	1.029563014	-0.220755449	0.048732968
5	1.208304597	-0.042013865	0.001765165
6	0.509901951	-0.740416511	0.54821661
7	1.860107524	0.609789061	0.371842699
8	1.208304597	-0.042013865	0.001765165
9	0.509901951	-0.740416511	0.54821661
10	1.029563014	-0.220755449	0.048732968

Table 23: Repeatability Data - Point 3 - Robot 1.

lbar	0.992467463
Sl	0.496090799
RP	2.480739861

A4.4.4 Point 2: Accuracy and Repeatability – Robot 1

Table 24: Accuracy Data - Point 2 - Robot 1.

accuracy	point 2
xbar	-28.9
ybar	28
zbar	111
AP	2.491987

Table 25: Repeatability Data Calculations - Point 2 - Robot 1.

	repeatability	POINT 2	
j	**lj**	**lj - lbar**	**(lj - lbar)^2**
1	1.004987562	-0.245330901	0.060187251
2	0.1	-1.150318463	1.323232566
3	1.345362405	0.095043942	0.009033351
4	0.1	-1.150318463	1.323232566
5	1.004987562	-0.245330901	0.060187251
6	0.1	-1.150318463	1.323232566
7	1.486606875	0.236288412	0.055832214
8	0.1	-1.150318463	1.323232566
9	1.004987562	-0.245330901	0.060187251
10	1.345362405	0.095043942	0.009033351

Table 26: Repeatability Data - Point 2 - Robot 1.

lbar	0.759229437
Sl	0.785096663
RP	3.114519426

A3.4.5 Point 1: Accuracy and Repeatability – Robot 1

Table 27: Accuracy Data - Point 1 - Robot 1.

accuracy	point 1
xbar	1
ybar	-0.7
zbar	111
AP	1.577973

Table 28: Repeatability Data Calculations - Point 1 - Robot 1.

	repeatability	POINT 1	
j	**lj**	**lj - lbar**	**(lj - lbar)^2**
1	0.3	-0.950318463	0.903105181
2	0.3	-0.950318463	0.903105181
3	0.3	-0.950318463	0.903105181
4	0.7	-0.550318463	0.30285041
5	0.3	-0.950318463	0.903105181
6	0.7	-0.550318463	0.30285041
7	0.3	-0.950318463	0.903105181
8	0.3	-0.950318463	0.903105181
9	0.7	-0.550318463	0.30285041
10	0.3	-0.950318463	0.903105181

Table 29: Repeatability Data - Point 1 - Robot 1.

lbar	0.42
Sl	0.896306464
RP	3.108919392

A4.5 Accuracy and Repeatability – Robot 2

The following is the resultant accuracy (AP) and repeatability (RP) that was calculated from the achieved x (xi), y (yi) and z (zi) positions at each point.

A4.5.1 Point 5: Accuracy and Repeatability – Robot 2

Table 30: Accuracy Data - Point 5 - Robot 2.

accuracy	point 5
xbar	27.7
ybar	27
zbar	112
AP	4.276681

Table 31: Repeatability Data Calculations - Point 5 - Robot 2.

	repeatability	POINT 5	
j	**lj**	**lj - lbar**	**(lj - lbar)^2**
1	1.220655562	0.022934463	0.00052599
2	1.044030651	-0.153690448	0.023620754
3	2.022374842	0.824653743	0.680053796
4	1.044030651	-0.153690448	0.023620754
5	1.220655562	0.022934463	0.00052599
6	1.220655562	0.022934463	0.00052599
7	0.3	-0.897721099	0.805903171
8	1.640121947	0.442400848	0.19571851
9	1.044030651	-0.153690448	0.023620754
10	1.220655562	0.022934463	0.00052599

Table 32: Repeatability Data - Point 5 - Robot 2.

lbar	1.197721099
Sl	0.441542963
RP	2.522349989

A4.5.2 Point 4: Accuracy and Repeatability – Robot 2

Table 33: Accuracy Data - Point 4 - Robot 2.

accuracy	point 4
xbar	27.6
ybar	-31.4
zbar	112
AP	3.423449

Table 34: Repeatability Data Calculations - Point 4 - Robot 2.

	repeatability	POINT 4	
j	**lj**	**lj - lbar**	**(lj - lbar)^2**
1	0.721110255	-0.476610844	0.227157896
2	0.721110255	-0.476610844	0.227157896
3	0.848528137	-0.349192961	0.121935724
4	0.721110255	-0.476610844	0.227157896
5	0.565685425	-0.632035674	0.399469093
6	0.721110255	-0.476610844	0.227157896
7	0.565685425	-0.632035674	0.399469093
8	0.848528137	-0.349192961	0.121935724
9	1.456021978	0.258300879	0.066719344
10	0.721110255	-0.476610844	0.227157896

Table 35: Repeatability Data - Point 4 - Robot 2.

lbar	0.789000038
Sl	0.499479558
RP	2.287438712

A4.5.3 Point 3: Accuracy and Repeatability – Robot 2

Table 36: Accuracy Data - Point 3 - Robot 2.

accuracy	point 3
xbar	-32.7
ybar	-31.5
zbar	112
AP	3.679674

Table 37: Repeatability Data Calculations - Point 3 - Robot 2.

	repeatability	POINT 3	
j	**lj**	**lj - lbar**	**(lj - lbar)^2**
1	0.860232527	-0.337488572	0.113898536
2	1.392838828	0.195117729	0.038070928
3	0.583095189	-0.614625909	0.377765008
4	0.860232527	-0.337488572	0.113898536
5	0.583095189	-0.614625909	0.377765008
6	1.655294536	0.457573437	0.20937345
7	0.860232527	-0.337488572	0.113898536
8	0.583095189	-0.614625909	0.377765008
9	1.392838828	0.195117729	0.038070928
10	0.860232527	-0.337488572	0.113898536

Table 38: Repeatability Data - Point 3 - Robot 2.

lbar	0.963118787
Sl	0.456362974
RP	2.332207709

A4.5.4 Point 2: Accuracy and Repeatability – Robot 2

Table 39: Accuracy Data - Point 2 - Robot 2.

accuracy	point 2
xbar	-30.6
ybar	27.5
zbar	112
AP	3.257299

Table 40: Repeatability Data Calculations - Point 2 - Robot 2.

	repeatability	POINT 2	
j	**lj**	**lj - lbar**	**(lj - lbar)^2**
1	1.615549442	0.417828343	0.174580525
2	0.640312424	-0.557408675	0.310704431
3	0.781024968	-0.416696131	0.173635666
4	0.781024968	-0.416696131	0.173635666
5	0.640312424	-0.557408675	0.310704431
6	0.781024968	-0.416696131	0.173635666
7	0.640312424	-0.557408675	0.310704431
8	0.781024968	-0.416696131	0.173635666
9	0.640312424	-0.557408675	0.310704431
10	2.051828453	0.854107354	0.729499372

Table 41: Repeatability Data - Point 2 - Robot 2.

lbar	0.935272746
Sl	0.561885742
RP	2.620929972

A4.5.5 Point 1: Accuracy and Repeatability – Robot 2

Table 42: Accuracy Data - Point 1 - Robot 2.

accuracy	point 1
xbar	-2.4
ybar	-3
zbar	112
AP	4.331282

Table 43: Repeatability Data Calculations - Point 1 - Robot 2.

	repeatability	POINT 1	
j	**lj**	**lj - lbar**	**(lj - lbar)^2**
1	0.4	-0.797721099	0.636358951
2	1.077032961	-0.120688137	0.014565626
3	0.6	-0.597721099	0.357270512
4	1.077032961	-0.120688137	0.014565626
5	1.166190379	-0.03153072	0.000994186
6	0.4	-0.797721099	0.636358951
7	0.4	-0.797721099	0.636358951
8	0.6	-0.597721099	0.357270512
9	1.077032961	-0.120688137	0.014565626
10	0.6	-0.597721099	0.357270512

Table 44: Repeatability Data - Point 1 - Robot 2.

lbar	0.739728926
Sl	0.579806429
RP	2.479148213

A4.6 Accuracy and Repeatability – Robot 3

The following is the resultant accuracy (AP) and repeatability (RP) that was calculated from the achieved x (xi), y (yi) and z (zi) positions at each point.

A4.6.1 Point 5: Accuracy and Repeatability – Robot 3

Table 45: Accuracy Data - Point 5 - Robot 3.

accuracy	point 5
xbar	28.6
ybar	29.3
zbar	108
AP	2.539685

Table 46: Repeatability Data Calculations - Point 5 - Robot 3.

	repeatability	POINT 5	
j	**lj**	**lj - lbar**	**(lj - lbar)^2**
1	1.431782106	0.215474857	0.046429414
2	0.5	-0.716307249	0.513096076
3	1.431782106	0.215474857	0.046429414
4	1.360147051	0.143839801	0.020689888
5	0.921954446	-0.294352804	0.086643573
6	0.670820393	-0.545486856	0.29755591
7	1.74642492	0.53011767	0.281024744
8	1.431782106	0.215474857	0.046429414
9	0.921954446	-0.294352804	0.086643573
10	1.74642492	0.53011767	0.281024744

Table 47: Repeatability Data - Point 5 - Robot 3.

lbar	1.216307249
Sl	0.43537554
RP	2.522433871

A4.6.2 Point 4: Accuracy and Repeatability – Robot 3

Table 48: Accuracy Data - Point 4 - Robot 3.

accuracy	point 4
xbar	31.6
ybar	-32.1
zbar	108
AP	3.312099

Table 49: Repeatability Data Calculations - Point 4 - Robot 3.

	repeatability	POINT 4	
j	**lj**	**lj - lbar**	**(lj - lbar)^2**
1	0.608276253	-0.608030996	0.369701693
2	0.98488578	-0.231421469	0.053555896
3	1.170469991	-0.045837258	0.002101054
4	0.608276253	-0.608030996	0.369701693
5	0.98488578	-0.231421469	0.053555896
6	1.170469991	-0.045837258	0.002101054
7	1.081665383	-0.134641867	0.018128432
8	1.170469991	-0.045837258	0.002101054
9	0.608276253	-0.608030996	0.369701693
10	0.98488578	-0.231421469	0.053555896

Table 50: Repeatability Data - Point 4 - Robot 3.

lbar	0.937256146
Sl	0.379210344
RP	2.074887176

A4.6.3 Point 3: Accuracy and Repeatability – Robot 3

Table 51: Accuracy Data - Point 3 - Robot 3.

accuracy	point 3
xbar	-28.4
ybar	-31.4
zbar	108
AP	2.918904

Table 52: Repeatability Data Calculations - Point 3 - Robot 3.

	repeatability	POINT 3	
j	**lj**	**lj - lbar**	**(lj - lbar)^2**
1	0.721110255	-0.495196994	0.245220063
2	1.456021978	0.239714728	0.057463151
3	1.456021978	0.239714728	0.057463151
4	0.721110255	-0.495196994	0.245220063
5	0.721110255	-0.495196994	0.245220063
6	0.848528137	-0.367779112	0.135261475
7	0.721110255	-0.495196994	0.245220063
8	0.565685425	-0.650621824	0.423308758
9	1.708800749	0.4924935	0.242549847
10	0.721110255	-0.495196994	0.245220063

Table 53: Repeatability Data - Point 3 - Robot 3.

lbar	0.964060954
Sl	0.487869142
RP	2.427668381

A4.6.4 Point 2: Accuracy and Repeatability – Robot 3

Table 54: Accuracy Data - Point 2 - Robot 3.

accuracy	point 2
xbar	-29.1
ybar	29.3
zbar	108
AP	2.302173

Table 55: Repeatability Data Calculations - Point 2 - Robot 3.

	repeatability	POINT 2	
j	**lj**	**lj - lbar**	**(lj - lbar)^2**
1	1.303840481	0.087533232	0.007662067
2	0.316227766	-0.900079483	0.810143076
3	2.024845673	0.808538424	0.653734383
4	0.707106781	-0.509200468	0.259285117
5	0.316227766	-0.900079483	0.810143076
6	1.303840481	0.087533232	0.007662067
7	0.707106781	-0.509200468	0.259285117
8	1.140175425	-0.076131824	0.005796055
9	0.316227766	-0.900079483	0.810143076
10	0.948683298	-0.267623951	0.071622579

Table 56: Repeatability Data - Point 2 - Robot 3.

lbar	0.908428222
Sl	0.640787416
RP	2.83079047

A4.6.5 Point 1: Accuracy and Repeatability – Robot 3

Table 57: Accuracy Data - Point 1 - Robot 3.

accuracy	point 1
xbar	-0.5
ybar	-0.7
zbar	108
AP	2.177154

Table 58: Repeatability Data Calculations - Point 1 - Robot 3.

	repeatability	POINT 1	
j	**lj**	**lj - lbar**	**(lj - lbar)^2**
1	0.583095189	-0.63321206	0.400957513
2	0.583095189	-0.63321206	0.400957513
3	0.583095189	-0.63321206	0.400957513
4	0.860232527	-0.356074723	0.126789208
5	0.860232527	-0.356074723	0.126789208
6	0.583095189	-0.63321206	0.400957513
7	0.583095189	-0.63321206	0.400957513
8	0.583095189	-0.63321206	0.400957513
9	0.860232527	-0.356074723	0.126789208
10	0.583095189	-0.63321206	0.400957513

Table 59: Repeatability Data - Point 1 - Robot 3.

lbar	0.666236391
Sl	0.595078913
RP	2.45147313

A5. APPENDIX E: COMBINED PLATFORM ACCURACY AND REPEATABILITY DATA

A5.1 Accuracy and Repeatability for Combined System G-Code:

```
G00 X0 Y0 Z270 R0 P0 Ya0
G00 X0 Y0 Z95 R0 P0 Ya0
G00 X30 Y30 Z95 R0 P0 Ya0
G00 X30 Y-30 Z95 R0 P0 Ya0
G00 X-30 Y-30 Z95 R0 P0 Ya0
G00 X-30 Y30 Z95 R0 P0 Ya0
G00 X0 Y0 Z95 R0 P0 Ya0
G28
G00 X0 Y0 Z270 R0 P0 Ya0
```

A5.2 Raw Data for the Combined System at Each Point

Table 60: Accuracy Data - Combined system.

accuracy - COMBINED SYSTEM															
	GOAL - i														
	5			4			3			2			1		
	xi	yi	zi	xi	yi	zi	xi	yi	zi	xi	yi	zi	xi	yi	zi
	30	30	95	30	-30	95	-30	-30	95	-30	30	95	0	0	95
j															
1	30	31	93	31	-27	93	-31	-30	93	-31	32	93	0	0	93
2	27	29	93	28	-30	93	-30	-29	93	-30	28	93	0	1	93
3	30	30	93	28	-30	93	-29	-32	93	-31	31	93	-1	0	93
4	28	31	93	29	-30	93	-29	-30	93	-30	30	93	0	1	93
5	30	28	93	28	-29	93	-29	-32	93	-32	29	93	-1	1	93
6	28	30	93	30	-29	93	-30	-31	93	-30	30	93	-1	0	93
7	28	29	93	29	-31	93	-31	-32	93	-30	29	93	0	0	93
8	29	31	93	28	-30	93	-30	-29	93	-32	29	93	-1	1	93
9	27	31	93	30	-28	93	-28	-31	93	-30	31	93	0	1	93
10	29	28	93	28	-29	93	-29	-32	93	-31	31	93	-1	0	93
TOT	286	298	930	289	-293	930	-296	-308	930	-307	300	930	-5	5	930

A5.3 Graphs of Achieved Positions

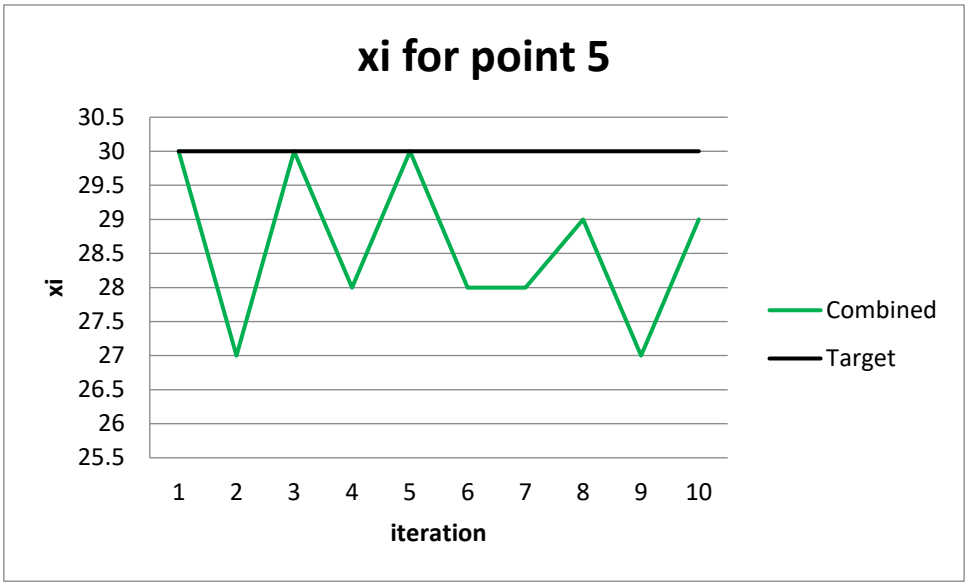

Figure 106: Graph of xi for point 5 for combined system.

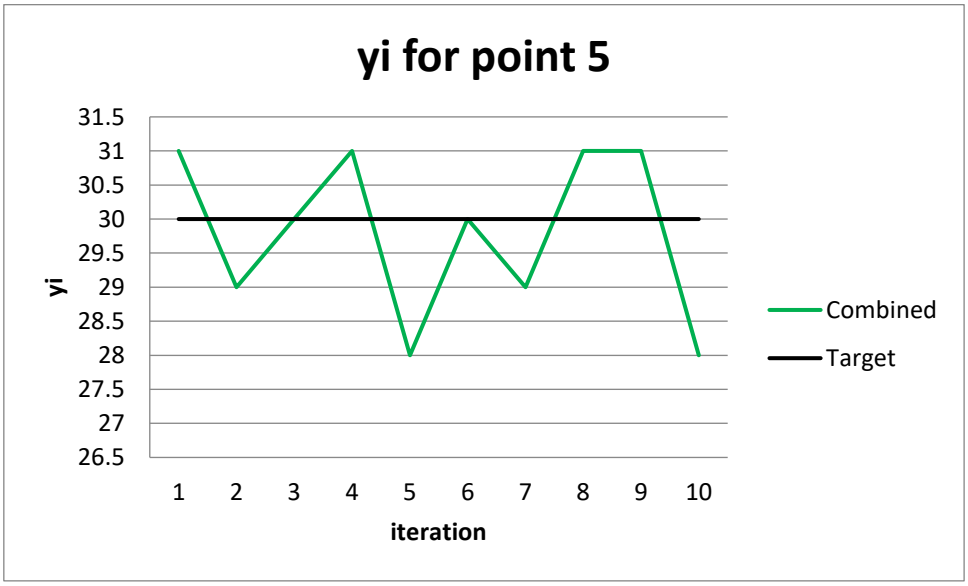

Figure 107: Graph of yi for point 5 for combined system.

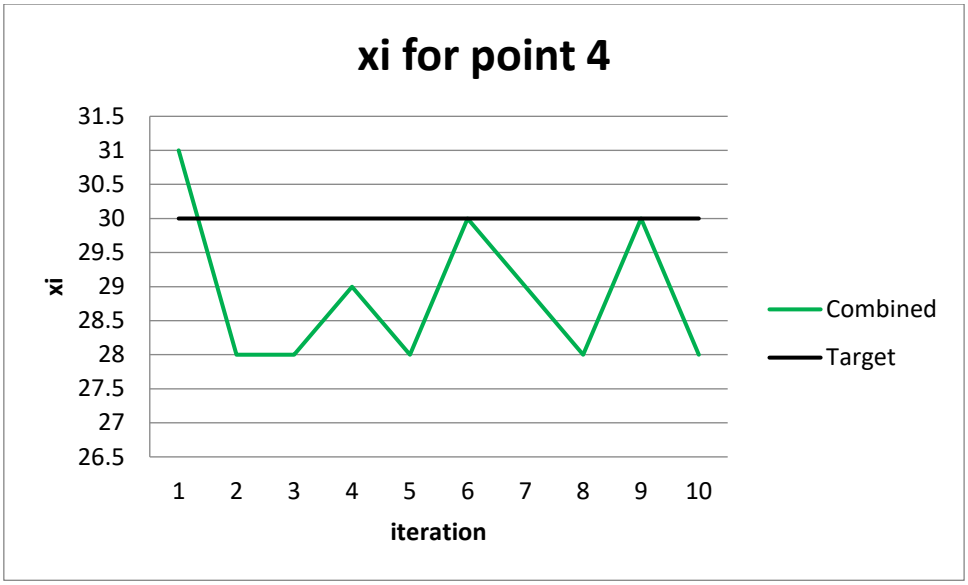

Figure 108: Graph of xi for point 4 for combined system.

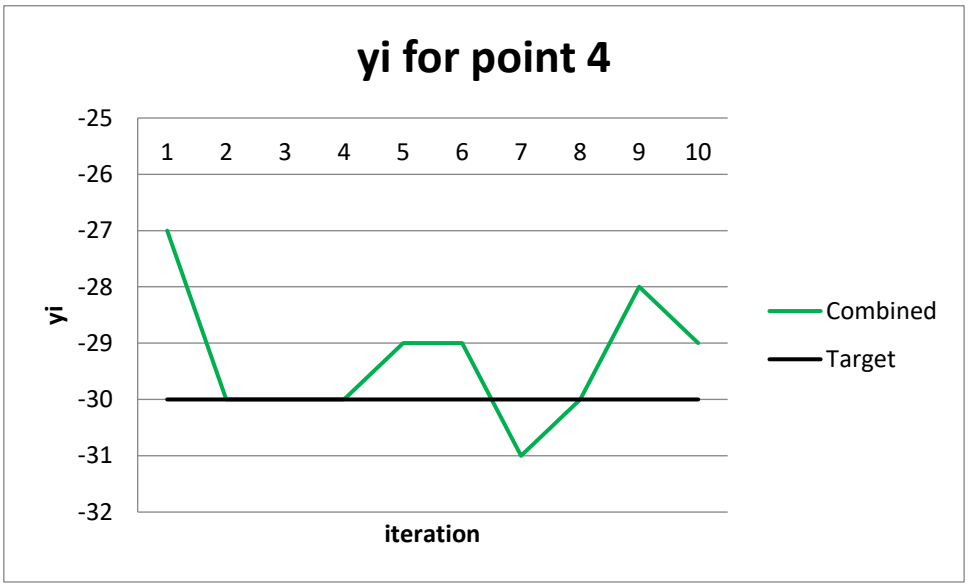

Figure 109: Graph of yi for point 4 for combined system.

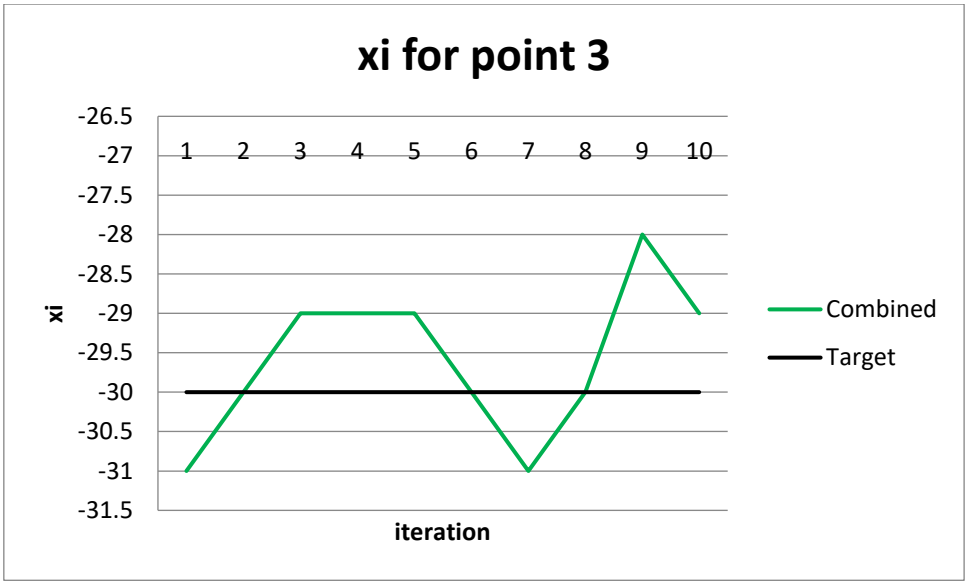

Figure 110: Graph of xi for point 3 for combined system.

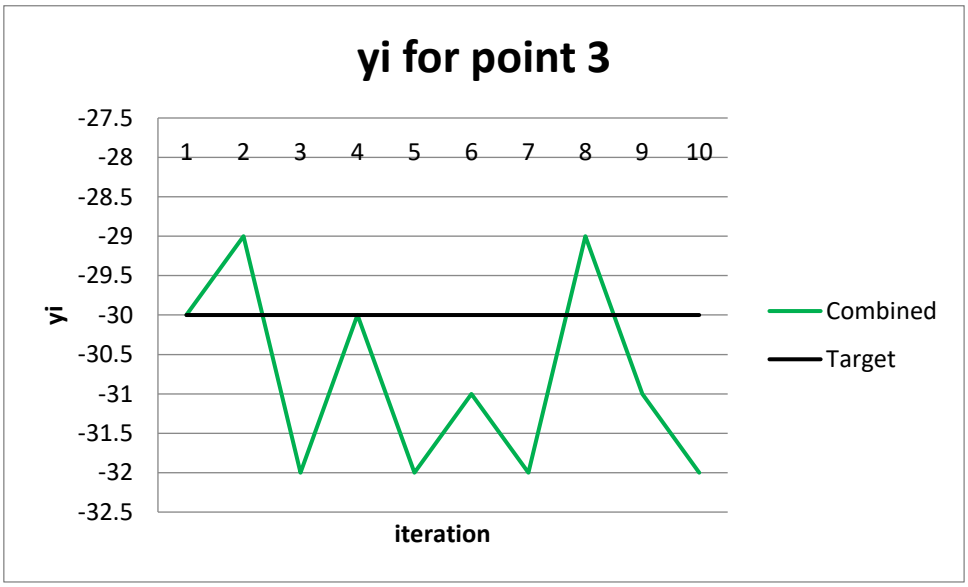

Figure 111: Graph of yi for point 3 for combined system.

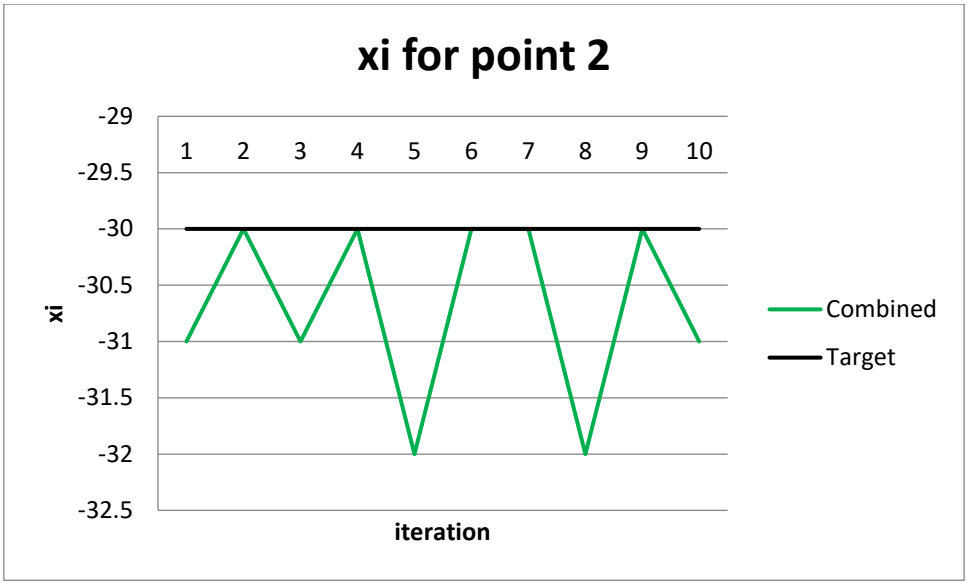

Figure 112: Graph of xi for point 2 for combined system.

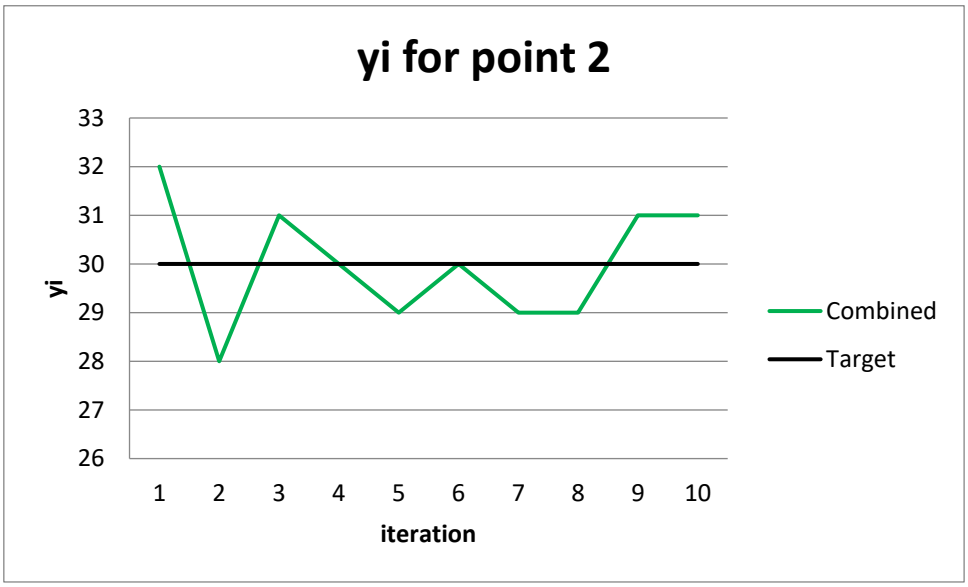

Figure 113: Graph of yi for point 2 for combined system.

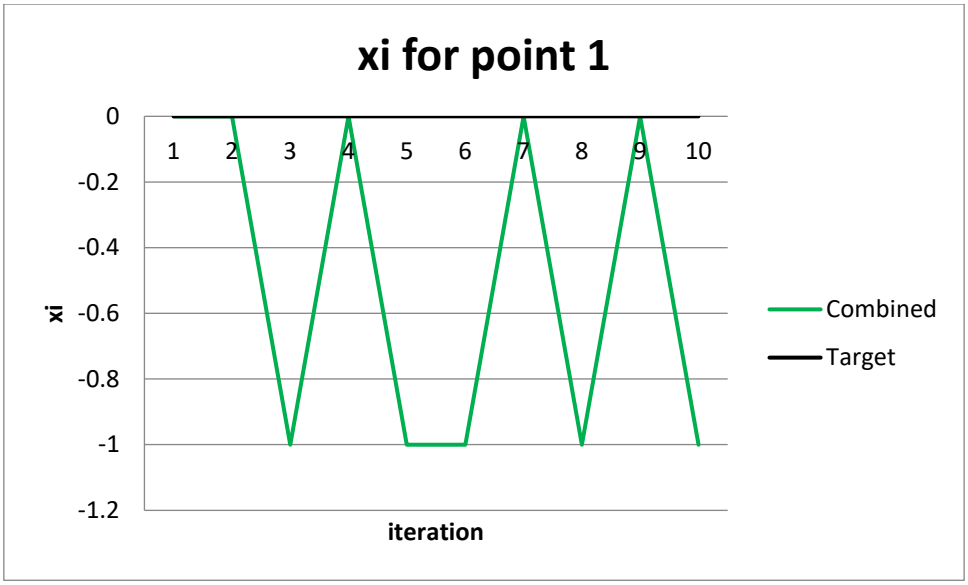

Figure 114: Graph of xi for point 1 for combined system.

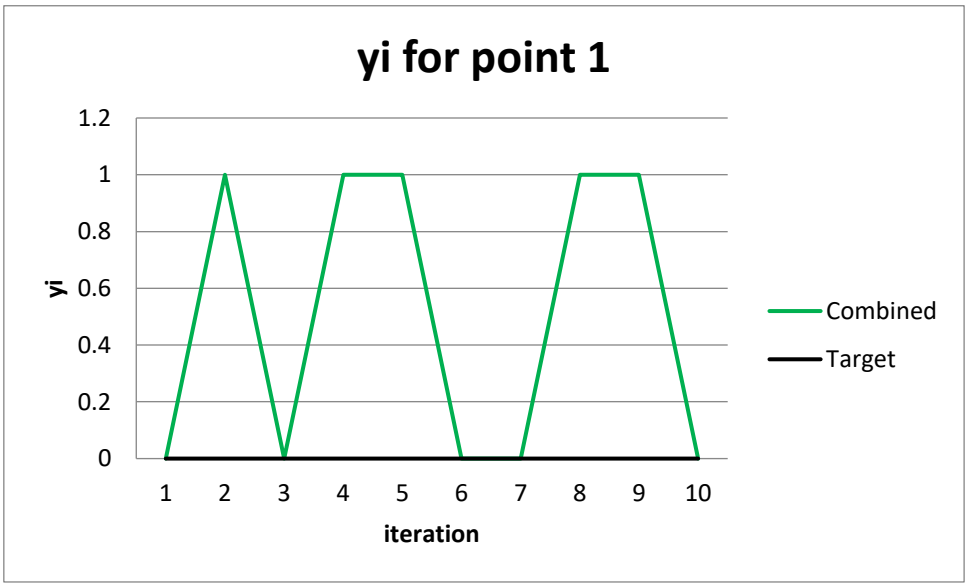

Figure 115: Graph of yi for point 1 for combined system.

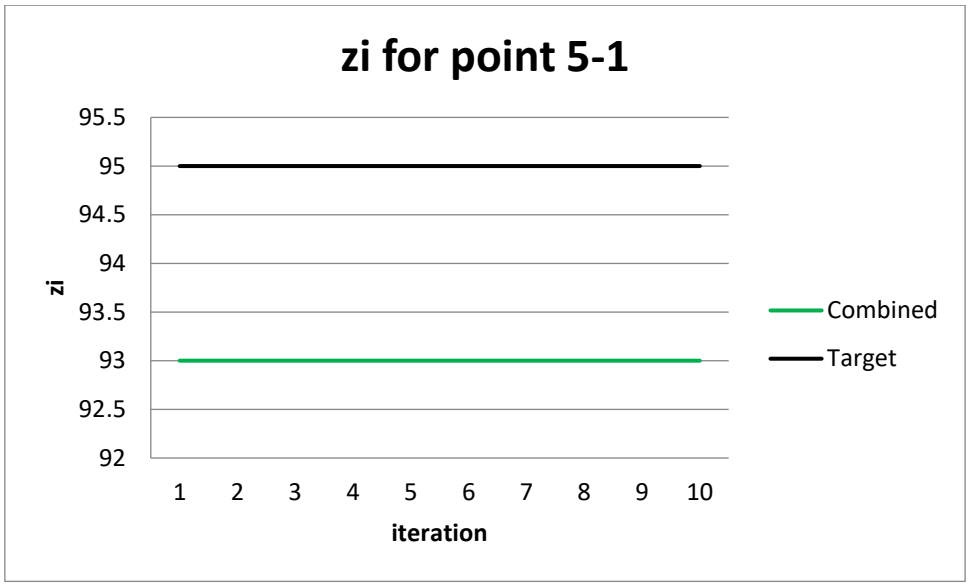

Figure 116: Graph of zi for point 5-1 for combined system.

A5.4 Accuracy and Repeatability – Combined System

The following is the resultant accuracy (AP) and repeatability (RP) that was calculated from the achieved x (xi), y (yi) and z (zi) positions at each point.

A5.4.1 Point 5: Accuracy and Repeatability – Combined System

Table 61: Accuracy Data - Point 5 - Combined system.

accuracy	point 5
xbar	28.6
ybar	29.8
zbar	93
AP	2.44949

Table 62: Repeatability Data Calculations - Point 5 - Combined system.

	repeatability	POINT 5	
j	**lj**	**lj - lbar**	**(lj - lbar)^2**
1	1.843908891	0.302884495	0.091739018
2	1.788854382	0.247829986	0.061419702
3	1.414213562	-0.126810834	0.016080988
4	1.341640786	-0.19938361	0.039753824
5	2.28035085	0.739326454	0.546603606
6	0.632455532	-0.908568864	0.825497381
7	1	-0.541024396	0.292707397
8	1.264911064	-0.276113332	0.076238572
9	2	0.458975604	0.210658605
10	1.843908891	0.302884495	0.091739018

Table 63: Repeatability Data - Point 5 - Combined system.

lbar	1.541024396
Sl	0.500270828
RP	3.041836879

A5.4.2 Point 4: Accuracy and Repeatability – Combined System

Table 64: Accuracy Data - Point 4 - Combined system.

accuracy	point 4
xbar	28.9
ybar	-29.3
zbar	93
AP	2.387467

Table 65: Repeatability Data Calculations - Point 4 - Combined system.

	repeatability	POINT 4	
j	**lj**	**lj - lbar**	**(lj - lbar)^2**
1	3.1144823	1.573457904	2.475769777
2	1.140175425	-0.400848971	0.160679897
3	1.140175425	-0.400848971	0.160679897
4	0.707106781	-0.833917615	0.695418588
5	0.948683298	-0.592341098	0.350867976
6	1.140175425	-0.400848971	0.160679897
7	1.702938637	0.161914241	0.026216221
8	1.140175425	-0.400848971	0.160679897
9	1.702938637	0.161914241	0.026216221
10	0.948683298	-0.592341098	0.350867976

Table 66: Repeatability Data - Point 4 - Combined system.

lbar	1.368553465
Sl	0.712435288
RP	3.505859328

A5.4.3 Point 3: Accuracy and Repeatability – Combined System

Table 67: Accuracy Data - Point 3 - Combined system.

accuracy	point 3
xbar	-29.6
ybar	-30.8
zbar	93
AP	2.19089

Table 68: Repeatability Data Calculations - Point 3 - Combined system.

	repeatability	POINT 3	
j	**lj**	**lj - lbar**	**(lj - lbar)^2**
1	1.61245155	0.071427154	0.005101838
2	1.843908891	0.302884495	0.091739018
3	1.341640786	-0.19938361	0.039753824
4	1	-0.541024396	0.292707397
5	1.341640786	-0.19938361	0.039753824
6	0.447213595	-1.093810801	1.196422067
7	1.843908891	0.302884495	0.091739018
8	1.843908891	0.302884495	0.091739018
9	1.61245155	0.071427154	0.005101838
10	1.341640786	-0.19938361	0.039753824

Table 69: Repeatability Data - Point 3 - Combined system.

lbar	1.422876573
Sl	0.458719433
RP	2.799034872

A5.4.4 Point 2: Accuracy and Repeatability – Combined System

Table 70: Accuracy Data - Point 2 - Combined system.

accuracy	point 2
xbar	-30.7
ybar	30
zbar	93
AP	2.118962

Table 71: Repeatability Data Calculations - Point 2 - Combined system.

	repeatability	POINT 2	
j	**lj**	**lj - lbar**	**(lj - lbar)^2**
1	2.022374842	0.481350446	0.231698251
2	2.11896201	0.577937614	0.334011886
3	1.044030651	-0.496993745	0.247002783
4	0.7	-0.841024396	0.707322035
5	1.640121947	0.099097551	0.009820325
6	0.7	-0.841024396	0.707322035
7	1.220655562	-0.320368834	0.10263619
8	1.640121947	0.099097551	0.009820325
9	1.220655562	-0.320368834	0.10263619
10	1.044030651	-0.496993745	0.247002783

Table 72: Repeatability Data - Point 2 - Combined system.

lbar	1.335095317
Sl	0.547648793
RP	2.978041695

A5.4.5 Point 1: Accuracy and Repeatability – Combined System

Table 73: Accuracy Data - Point 1 - Combined system.

accuracy	point 1
xbar	-0.5
ybar	0.5
zbar	93
AP	2.12132

Table 74: Repeatability Data Calculations - Point 1 - Combined system.

	repeatability	POINT 1	
j	**lj**	**lj - lbar**	**(lj - lbar)^2**
1	0.707106781	-0.833917615	0.695418588
2	0.707106781	-0.833917615	0.695418588
3	0.707106781	-0.833917615	0.695418588
4	0.707106781	-0.833917615	0.695418588
5	0.707106781	-0.833917615	0.695418588
6	0.707106781	-0.833917615	0.695418588
7	0.707106781	-0.833917615	0.695418588
8	0.707106781	-0.833917615	0.695418588
9	0.707106781	-0.833917615	0.695418588
10	0.707106781	-0.833917615	0.695418588

Table 75: Repeatability Data - Point 1 - Combined system.

lbar	0.707106781
Sl	0.879026348
RP	3.344185825

A6. APPENDIX F: IMAGES

Figure 117: Individual RobotArm with marker - front view.

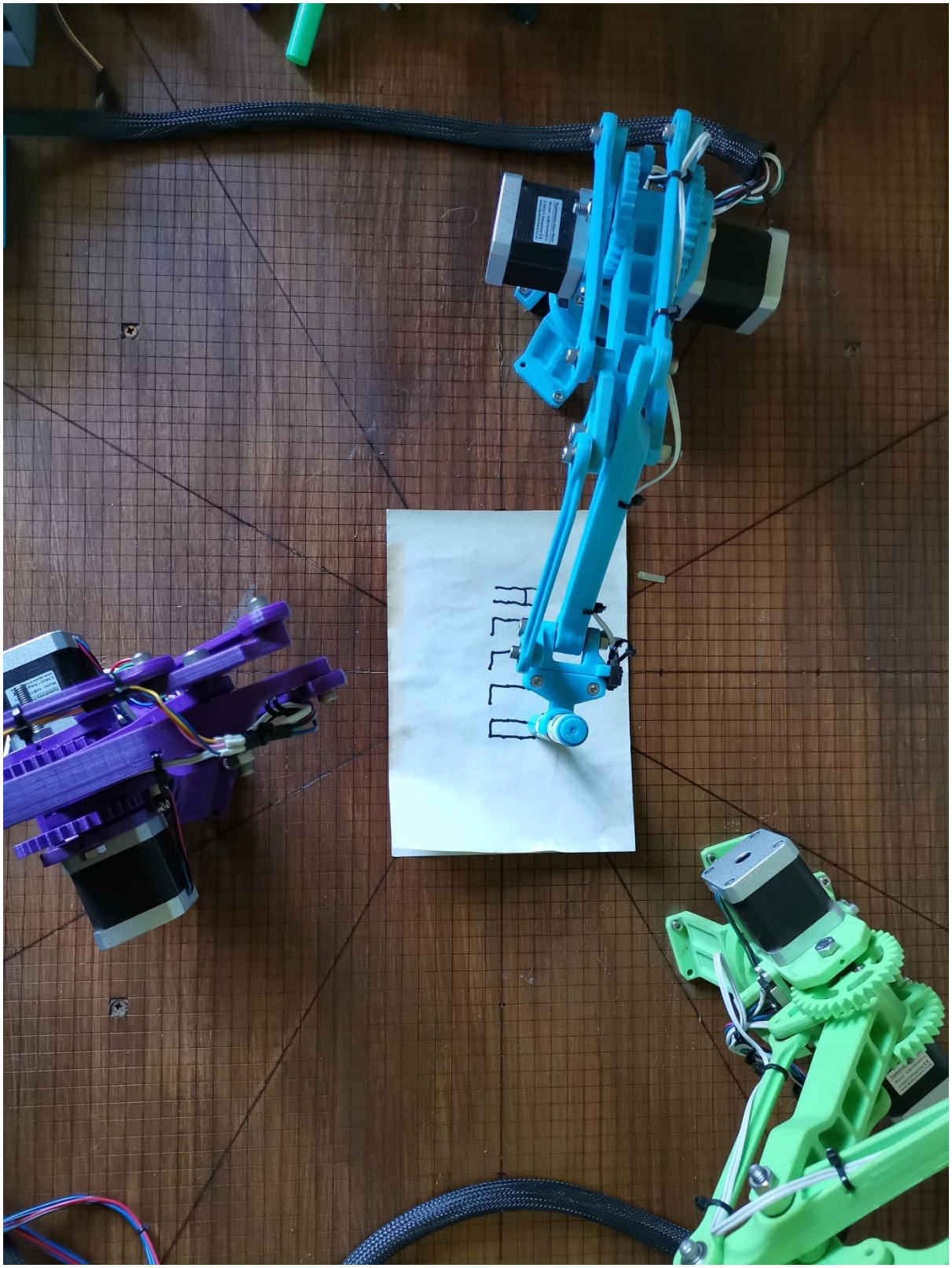

Figure 118: Individual RobotArm with marker - top view – collaborative workspace.

Figure 119: Limit switches for homing.

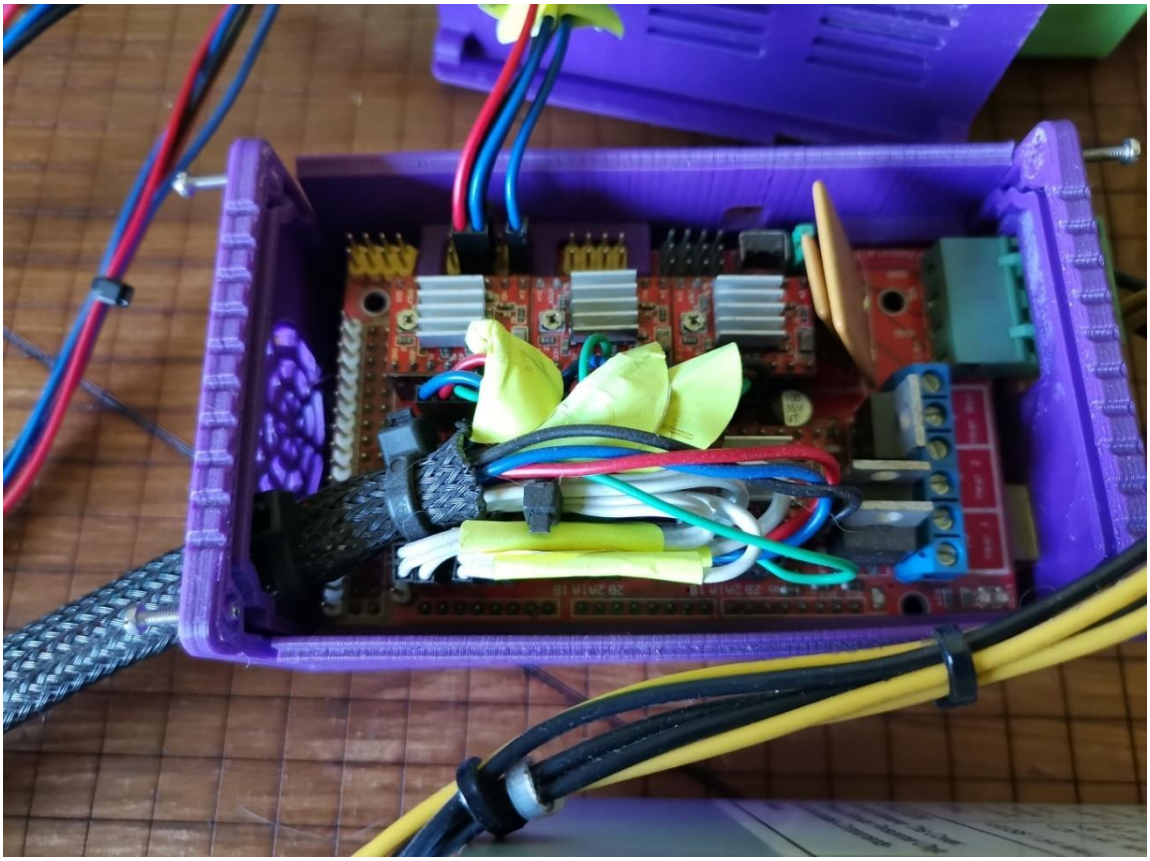

Figure 120: Electronics.

Figure 121: Collaborate RobotArms - side view.

Figure 122: Collaborate RobotArms - top view.

Figure 123: Selection of end-effectors.

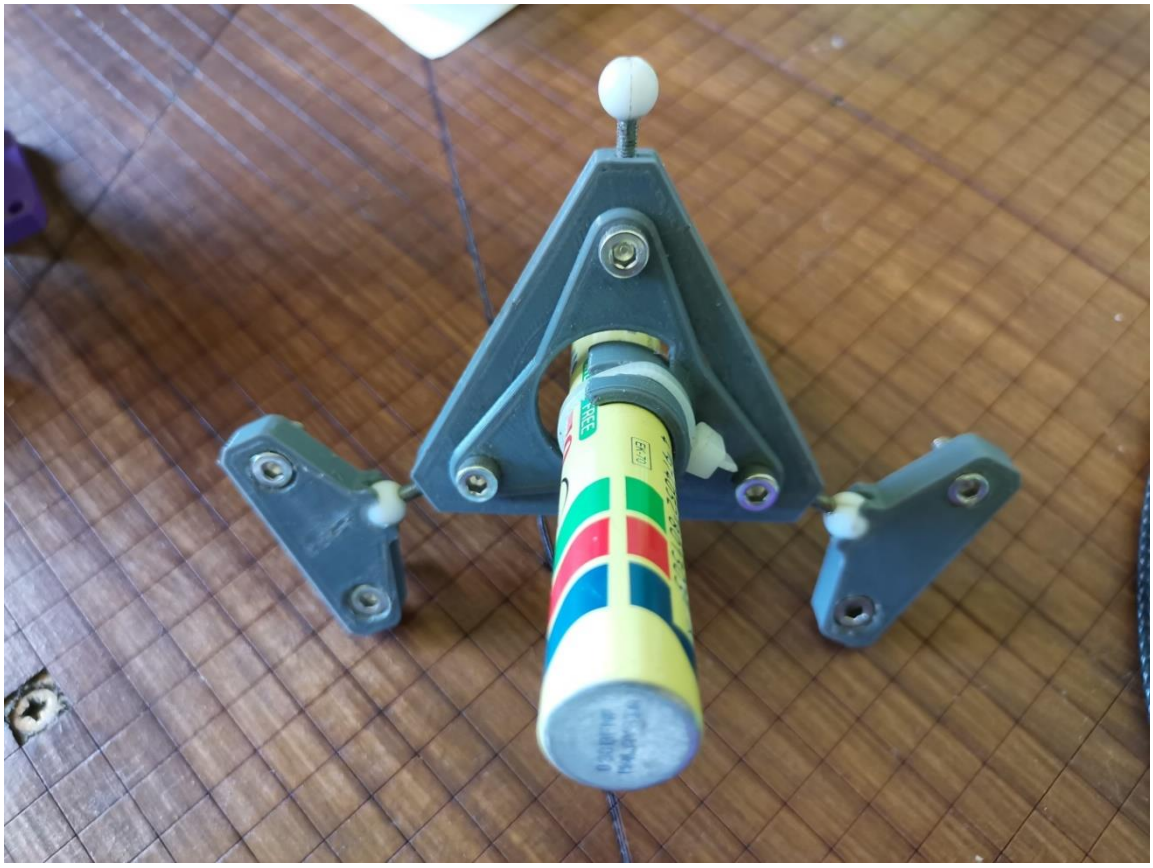

Figure 124: Combined end-effector.

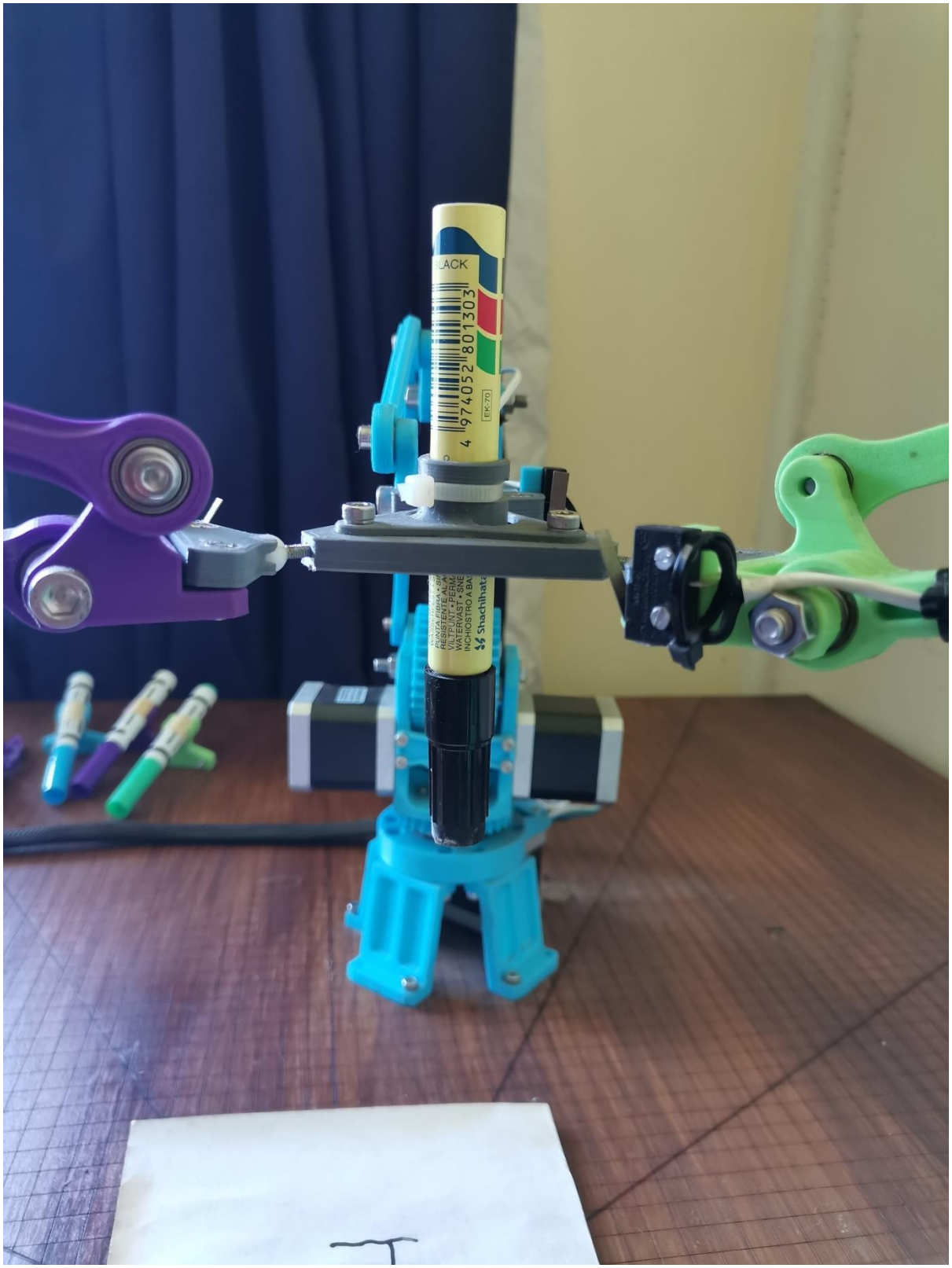

Figure 125: Combined RobotArms with marker pen - side view.

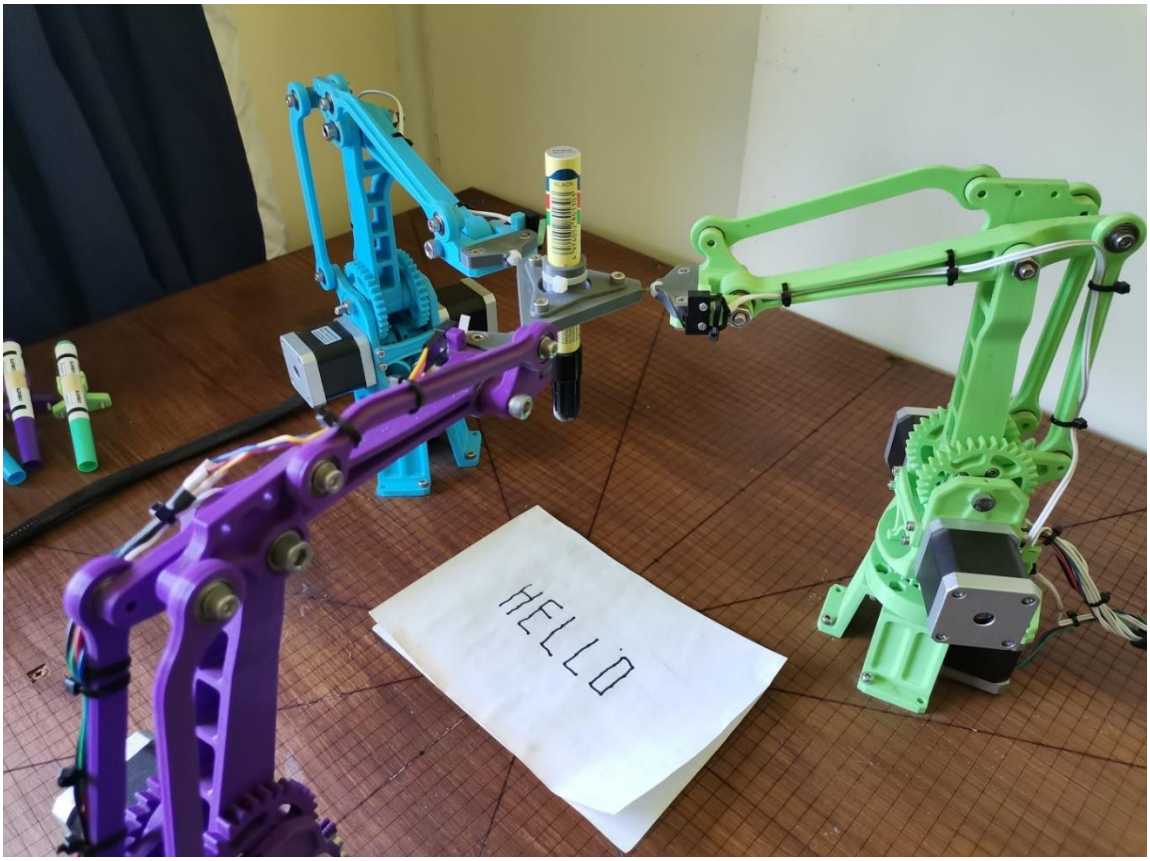

Figure 126: Combined RobotArms with marker pen.

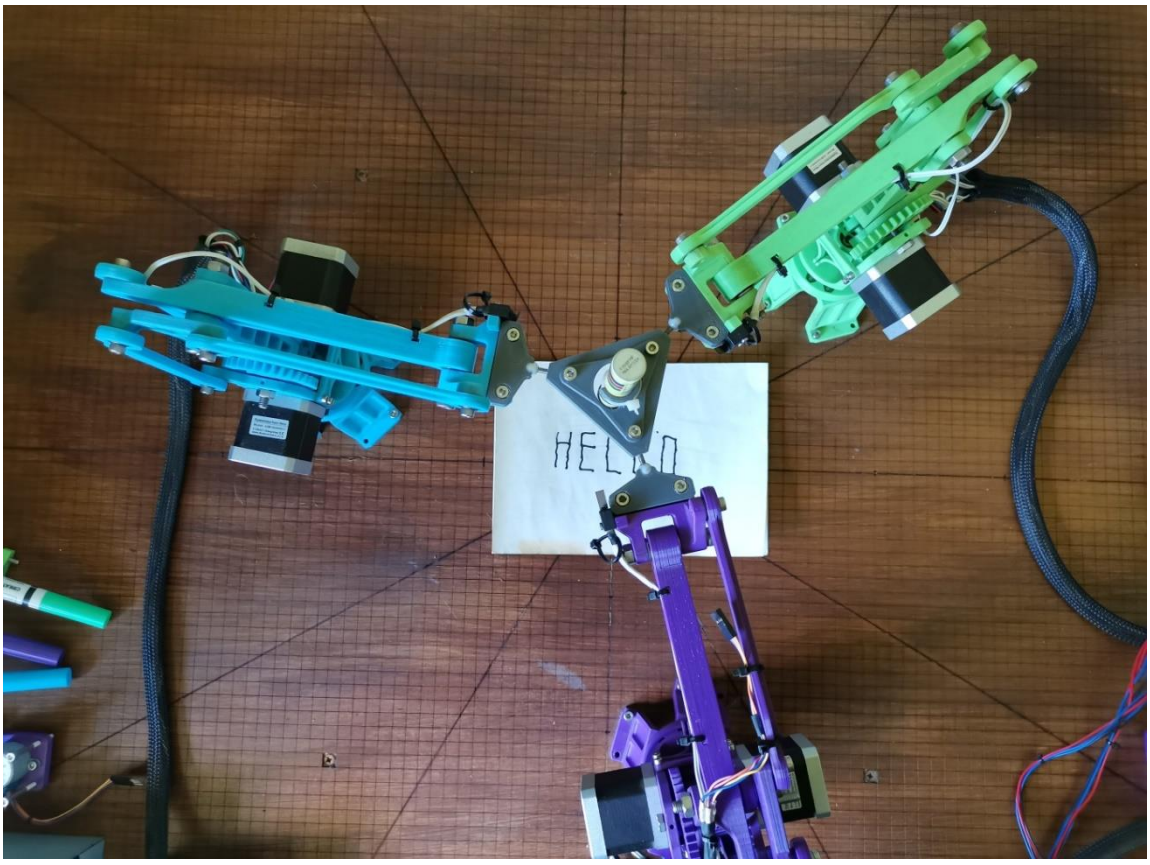

Figure 127: Combined RobotArms with marker pen - side view close.

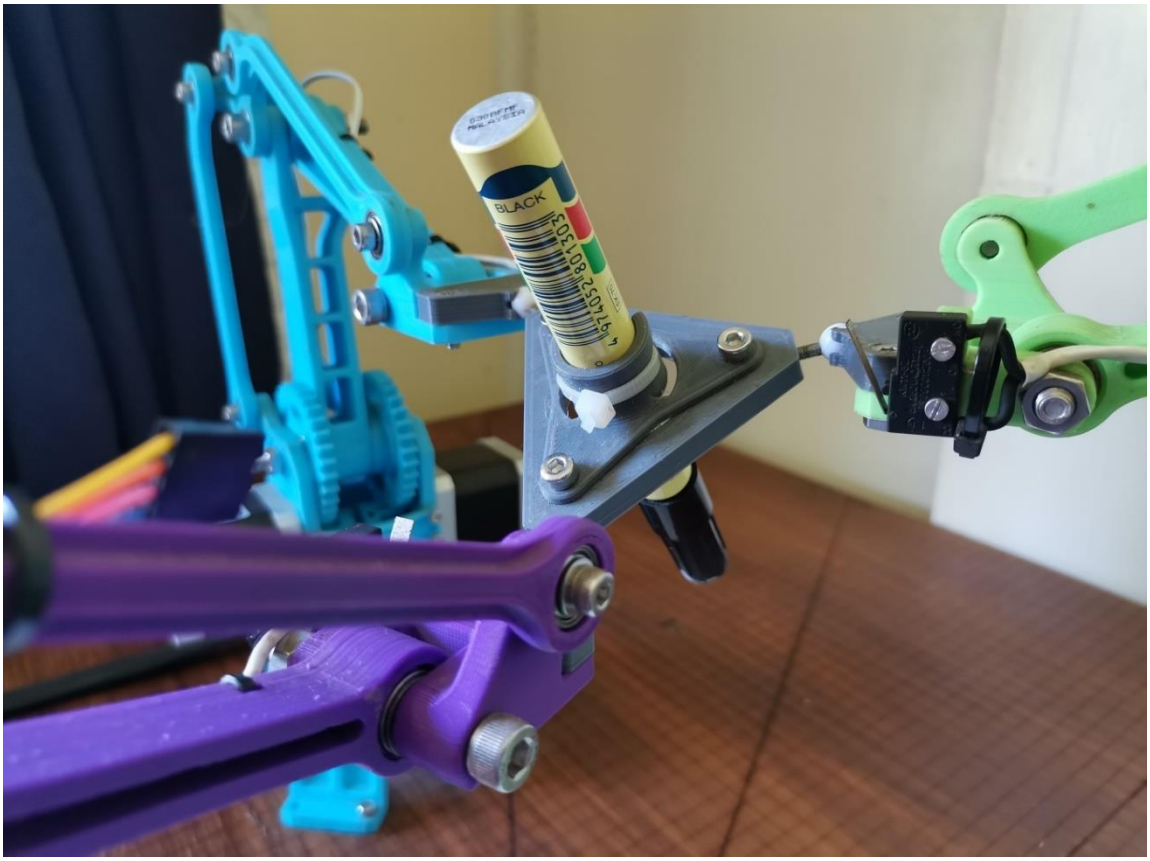

Figure 128: Combined RobotArms with marker pen – roll.

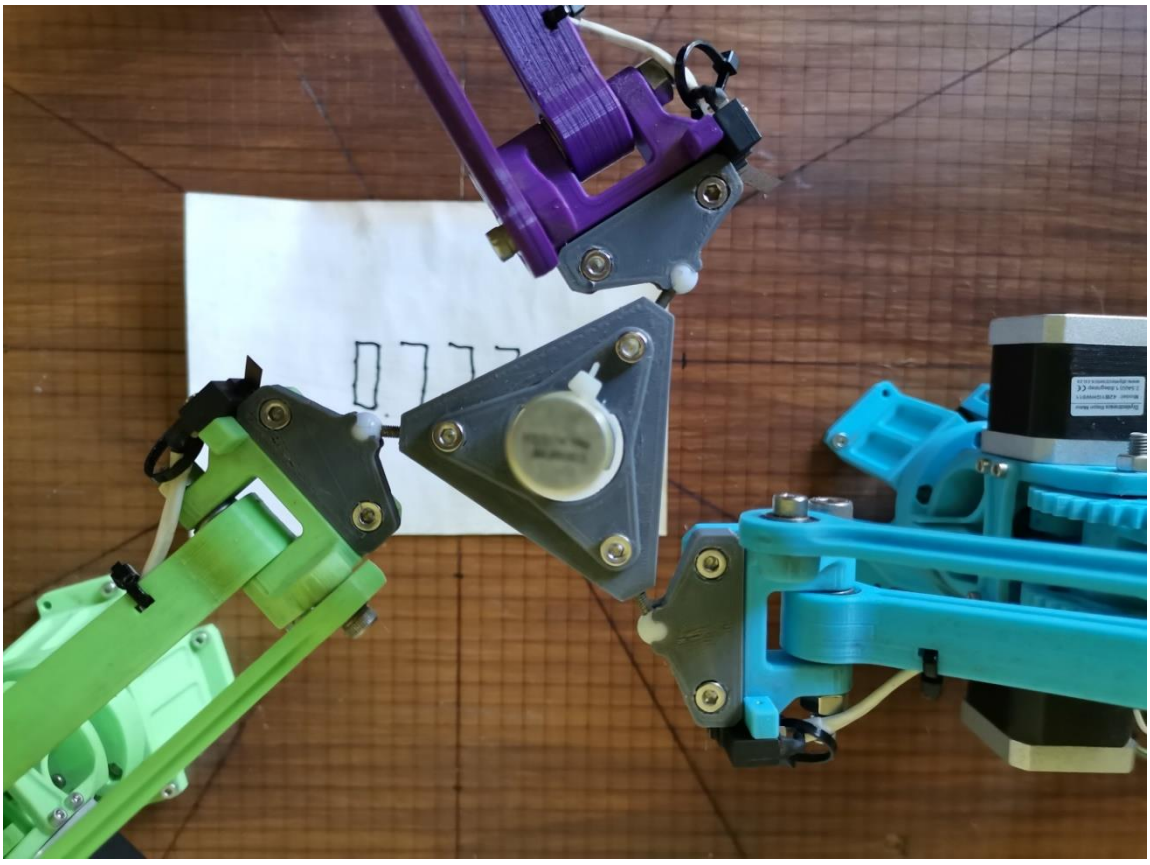

Figure 129: Combined RobotArms with marker pen – yaw.

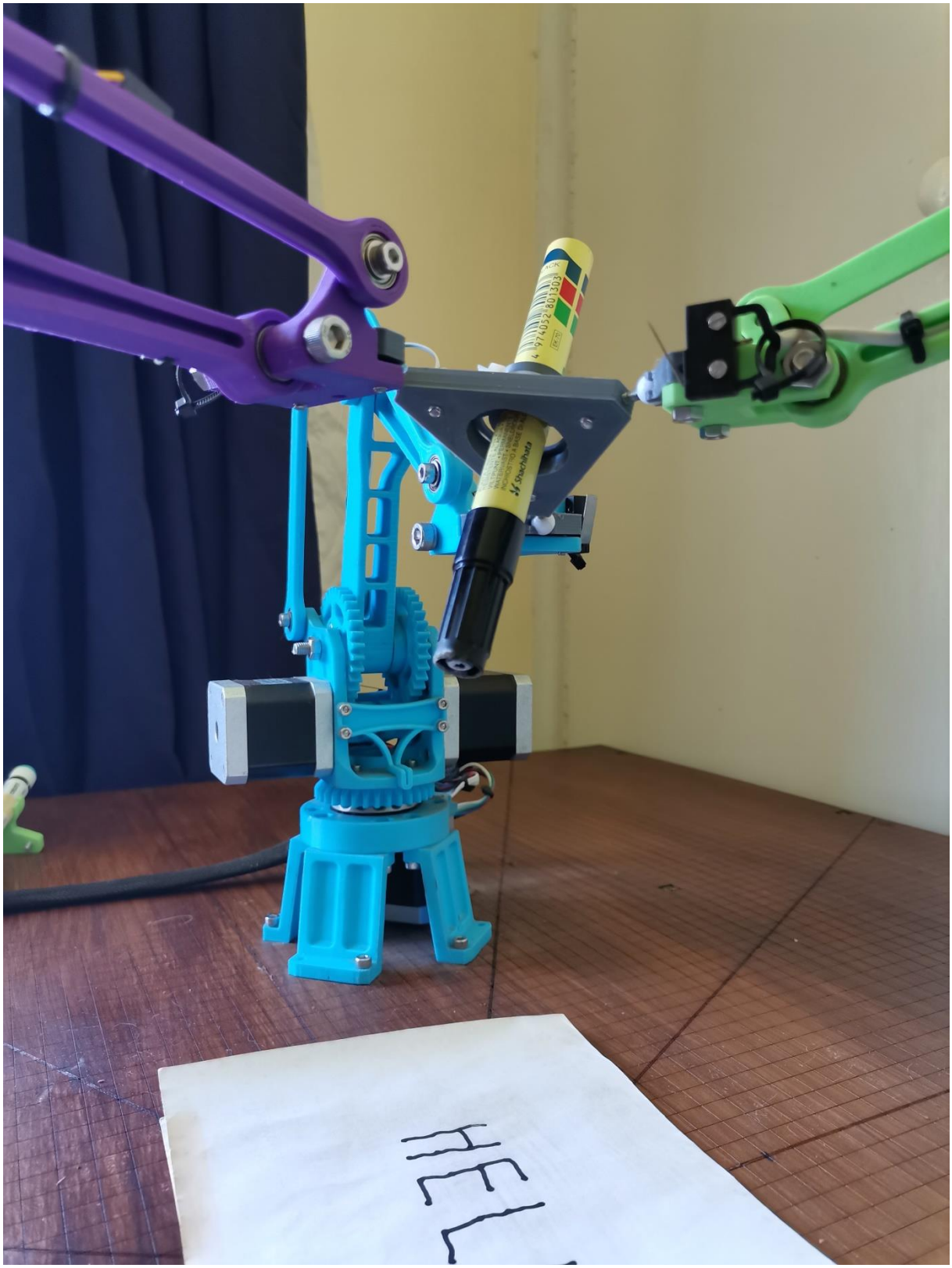

Figure 130: Combined RobotArms with marker pen - roll, pitch and yaw.

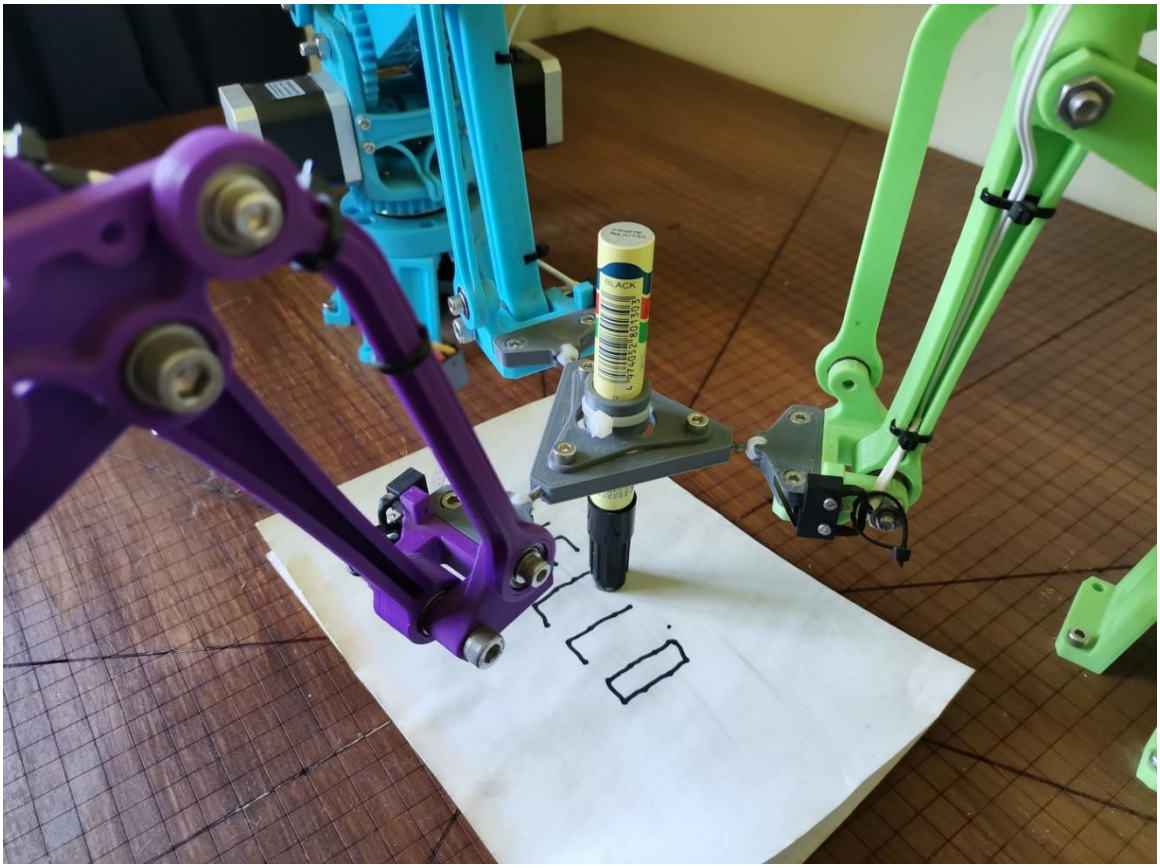

Figure 131: Combined RobotArms with marker pen working.

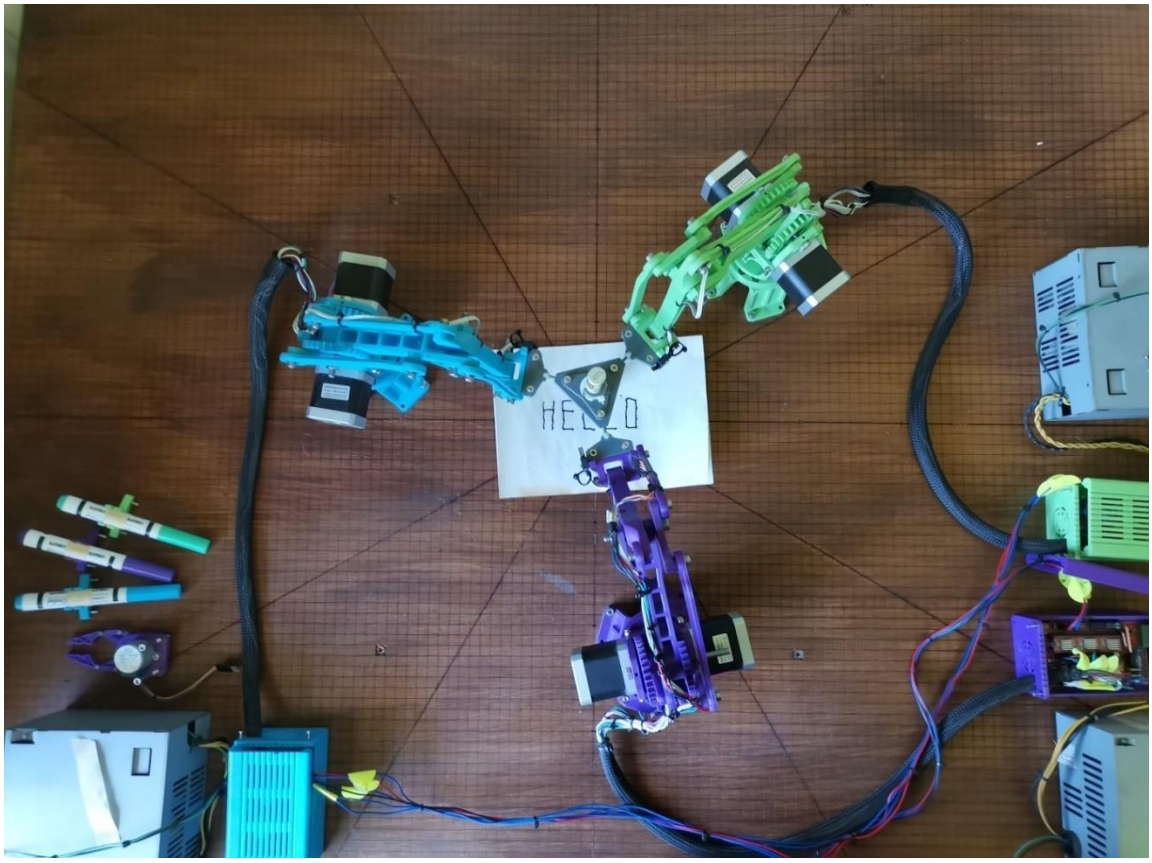

Figure 132: Combined RobotArms with marker pen working - top view.